Molecular cloud dynamics and star formation

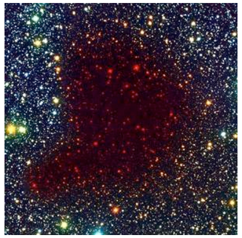
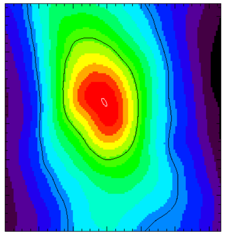

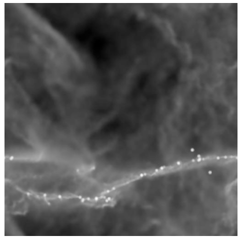

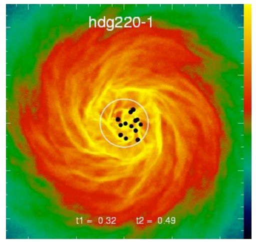

Ralf Klessen

Zentrum für Astronomie der Universität Heidelberg
Institut für Theoretische Astrophysik

thanks to ...

... the organizers for making this school happen!

... people in the group in Heidelberg:

Robi Banerjee, Paul Clark, Gustavo Dopcke, Philipp Girichidis, Simon Glover, Christoph Federrath, Milica Milosavljevic, Faviola Molina, Thomas Peters, Stefan Schmeja, Daniel Seifried, Rahul Shetty, Rowan Smith, Sharanya Sur, Hsiang-Hsu Wang

... many collaborators abroad!

- Structured PhD program
  - HGSFP: Heidelberg Graduate School for Fundamental Physics
    ----> http://www.fundamental-physics.uni-hd.de/

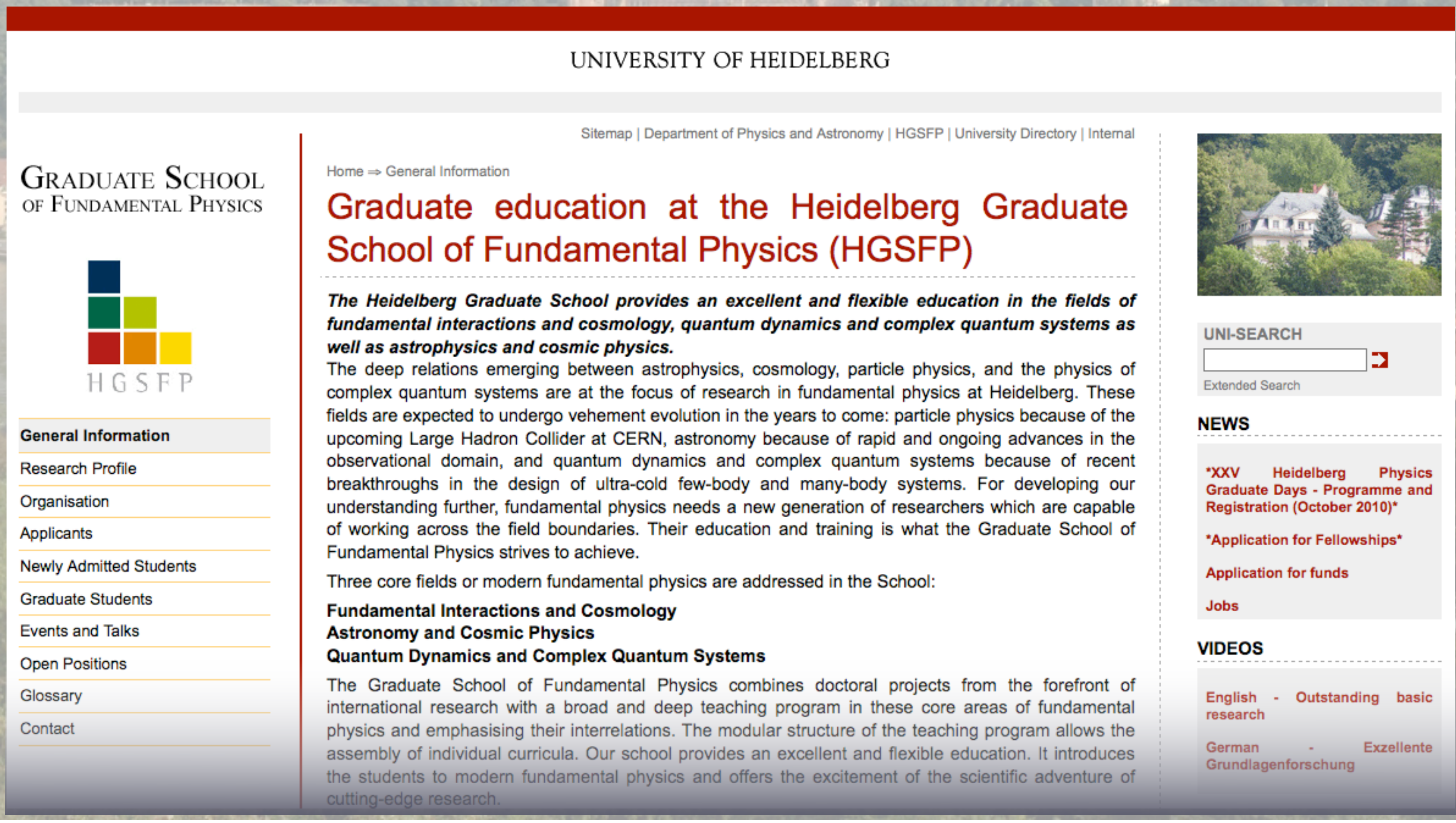

UNIVERSITY OF HEIDELBERG

Sitemap | Department of Physics and Astronomy | HGSFP | University Directory | Internal

GRADUATE SCHOOL OF FUNDAMENTAL PHYSICS

HGSFP

- General Information
- Research Profile
- Organisation
- Applicants
- Newly Admitted Students
- Graduate Students
- Events and Talks
- Open Positions
- Glossary
- Contact

Home ⇒ General Information

Graduate education at the Heidelberg Graduate School of Fundamental Physics (HGSFP)

The Heidelberg Graduate School provides an excellent and flexible education in the fields of fundamental interactions and cosmology, quantum dynamics and complex quantum systems as well as astrophysics and cosmic physics.
The deep relations emerging between astrophysics, cosmology, particle physics, and the physics of complex quantum systems are at the focus of research in fundamental physics at Heidelberg. These fields are expected to undergo vehement evolution in the years to come: particle physics because of the upcoming Large Hadron Collider at CERN, astronomy because of rapid and ongoing advances in the observational domain, and quantum dynamics and complex quantum systems because of recent breakthroughs in the design of ultra-cold few-body and many-body systems. For developing our understanding further, fundamental physics needs a new generation of researchers which are capable of working across the field boundaries. Their education and training is what the Graduate School of Fundamental Physics strives to achieve.

Three core fields or modern fundamental physics are addressed in the School:

Fundamental Interactions and Cosmology
Astronomy and Cosmic Physics
Quantum Dynamics and Complex Quantum Systems

The Graduate School of Fundamental Physics combines doctoral projects from the forefront of international research with a broad and deep teaching program in these core areas of fundamental physics and emphasising their interrelations. The modular structure of the teaching program allows the assembly of individual curricula. Our school provides an excellent and flexible education. It introduces the students to modern fundamental physics and offers the excitement of the scientific adventure of cutting-edge research.

UNI-SEARCH

Extended Search

NEWS

XXV Heidelberg Physics Graduate Days - Programme and Registration (October 2010)

Application for Fellowships

Application for funds

Jobs

VIDEOS

English - Outstanding basic research

German - Exzellente Grundlagenforschung

- Structured PhD program
  - IMPRS-HD: International Max Planck Research School for Astronomy and Cosmic Physics at the University of Heidelberg ---> http://www.mpia-hd.mpg.de/imprs-hd/

Disclaimer

- I try to cover the field as broadly as possible, however, there will clearly be a bias towards my personal interests and many examples will be from my own work.

Schedule

11h30--12h30	C6.1.	Formation of molecular clouds
16h00--17h00	C6.2.	Origin and statistical characteristics of ISM turbulence
17h00--18h00	C6.3.	Star (cluster) formation in molecular clouds
18h00--19h00	C6.4.	Stellar initial mass function

Literature

- Books

  - Stahler, S., & Palla, F., 2004, "The Formation of Stars" (Weinheim: Wiley-VCH)
  - Osterbrock, D., & Farland, G., 2006, "Astrophysics of Gaseous Nebulae & Active Galactic Nuclei, 2nd ed. (Sausalito: Univ. Science Books)
  - Lada, C. F., & Kylafis, N. D. 1999, "The Origin of Stars and Planetary Systems", NATO ASI Series 540 (Kluwer Academic Publisher)
  - Reipurth et al. 2007, "Protostars and Planets V" (University of Arizona Press)

Literature

- Review Articles
  - Mac Low, M.-M., Klessen, R.S., 2004, "The control of star formation by supersonic turbulence", Rev. Mod. Phys., 76, 125 - 194
  - Zinnecker, H., Yorke, McKee, C.F., Ostriker, E.C., 2008, "Toward Understanding Massive Star Formation", ARA&A, 45, 481 - 563
  - McKee, C.F., Ostriker, E.C., 2008, "Theory of Star Formation", ARA&A, 45, 565 - 687
  - Bromm, V., Larson, R.B., 2004, "The first stars", ARA&A, 42, 79 - 118

Lecture 1+2: ISM dynamics

- phases of the ISM
- how to observe the ISM
- formation of molecular clouds in convergent flows
  - chemistry
  - dynamics
- origin of ISM turbulence

inventory of Galactic disc component

- **stellar disc**
  - thin disc (80% of mass): stars of all ages 0-12Gyr
  - thick disc (5% of mass): older stars with lower metallicity
- **interstellar medium (ISM)**
  - gas (15% of mass): hot, warm, and cool component (atomic and molecular)
  - dust (<1% of gas mass): well mixed with the cool gas
  - cosmic rays: relativistic particles
  - magnetic fields: frozen to the gas (field lines are co-moving with the gas); energy density comparable to the kinetic energy of gas

Interstellar Matter: ISM

Abundances, scaled to 1.000.000 H atoms

element		atomic number	abundance
hydrogen	H	1	1.000.000
deuterium	$_1H^2$	1	16
helium	He	2	68.000
carbon	C	6	420
nitrogen	N	7	90
oxygen	O	8	700
neon	Ne	10	100
sodium	Na	11	2
magnesium	Mg	12	40
aluminium	Al	13	3
silicium	Si	14	38
sulfur	S	16	20
calcium	Ca	20	2
iron	Fe	26	34
nickel	Ni	28	2

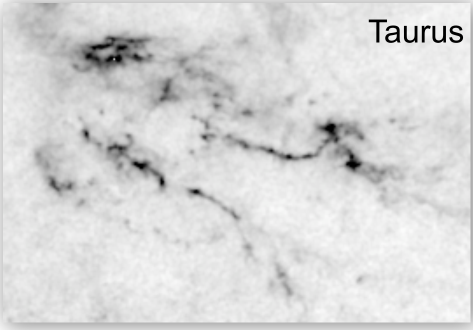

hydrogen is by far the most abundant element (more than 90% in number).

Phases of the ISM

Because hydrogen is the dominating element, the classification scheme is based on its chemical state:

ionized atomic hydrogeN	*HII (H^+)*	ionization
neutraler atomic hydrogen	*HI (H)*	dissociation
molecular hydrogen	*H_2*	

different regions consist of almost 100% of the appropriate phase, the transition regions between HII, H and H_2 are very thin.

star formation always takes place in dense and cold molecular clouds.

Phases of the ISM

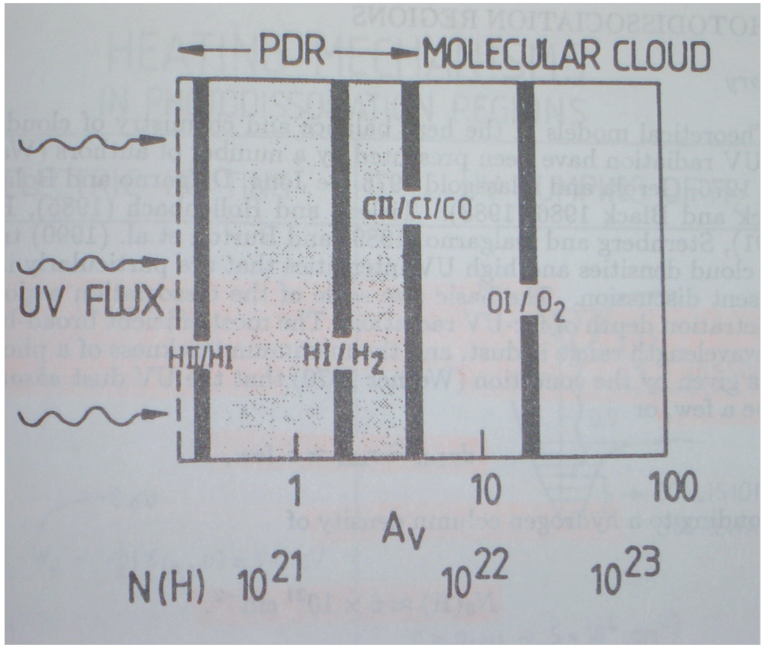

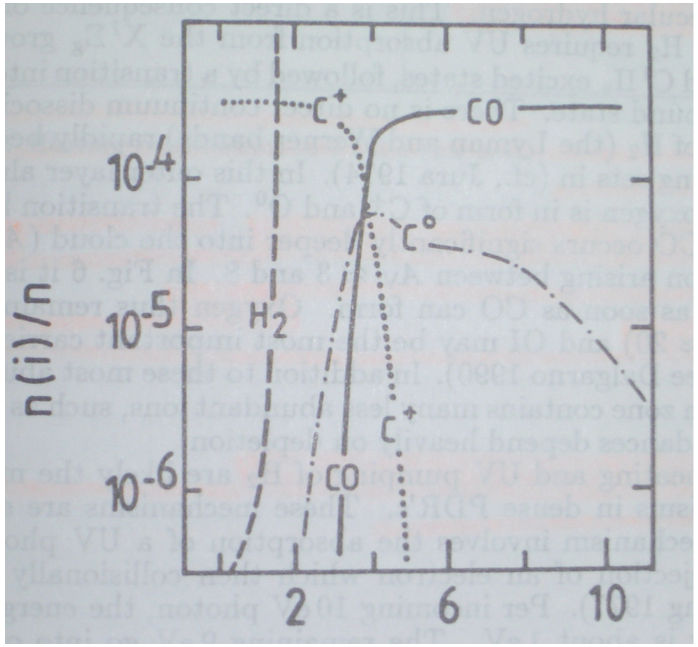

A_V

HII ⟵ HI ⟷ H$_2$ ⟶

density / column density increases ⟶

A_V denotes the extinction, the attenuation of radiation due to absorption (mostly on dust grains)

Life-cycle of ISM

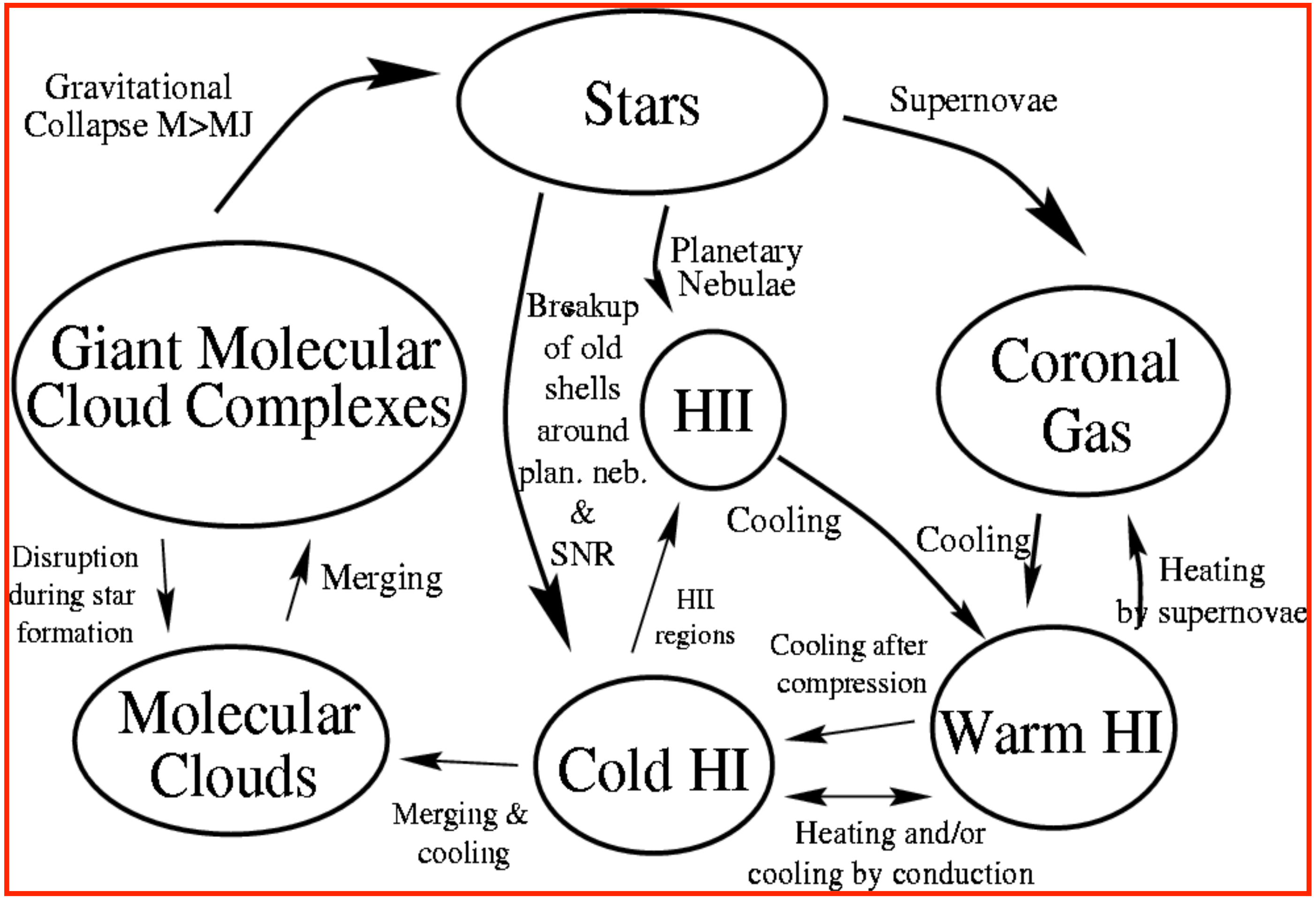

Life-cycle of ISM

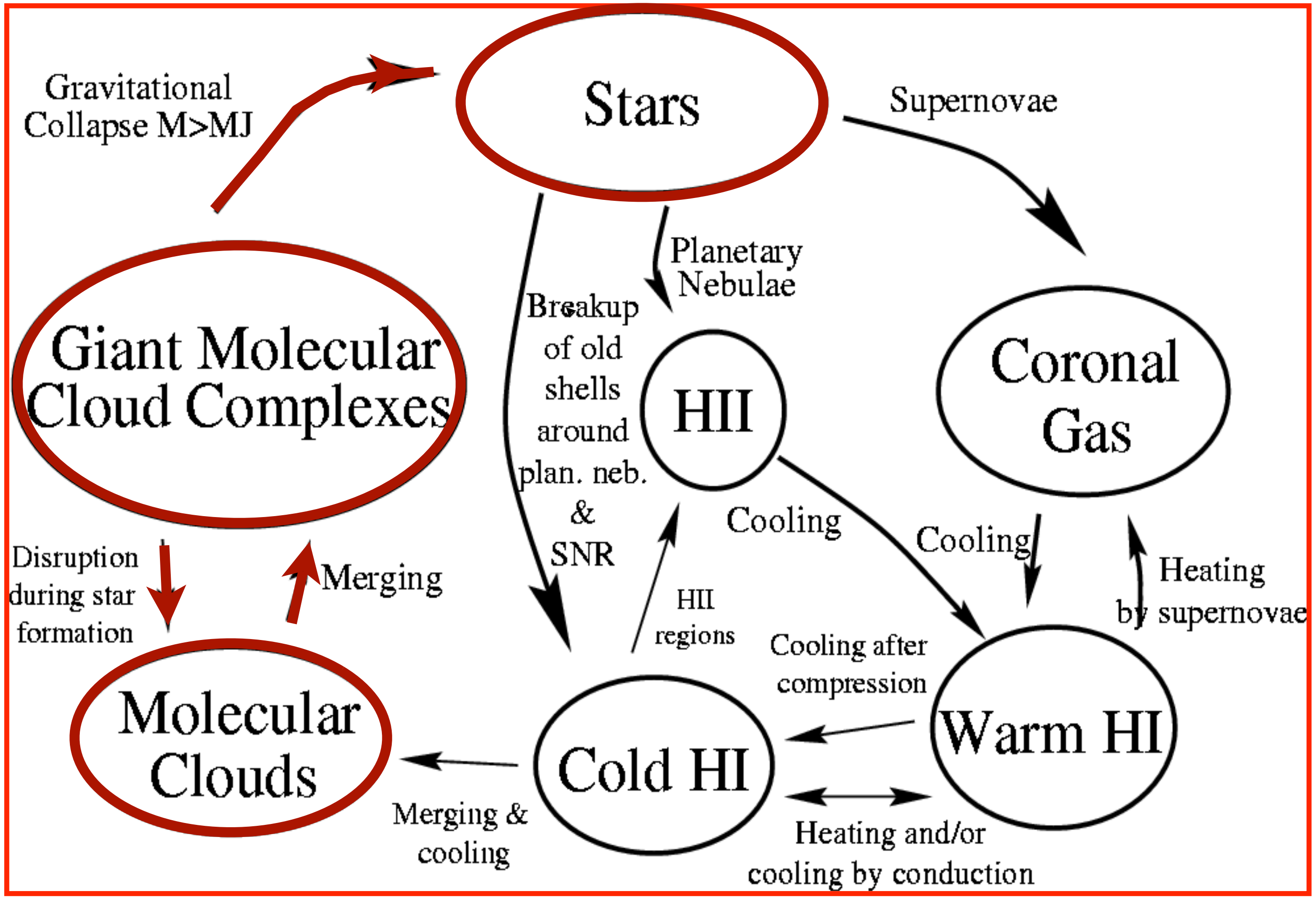

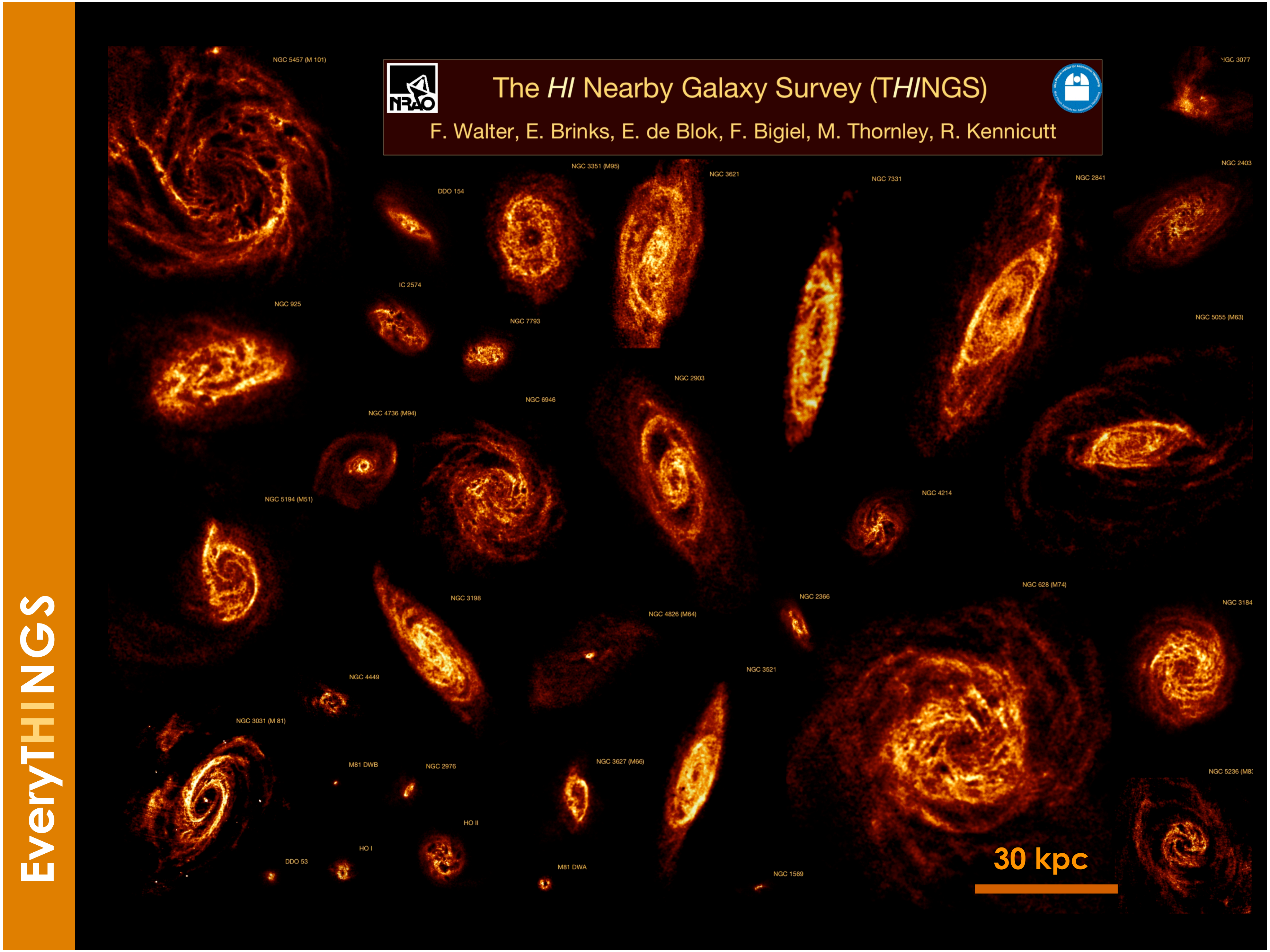
EveryTHINGS
The HI Nearby Galaxy Survey (THINGS)
F. Walter, E. Brinks, E. de Blok, F. Bigiel, M. Thornley, R. Kennicutt
NGC 5457 (M 101)
DDO 154
NGC 3351 (M95)
NGC 3621
NGC 7331
NGC 2841
NGC 2403
IC 2574
NGC 925
NGC 7793
NGC 5055 (M63)
NGC 2903
NGC 6946
NGC 4736 (M94)
NGC 5194 (M51)
NGC 4214
NGC 3198
NGC 4826 (M64)
NGC 2366
NGC 628 (M74)
NGC 3184
NGC 4449
NGC 3521
NGC 3031 (M 81)
M81 DWB
NGC 2976
NGC 3627 (M66)
HO II
HO I
DDO 53
M81 DWA
NGC 1569
30 kpc

HI Maps

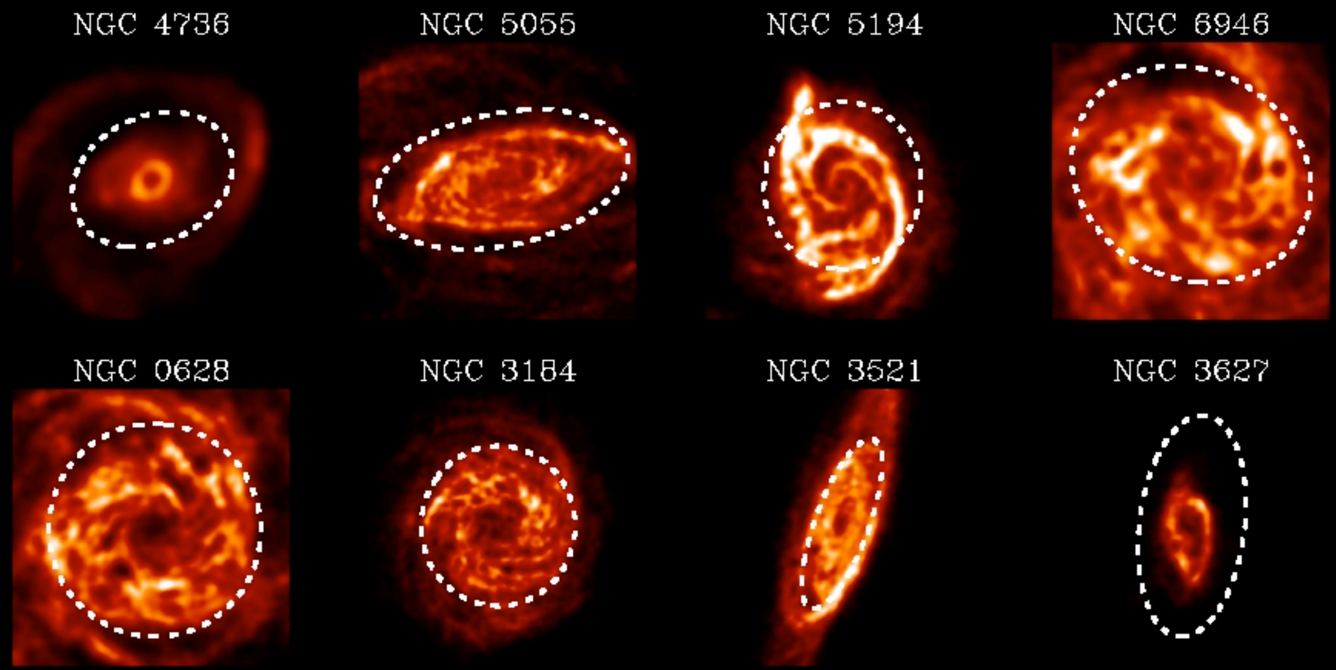

work by Frank Bigiel (now Berkeley)

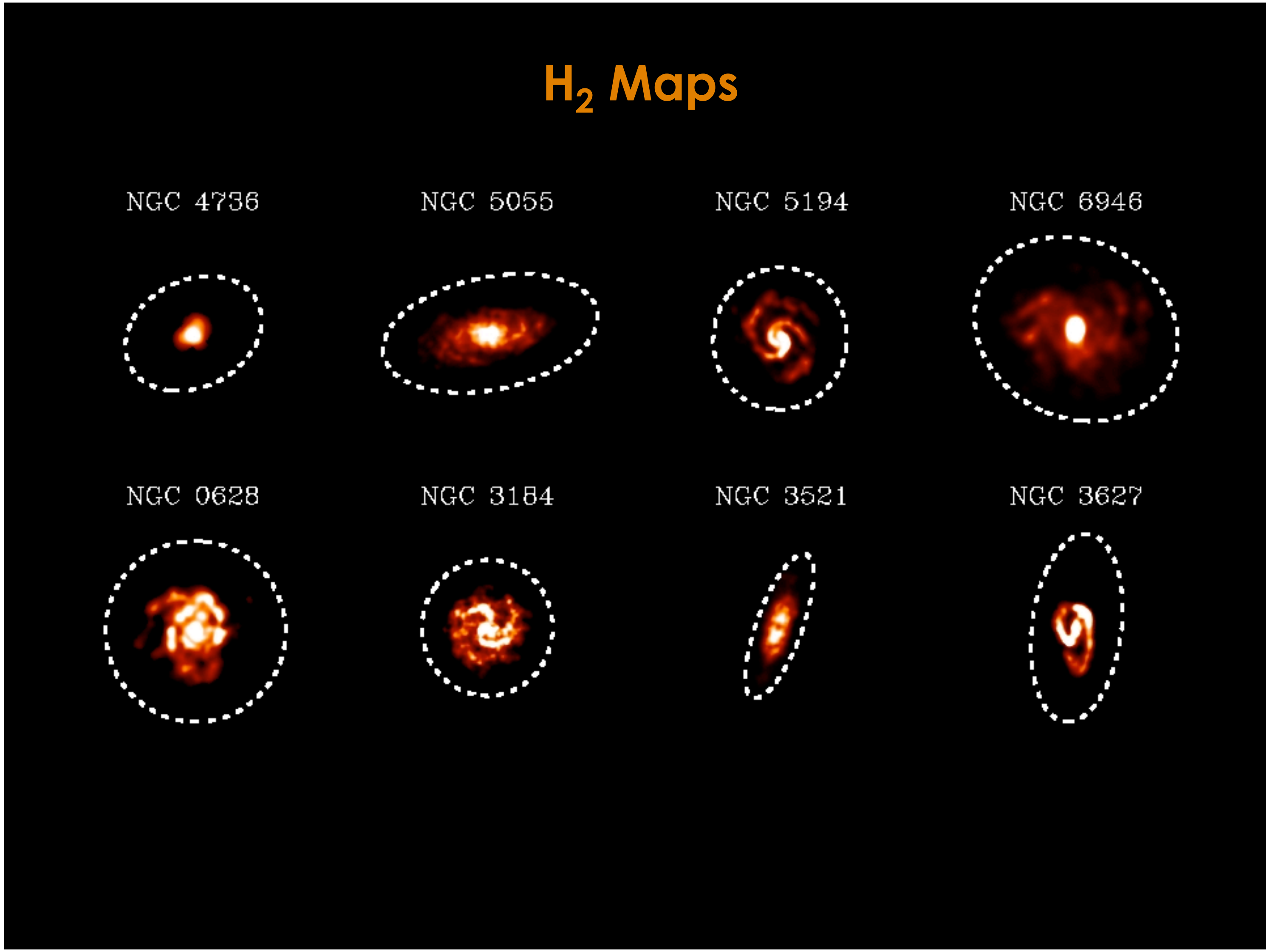

work by Frank Bigiel (now Berkeley)

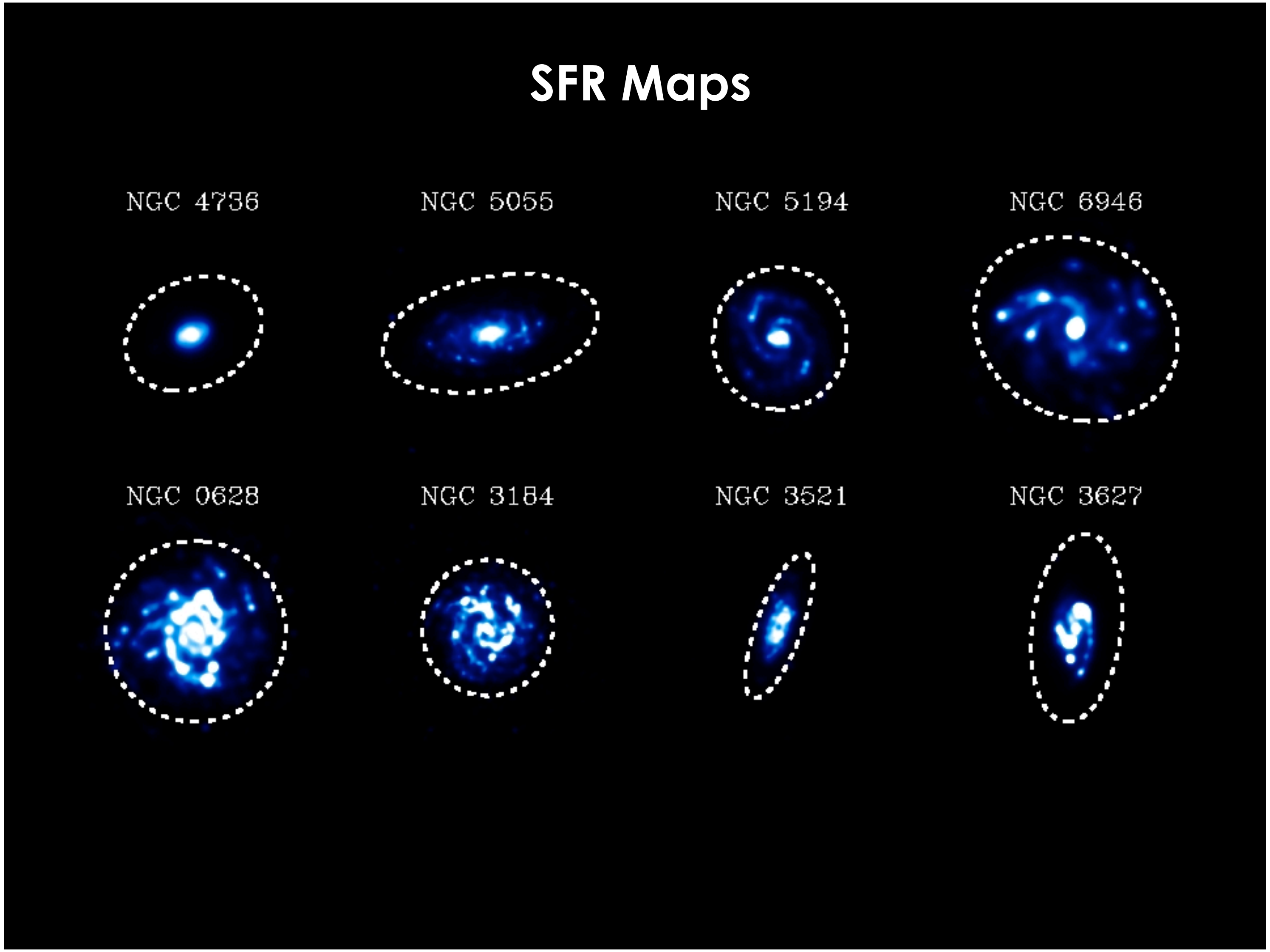

work by Frank Bigiel (now Berkeley)

Correlation between H_2 and HI

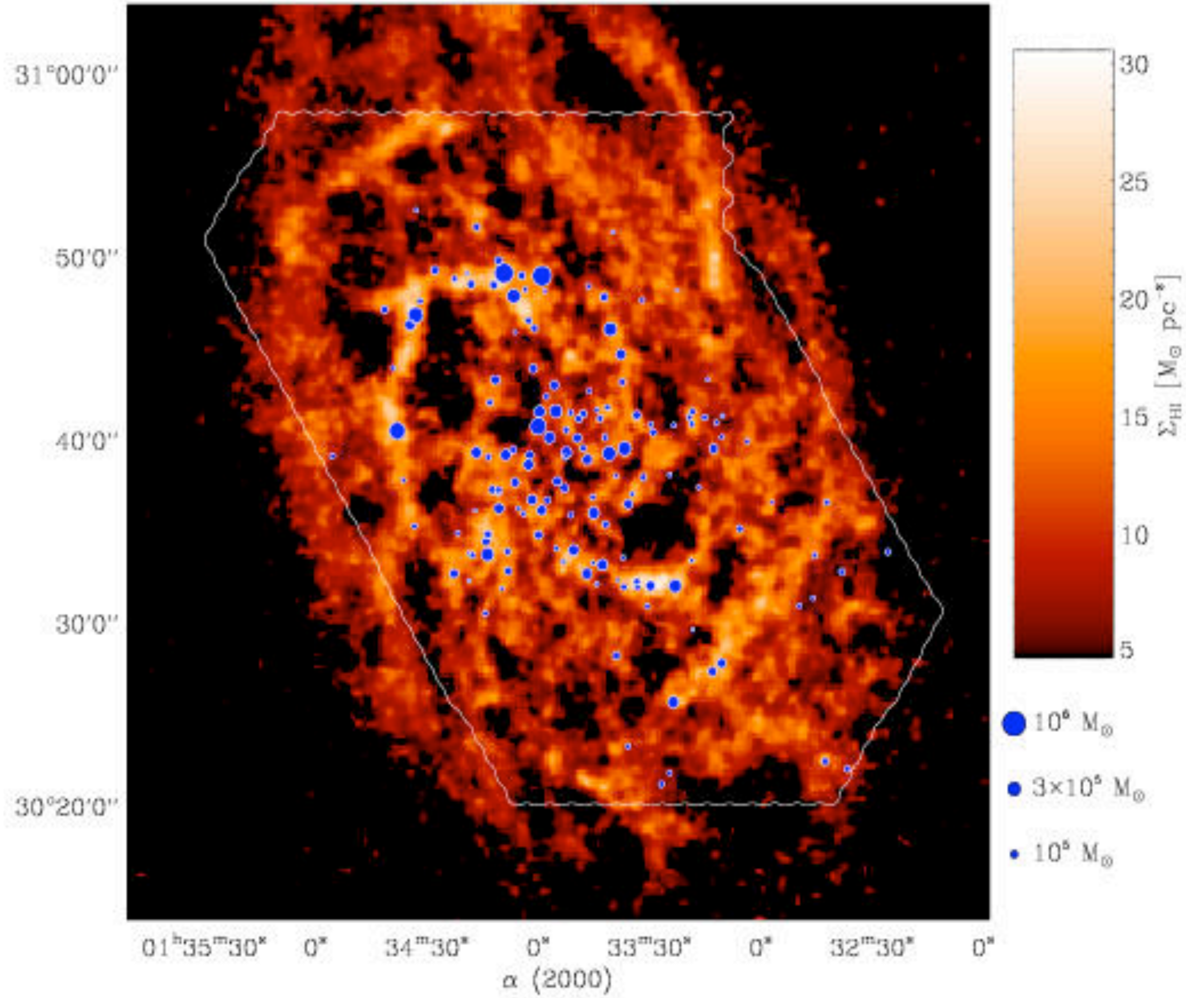

(Deul & van der Hulst 1987, Blitz et al. 2004)

Compare H_2 - HI in M33:

- H_2: BIMA-SONG Survey, see Blitz et al.
- HI: Observations with Westerbork Radio T.

H_2 clouds are seen in regions of high HI density
(in spiral arms and filaments)

Radial Distribution in Spirals

- HI versus H_2:
  - H_2 is restricted to the optical disk
  - while the HI extends 2 - 4 x optical radius
- HI hole or depression in the centers, sometimes compensated by H_2
- often H_2 is exponential like stars, HI does *not* follow in most cases

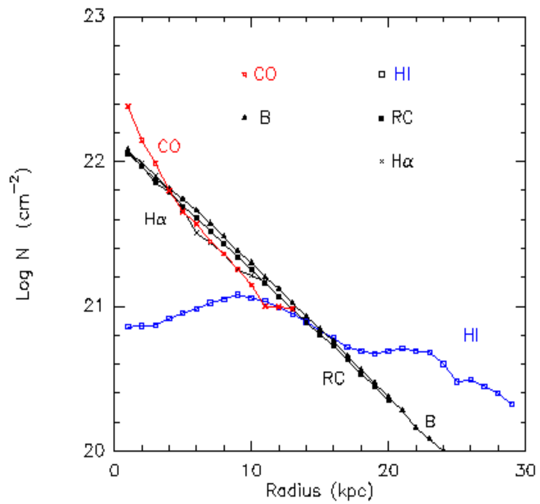

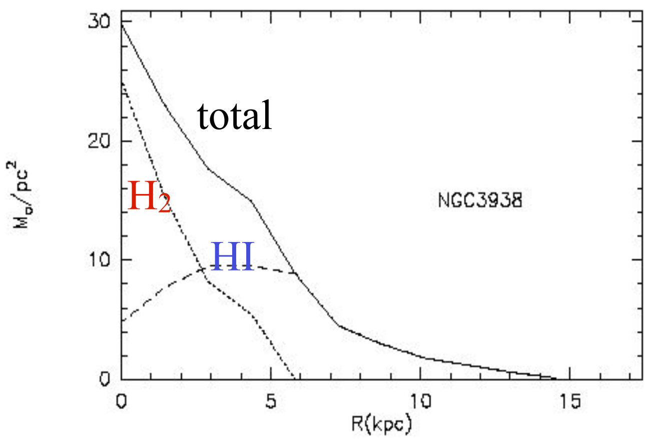

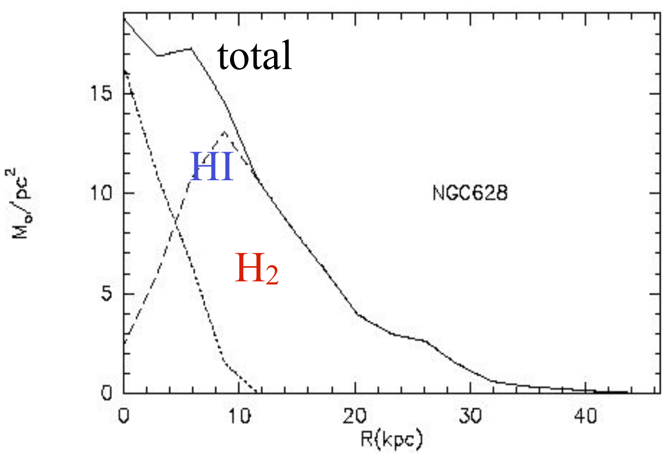

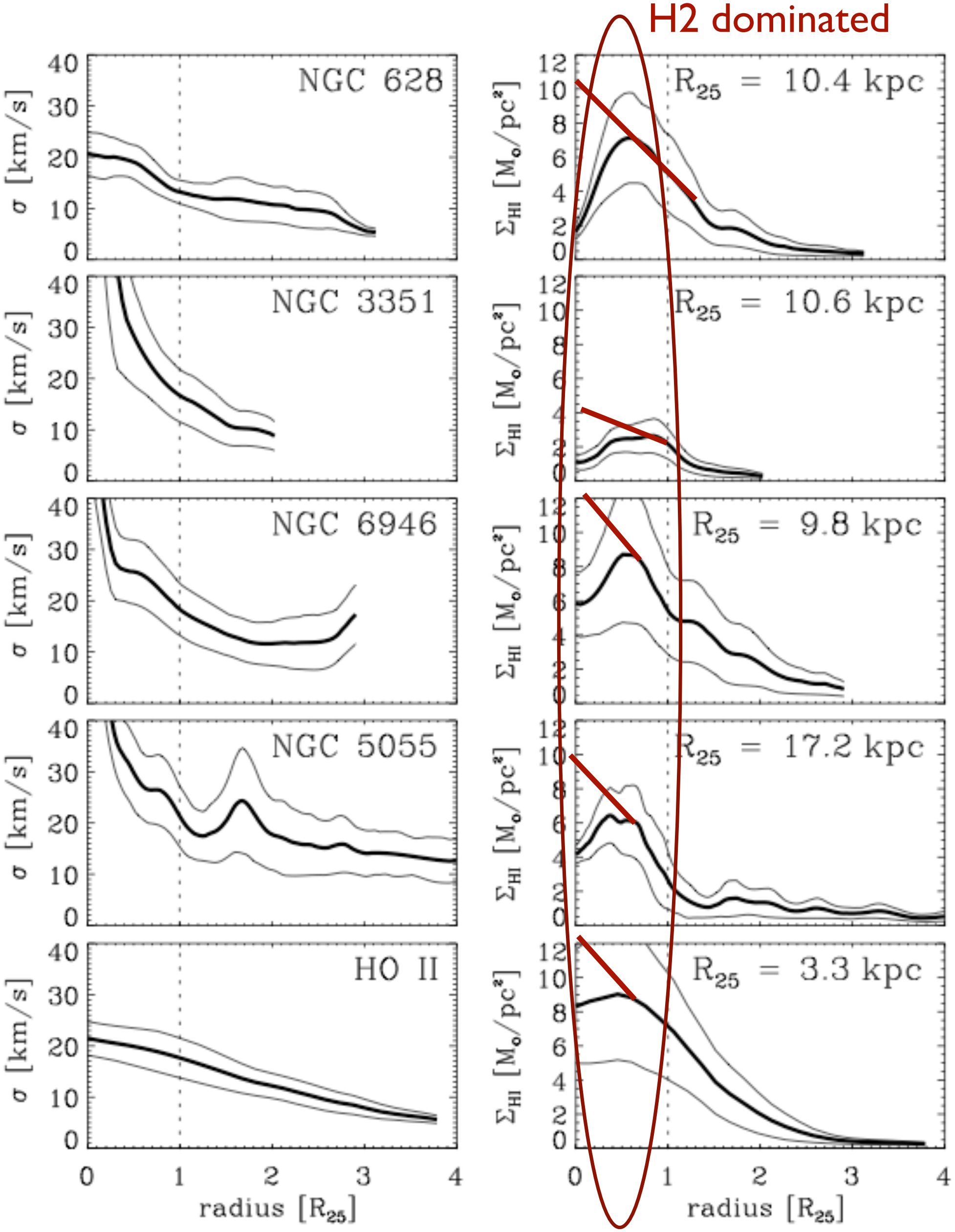
H2 dominated
NGC 628
NGC 3351
NGC 6946
NGC 5055
HO II
R25 = 10.4 kpc
R25 = 10.6 kpc
R25 = 9.8 kpc
R25 = 17.2 kpc
R25 = 3.3 kpc
σ [km/s]
Σ_HI [M_o/pc²]
radius [R25]

some important trends

- typically comparable amounts of H_2 and HI gas in the Galaxy
- in Milky Way $M(H_2) \sim 2 \times 10^9\, M_\odot$ and $M(H_2) \sim 6 \times 10^9\, M_\odot$
- But: Very different radial distribution
  - H_2 is centrally concentrated, and in a molecular ring at 4-8kpc (seen in our Galaxy, and in external ones)
  - HI depleted in the center and more radially extended
- H_2 is clumped in clouds and superclouds
- Velocity dispersion falls of slowly from σ_g= 20 km/s to 5 km/s (and this holds more or less for all spiral galaxies)

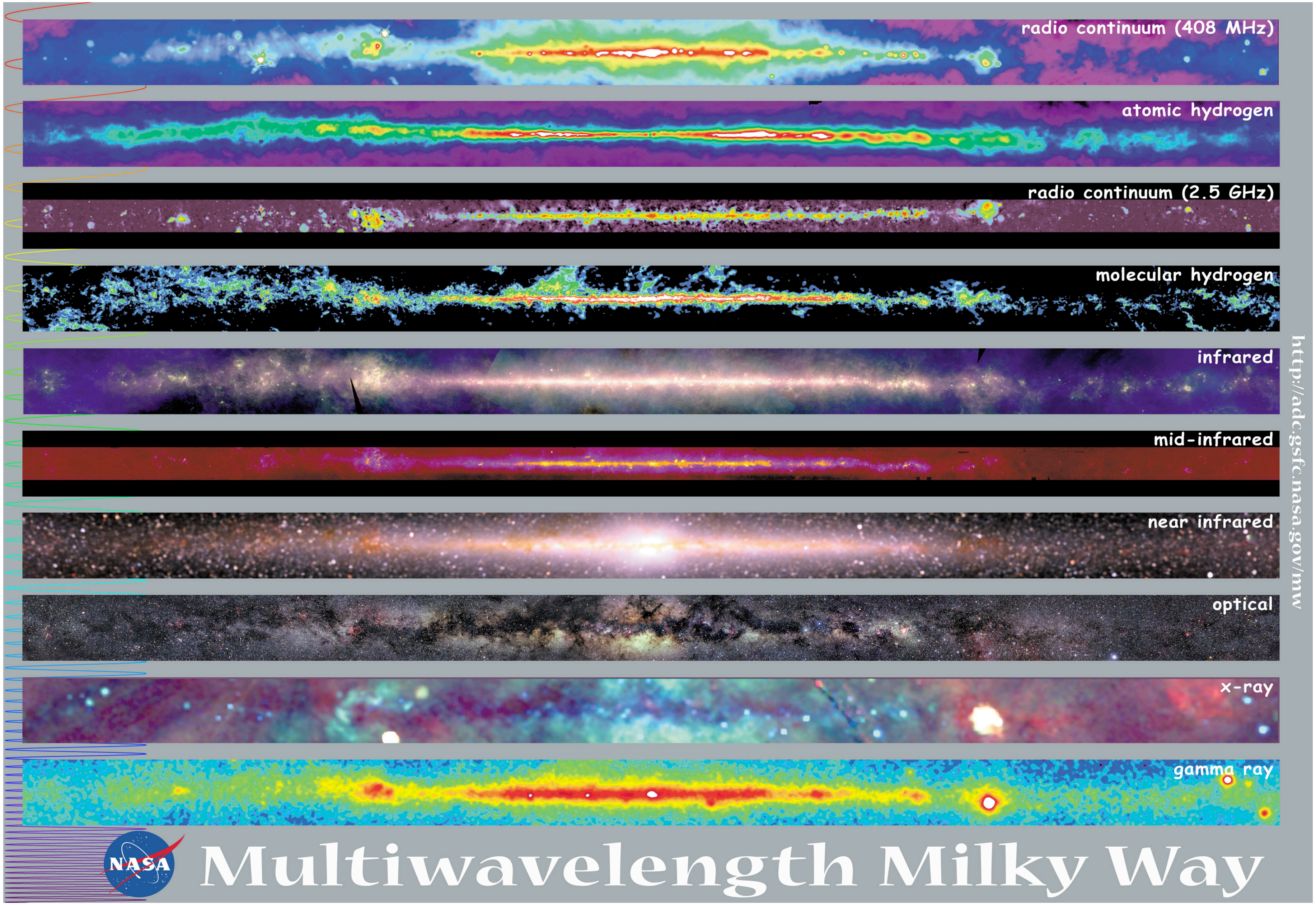
radio continuum (408 MHz)
atomic hydrogen
radio continuum (2.5 GHz)
molecular hydrogen
infrared
mid-infrared
near infrared
optical
x-ray
gamma ray
http://adc.gsfc.nasa.gov/mw
NASA
Multiwavelength Milky Way

Multi-wavelength observations

different wavelengths provide different information.

→astronomer use the full electromagnetic spectrum

- radio: interstellar gas (line emission -> velocity information)
- sub-mm range: dust (thermal emission)
- infrared & optical: stars
- x-rays: stars (coronae), supernovae remnants (very hot gas)
- γ-rays: supernovae remnants (radioactive decay, e.g. ^{26}Al), compact objects, merging of neutron stars (γ-ray burst)

dust

ingredients of the ISM

- **interstellar dust**
- smoothly distributed with HI
- and in dark (molecular) clouds

- rough distance of clouds by star counts: Wolf diagram
- mean absolute brightness M_1 and m_1 -> distance
- from m_1-m_2 -> depth
- clouds are typically at a distance of a few 100pc with an extinction of Δm=1-3mag
- clouds sharply concentrated to the galactic plane

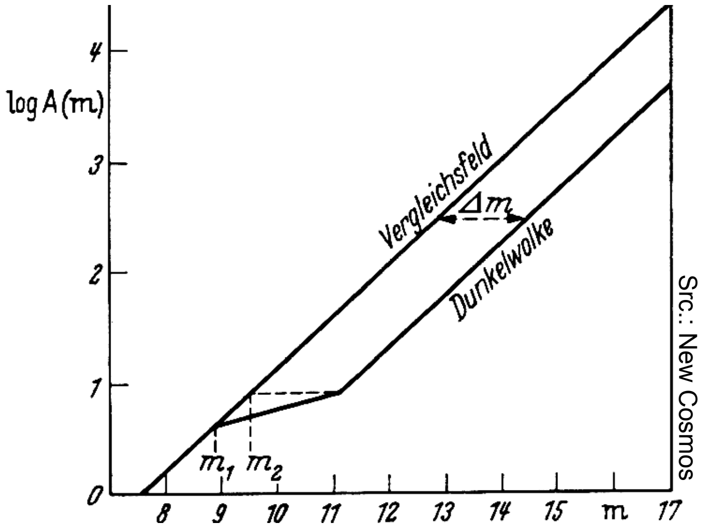

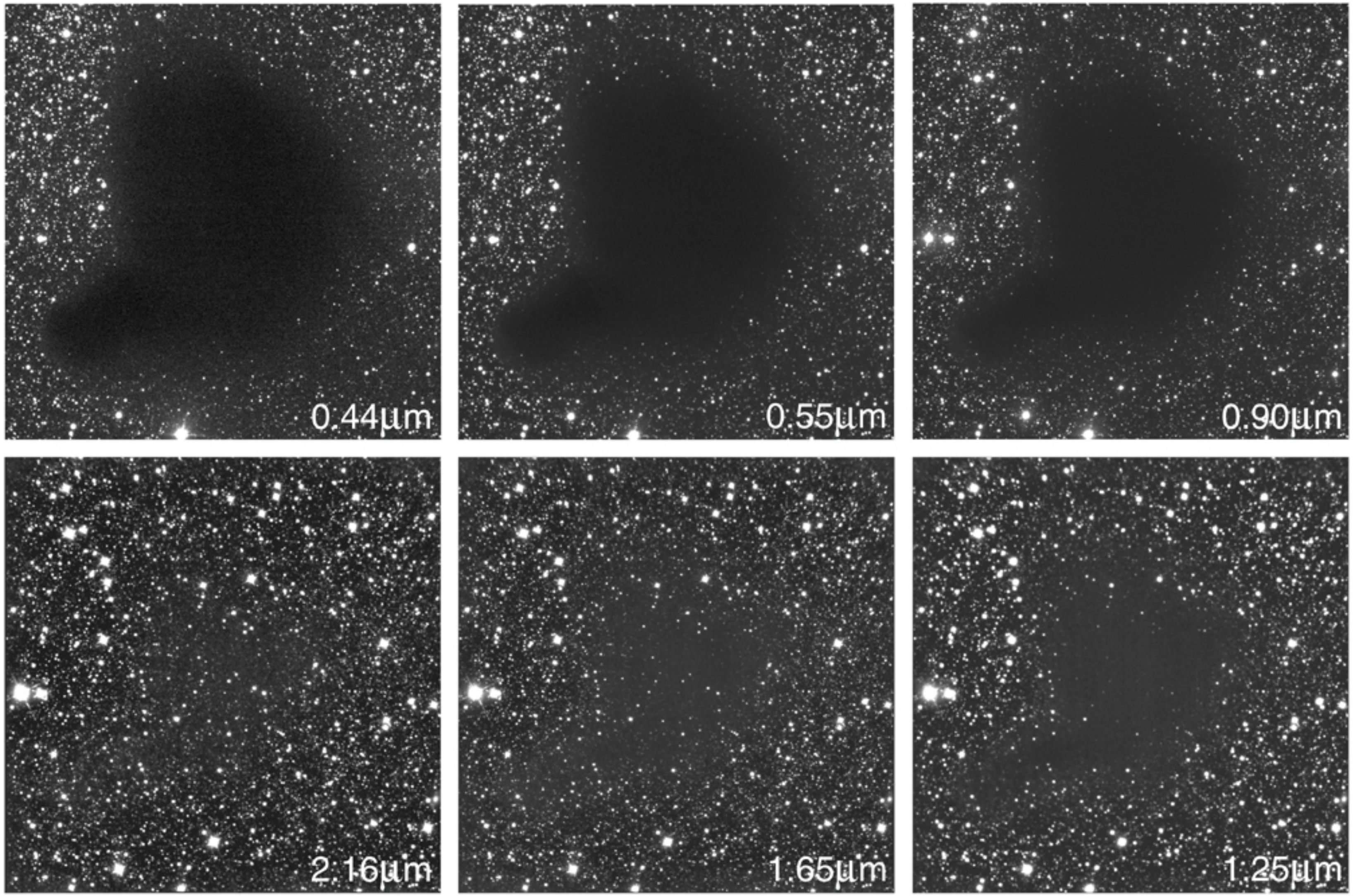

The Dark Cloud B68 at Different Wavelengths (NTT + SOFI)

ESO PR Photo 29b/99 (2 July 1999)

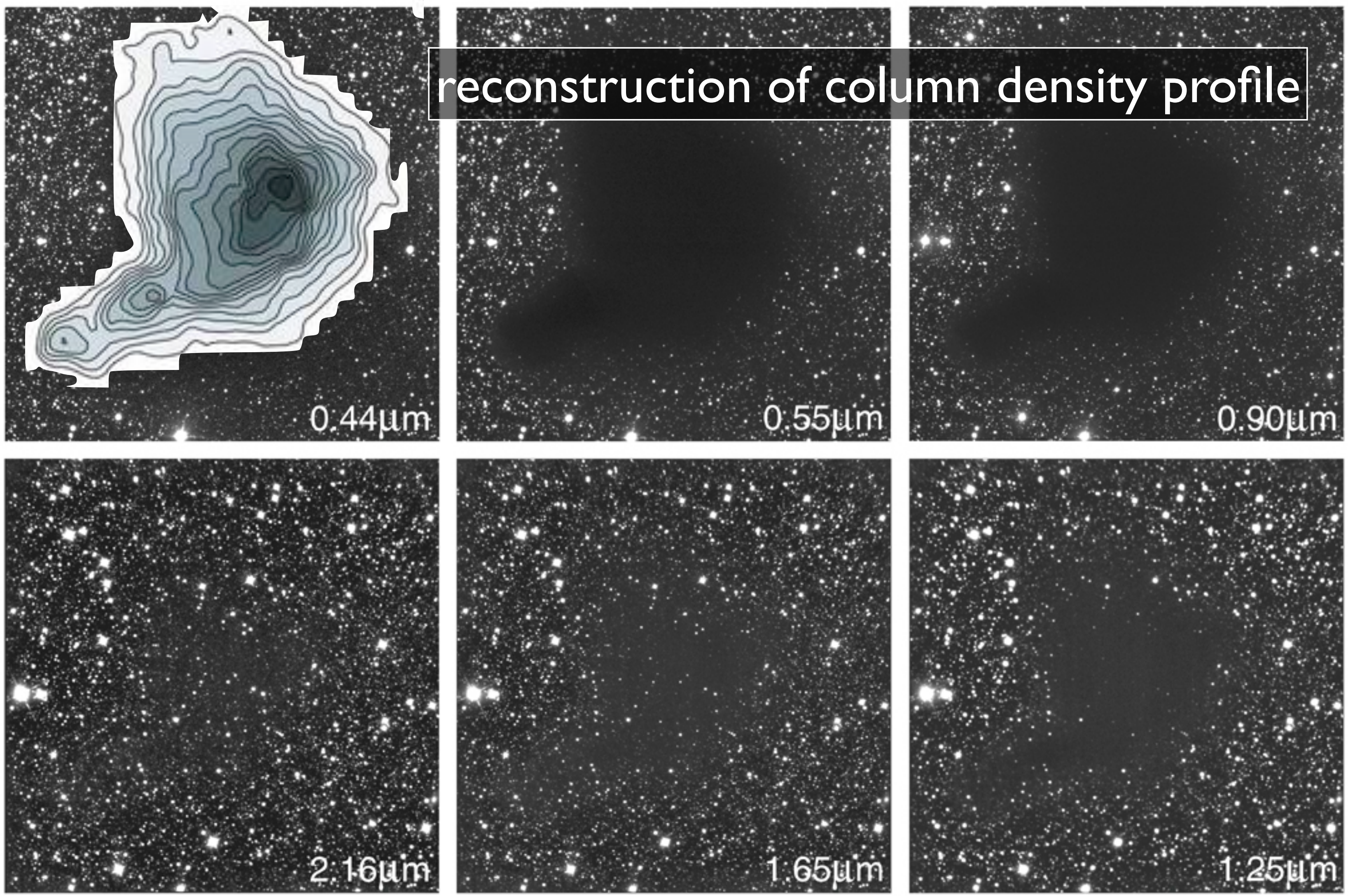

The Dark Cloud B68 at Different Wavelengths (NTT + SOFI)

ESO PR Photo 29b/99 (2 July 1999)

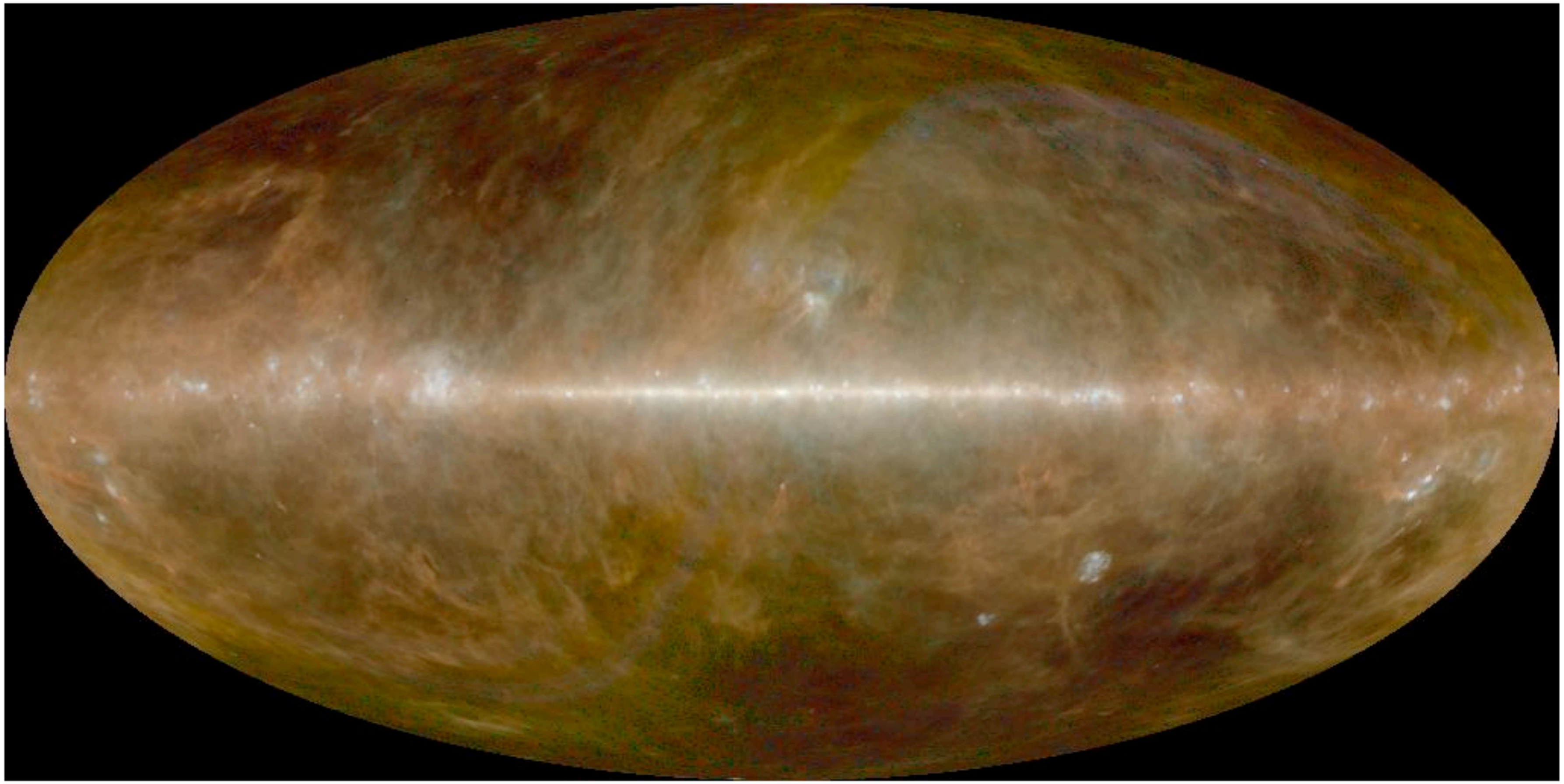

COBE Dirby results: Galactic foreground

DIRBE: Diffuse Infrared Background Experiment

atomic gas

Phases of interstellar matter

HI regions

Detection with 21cm line (1420 MHz, 6x10^{-6} eV))

Parallel spin (higher energy level) antiparallel spins (lower energy level)

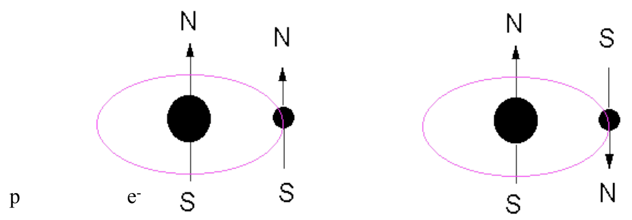

- Excitation by collisions (t_c ~ 500 yr)
- Deexcitation by radiation (t_r ~ 1x10^7 yr)
- (hyperfine structure transition)

Properties of HI gas

Galactic plane

mean density
n ~ 1 cm^{-3} (~1,7x10^{-18} g/cm^3)

envelope of MC's
cold clouds in disk
n ~ 10 ... 100 cm^{-3}
T_k > 100 K

matter
between clouds
n ~ 0,05 ... 0,2 cm^{-3}
T_k > 1000 K

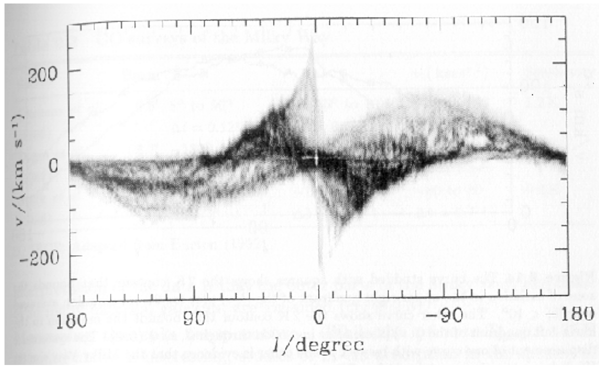

- forbidden transition
- n~1cm^{-3}, l~1pc~3x10^{18}cm, ¾ of atoms are excited
  → 10^{18} atoms cm^{-2} → t=10^{14}s → 10^4 transitions s^{-1}cm^{-2}pc^{-1}
- optically thin: $I_\nu = B_\nu \tau$~const. κ_ν~5.5x10^{-14} N_ν/T & B~T
- T dependence cancels → directly get cm^{-2} column NI

Radial velocity of 21cm radiation as function of galactic longitute (Leiden/Dwingeloo Survey)

molecular clouds

observing molecules

<u>*molecular Gas*</u>

H_2, CO, ...

transitions of two-atomic molecules

a) rotational transitions (needs dipole moment)

b) ro-vibrational transitions

c) electronic ro-vibrational transitions

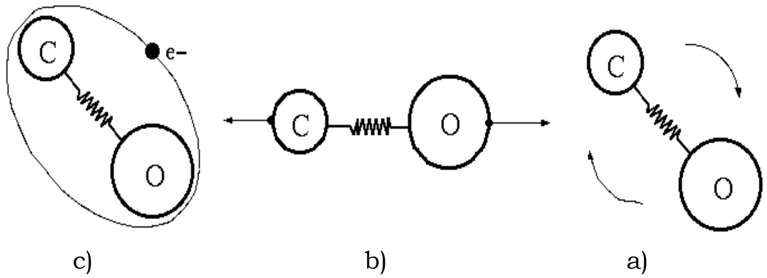

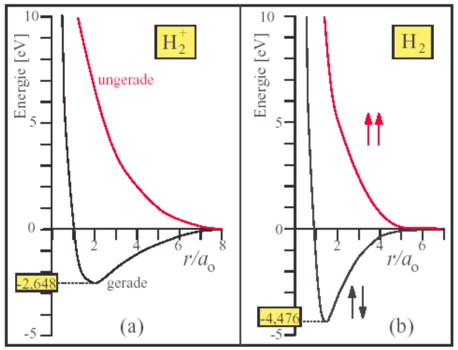

Abbildung 7.2: Energie von (a) H_2^+ (b) H_2 als Funktion des Abstands r der Kerne relativ zum Bohrschen Radius a_o.

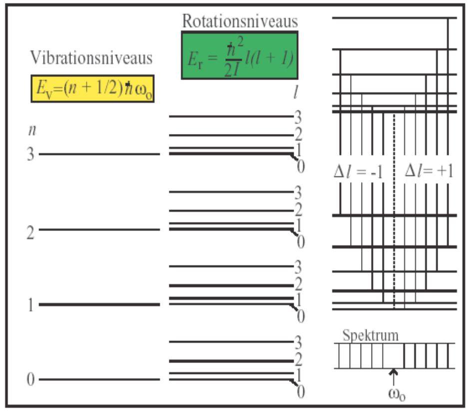

Abbildung 7.3: Rotations- und Vibrationsniveaus eines zweiatomigen Moleküls mit den nach den Auswahlregeln möglichen Übergängen.

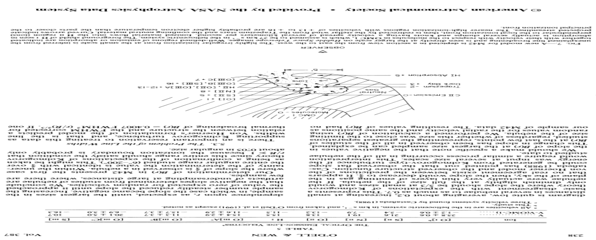

Niedrigste Rotations- und Schwingungsübergänge

	J = 1 – 0			n = 1 - 0		
	Frequenz	Wellenlänge	T	Frequenz	Wellenlänge	T
H_2	3,87 THz	77 µm	185 K	131 THz	2,28 µm	6300 K
^{12}CO	115 GHz	2,6 mm	5,5 K	64 THz	4,63 µm	3100 K

Phases of interstellar matter

Molecular Gas

Global properties of molecular clouds

	Temperature	Density	Radius	Mass	velocity gradient	E_{rot}/E_{pot}
diffuse molecular clouds (10 ... 50% of total H_2 mass)	T = 40 ... 80 K	n = 100 cm^{-3}				
Dark clouds/globules	T = 20 ... 40 K	n = 10^3 ... 10^4 cm^{-3}	R = 0,1 ... 5 pc	1 ... 10 $M_\odot$	0,5 ... 4 km/s/pc	10^{-3}... 0.3
Giant molecular clouds	T = 10 ... 50 K	n = 10^4 ... 10^6 cm^{-3}	R = 10 ... 100 pc	10^3 ... 10^6 $M_\odot$	0,1 ... 0,2 km/s/pc	10^{-4}... 0.1
Hot cores in MCs	T = 100 ... 300 K	n > 10^7 cm^{-3}	R < 0,1 pc	10 ... 100 $M_\odot$		

Giant molecular clouds are strongly concentrated in the galactic plane and towards the center of the Galaxy (similar holds for external galaxies)

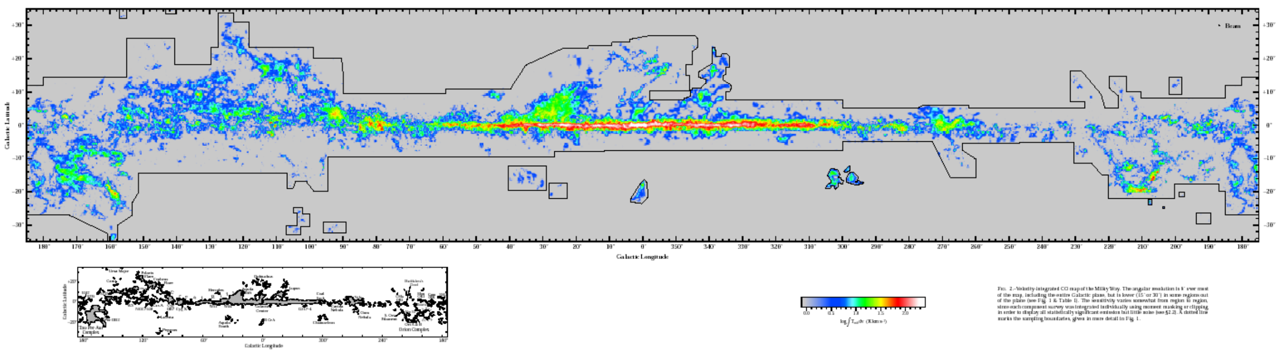

CO Survey of Milky Way
(Dame et al. 2001)

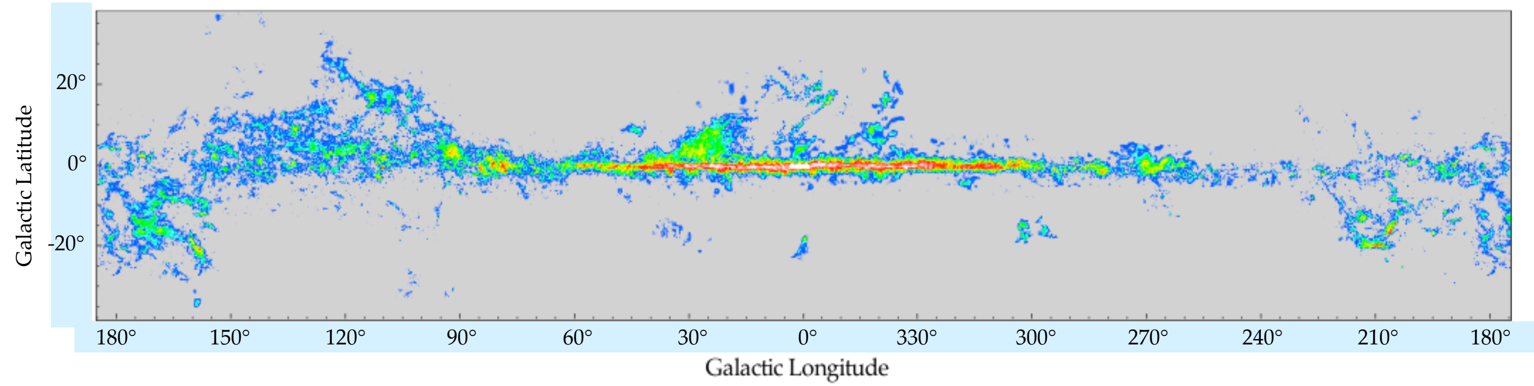

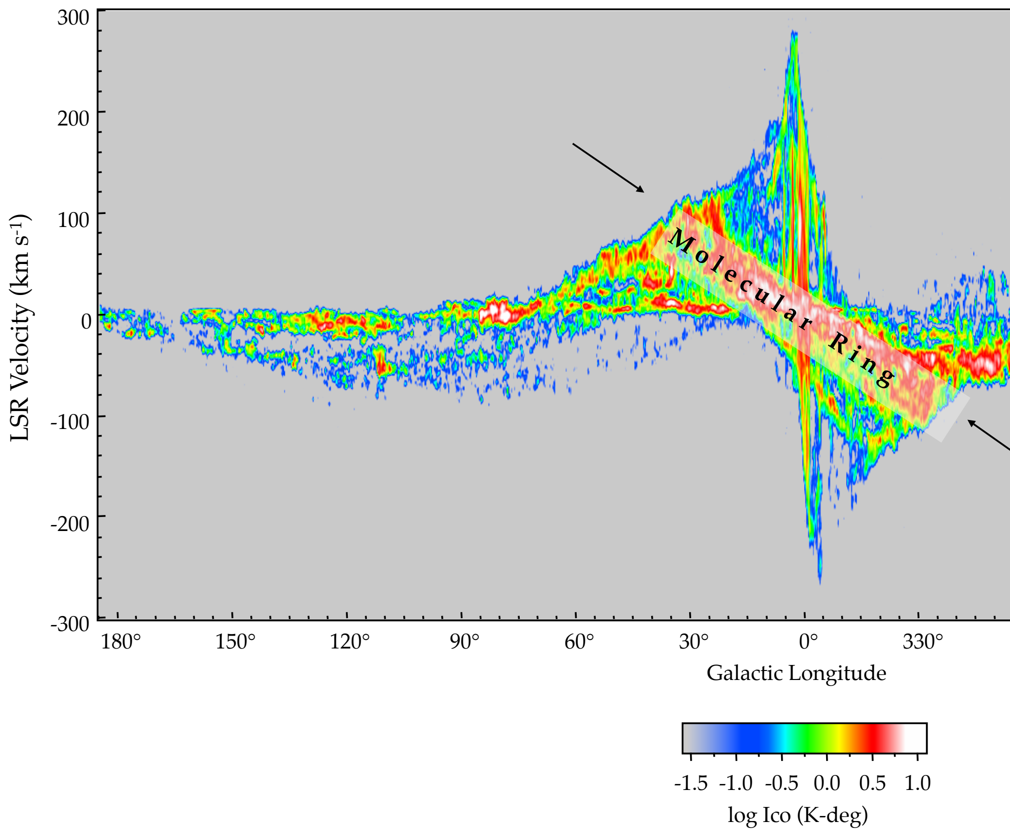

M_{tot} (H_2) ~ 2 x 10^9 M_o

M_{tot} (HI) ~ 6 x 10^9 M_o

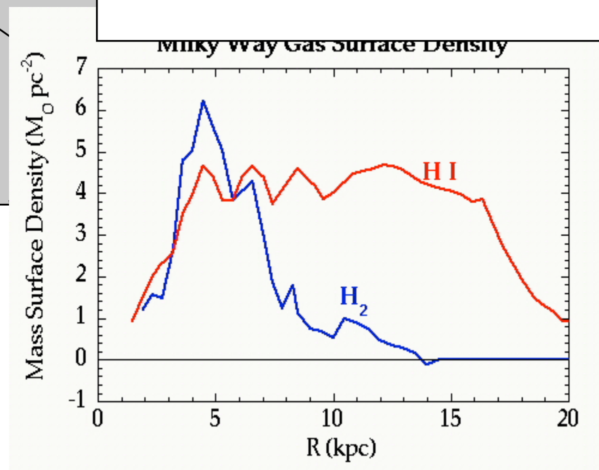

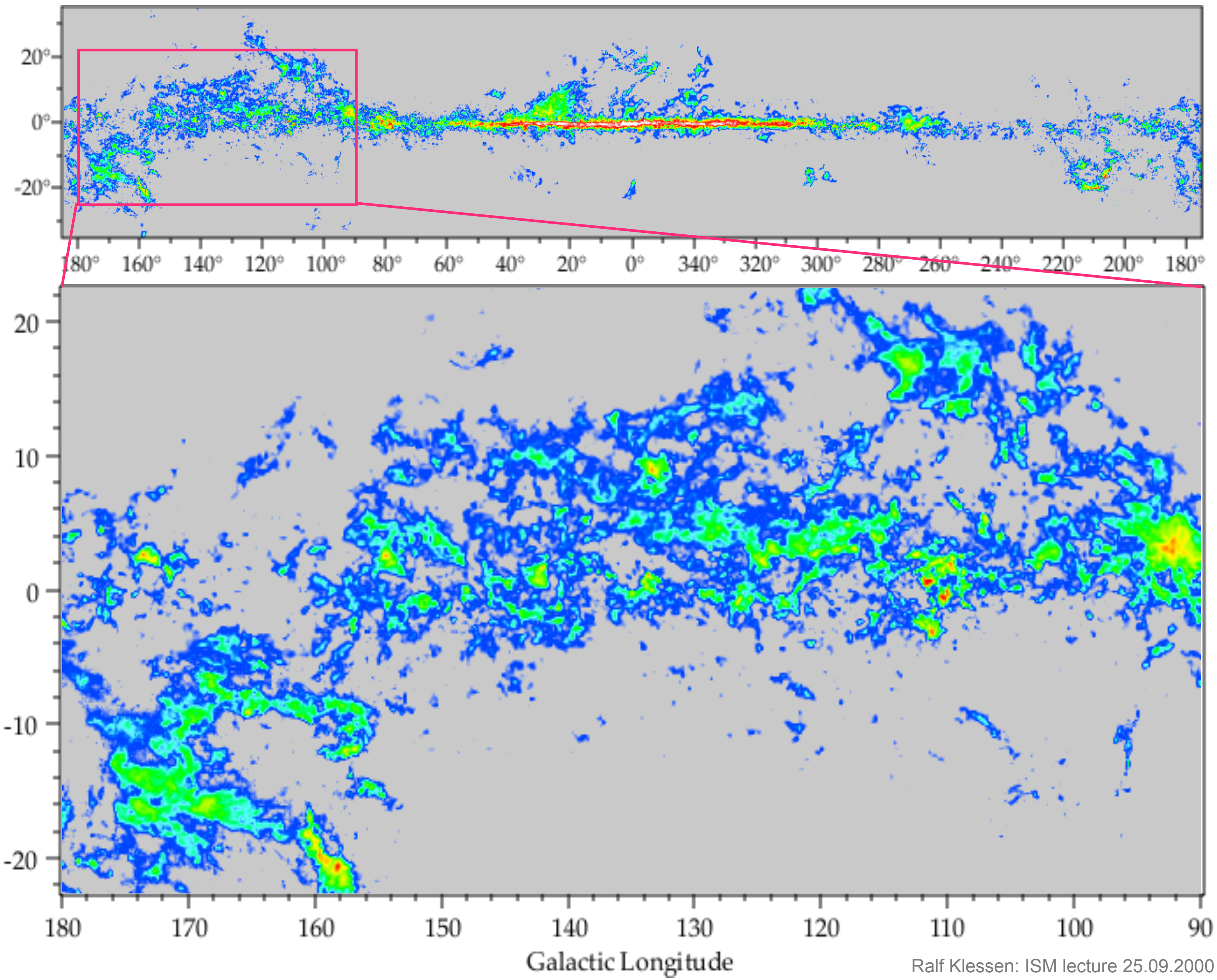

ata from Thomas Dame, CfA Harvard

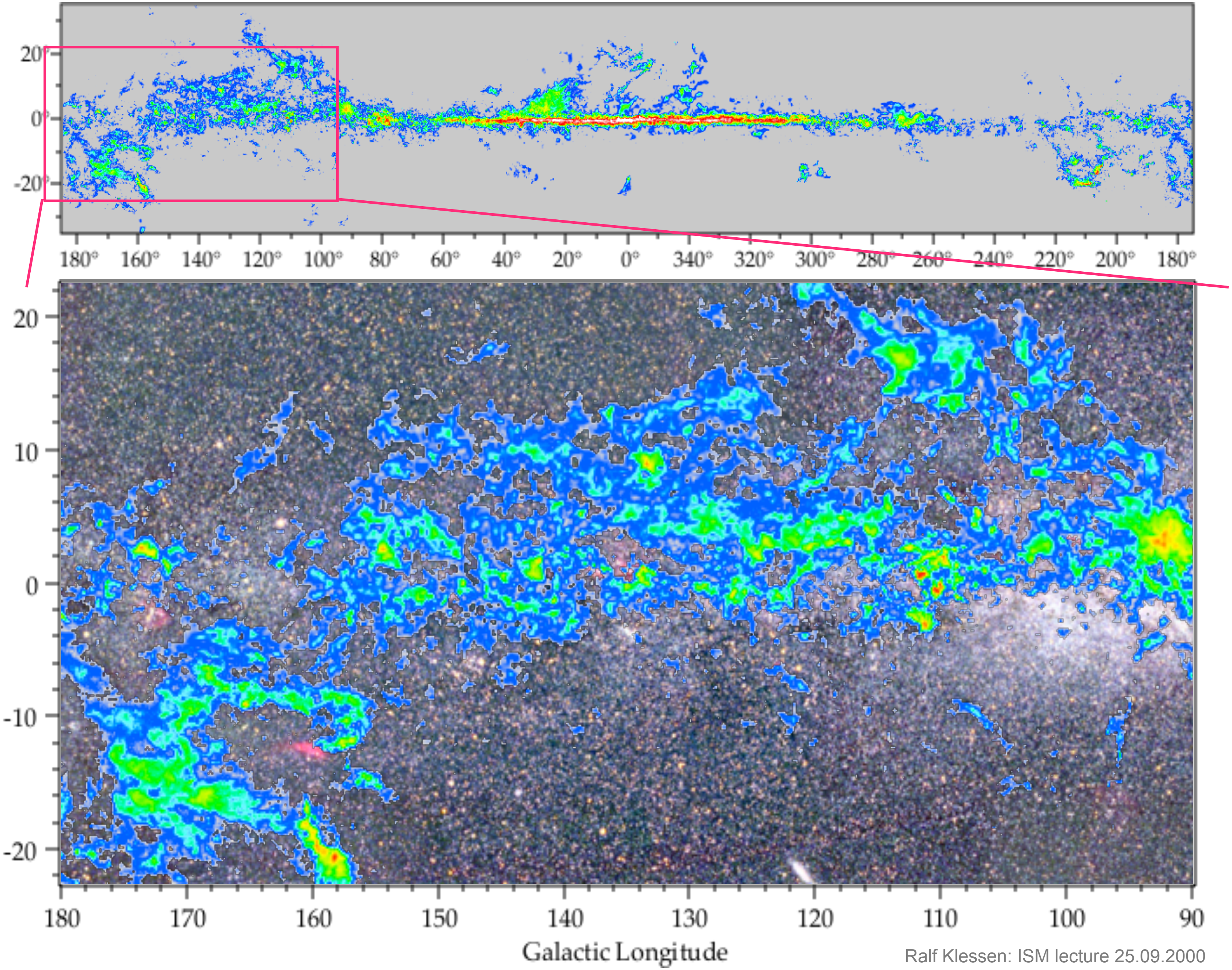

ata from Thomas Dame, CfA Harvard

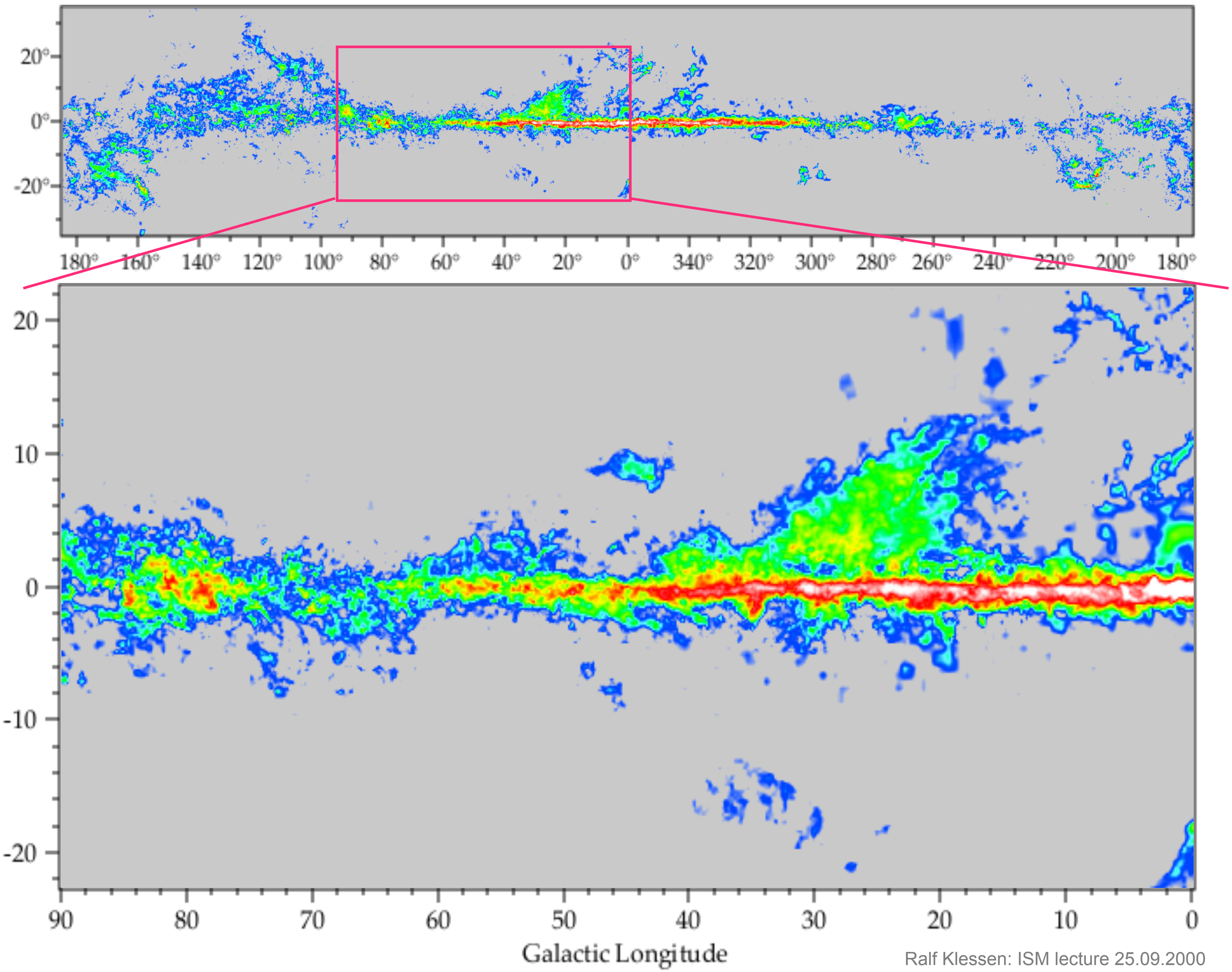

ata from Thomas Dame, CfA Harvard

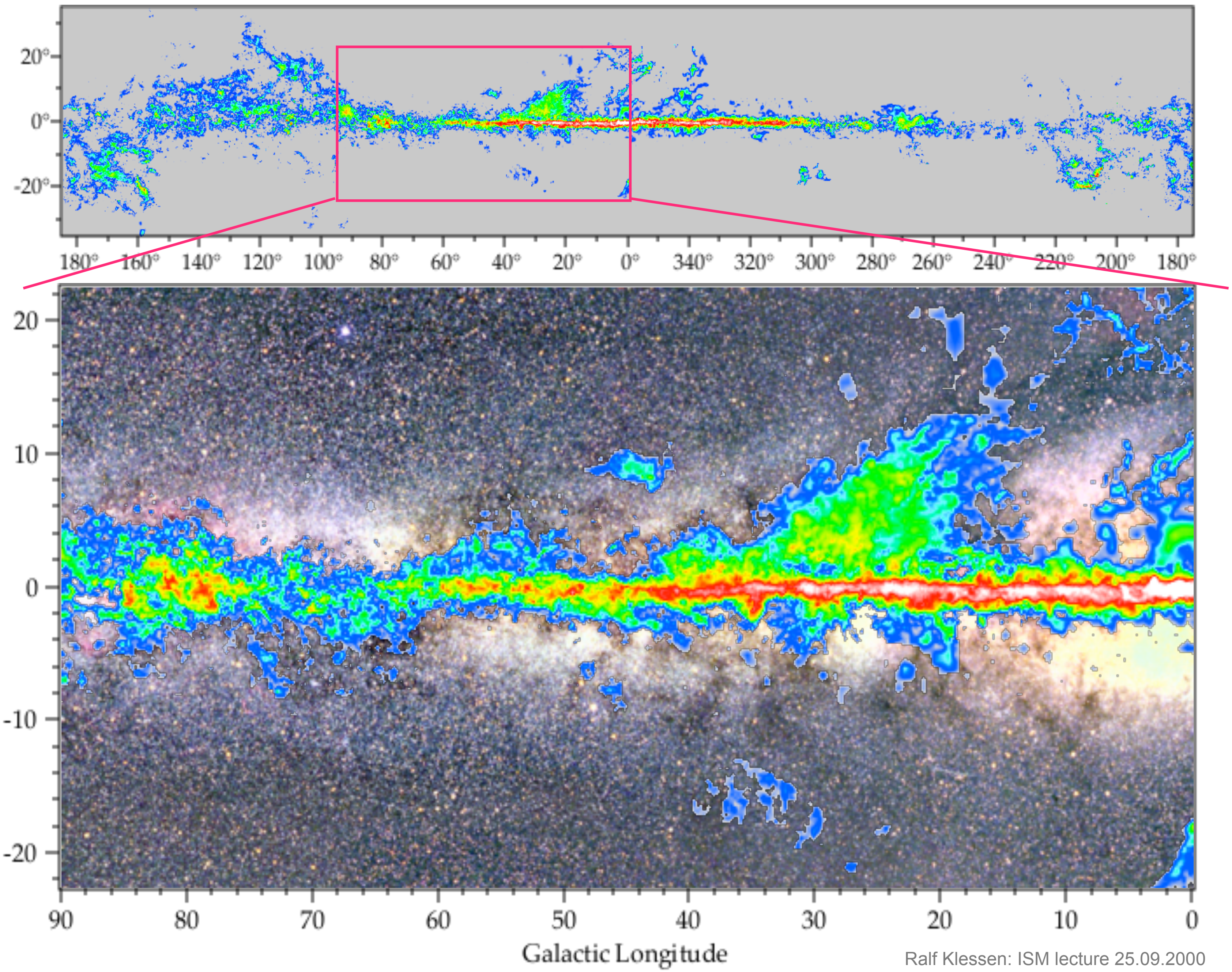

ata from Thomas Dame, CfA Harvard

ata from Thomas Dame, CfA Harvard

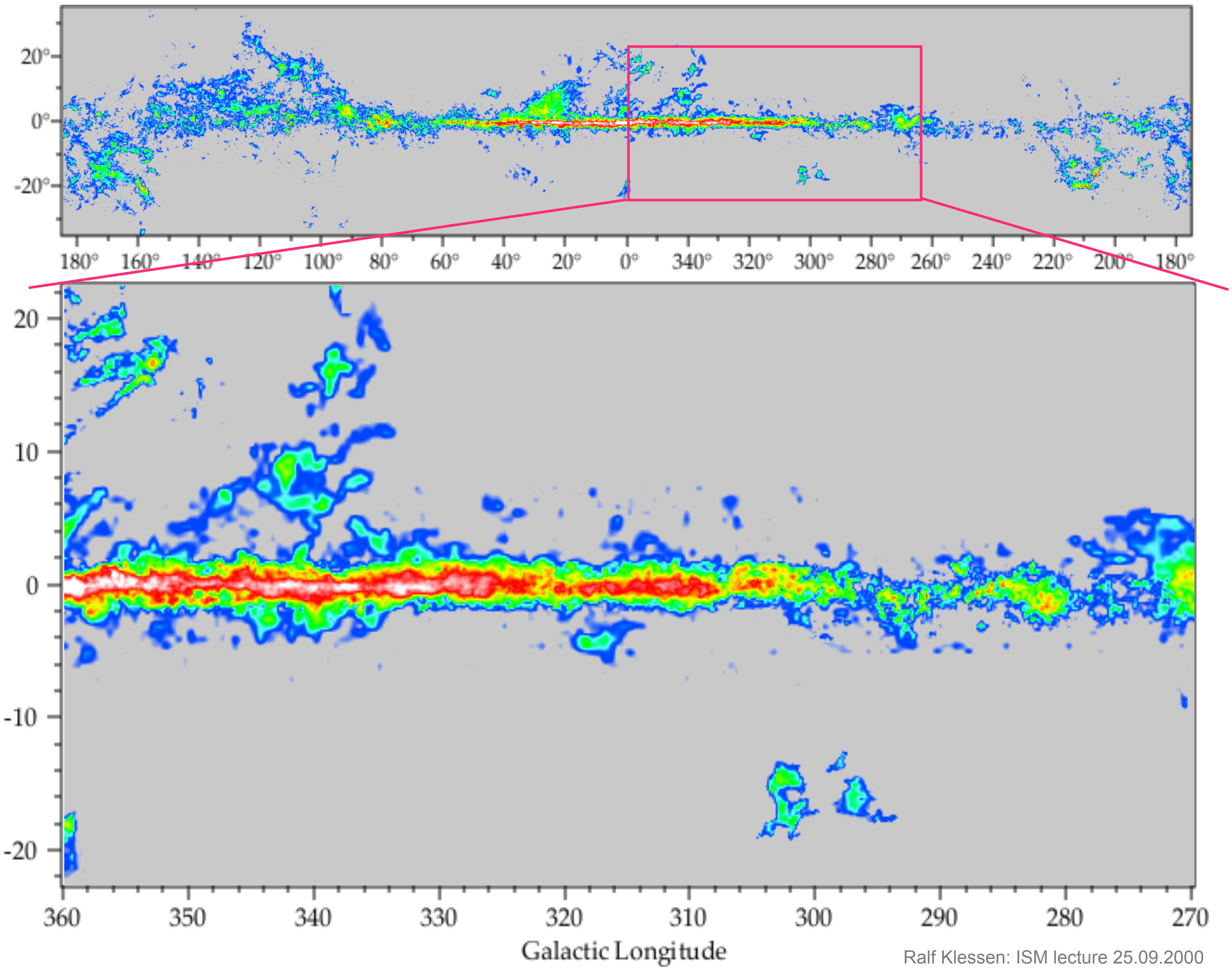

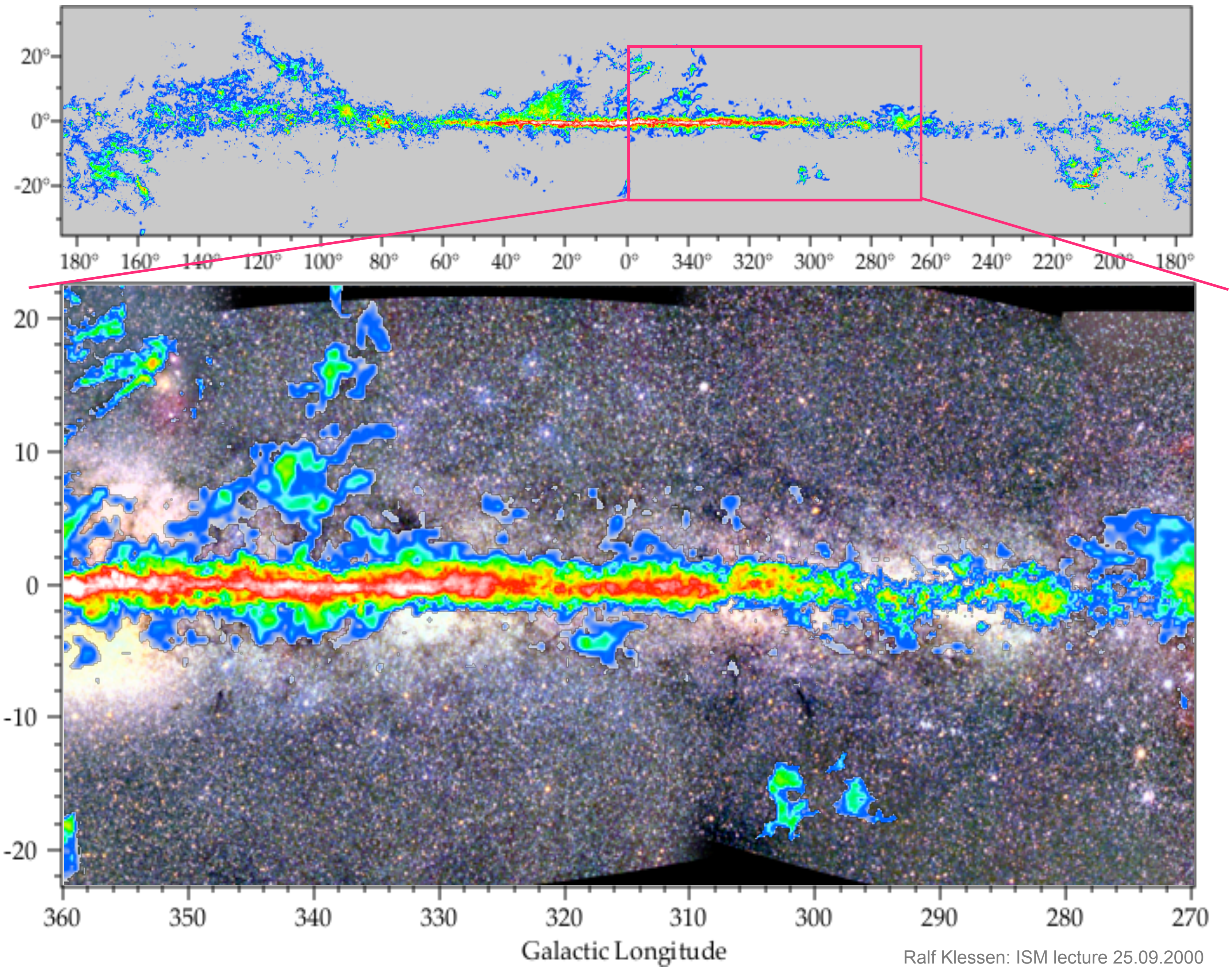

ata from Thomas Dame, CfA Harvard

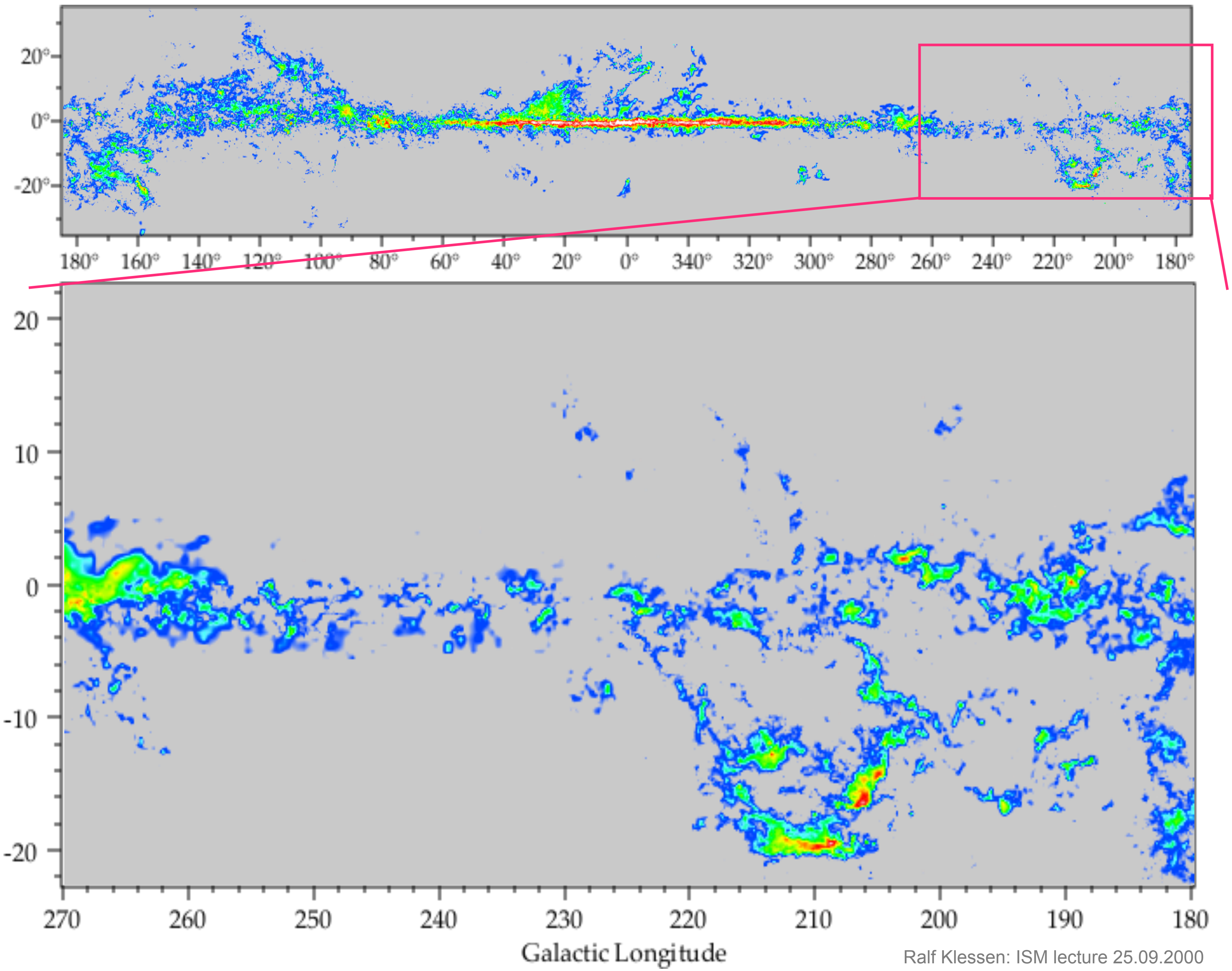

ata from Thomas Dame, CfA Harvard

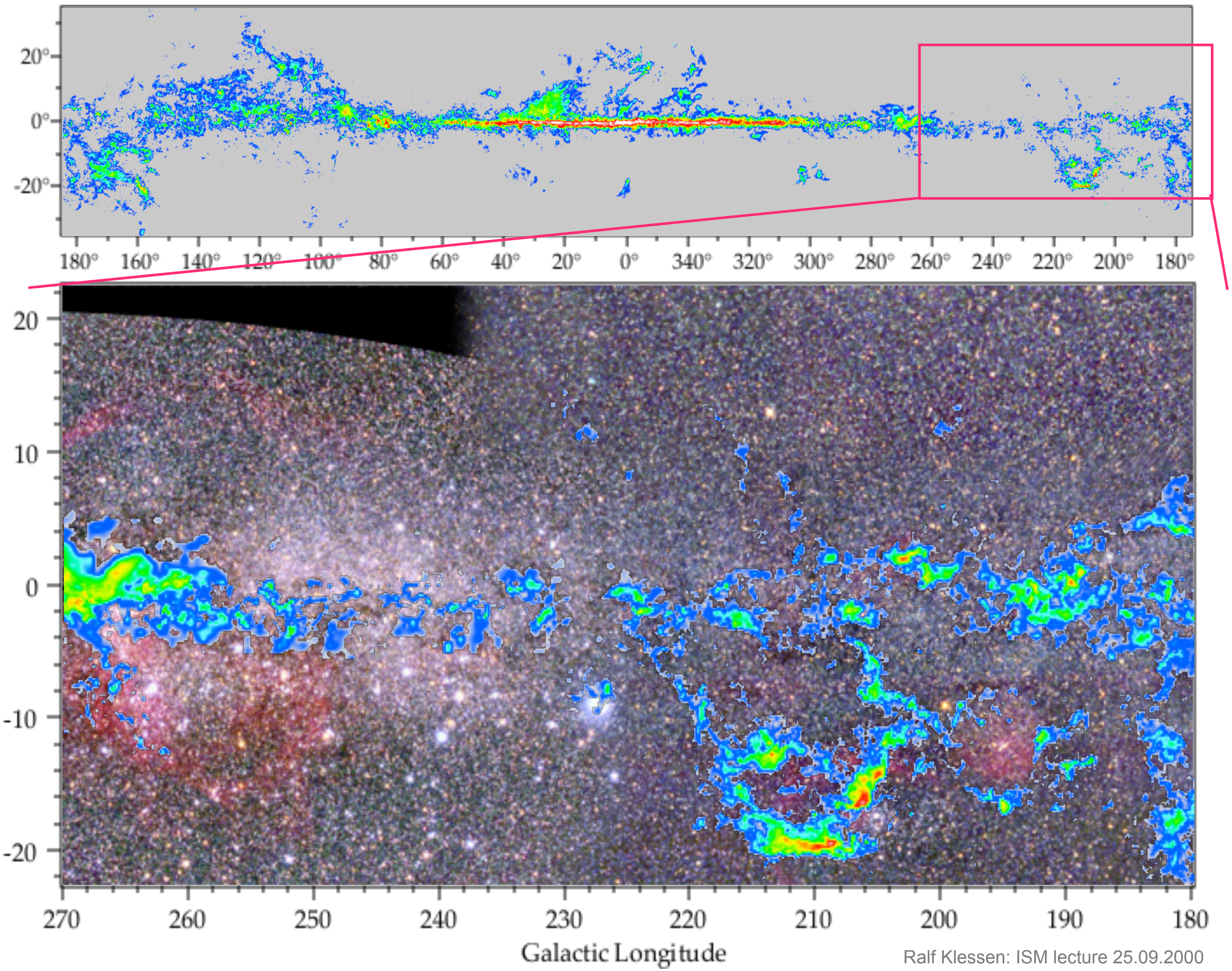

ata from Thomas Dame, CfA Harvard

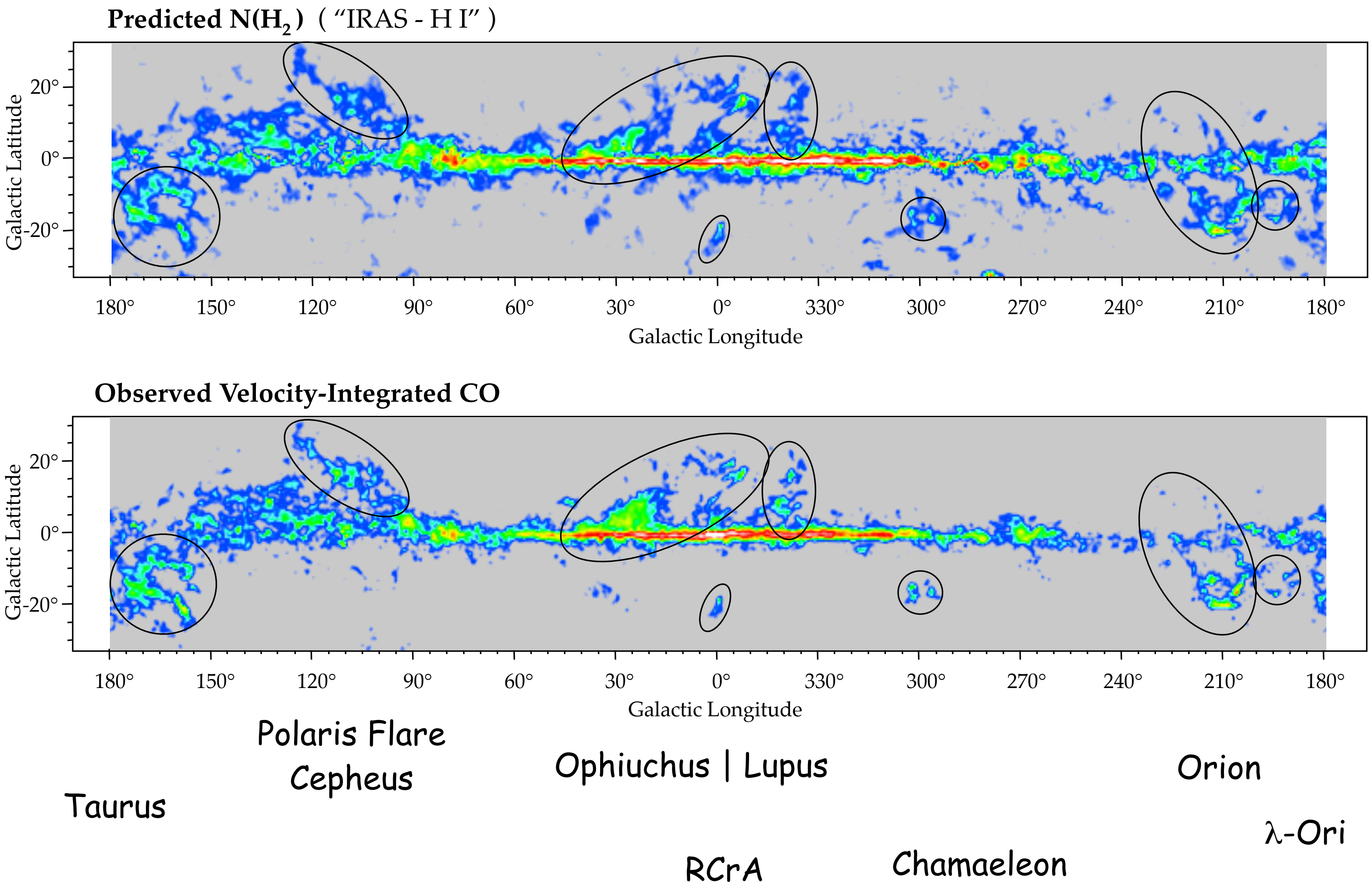

ata from Thomas Dame, CfA Harvard

nearby molecular clouds

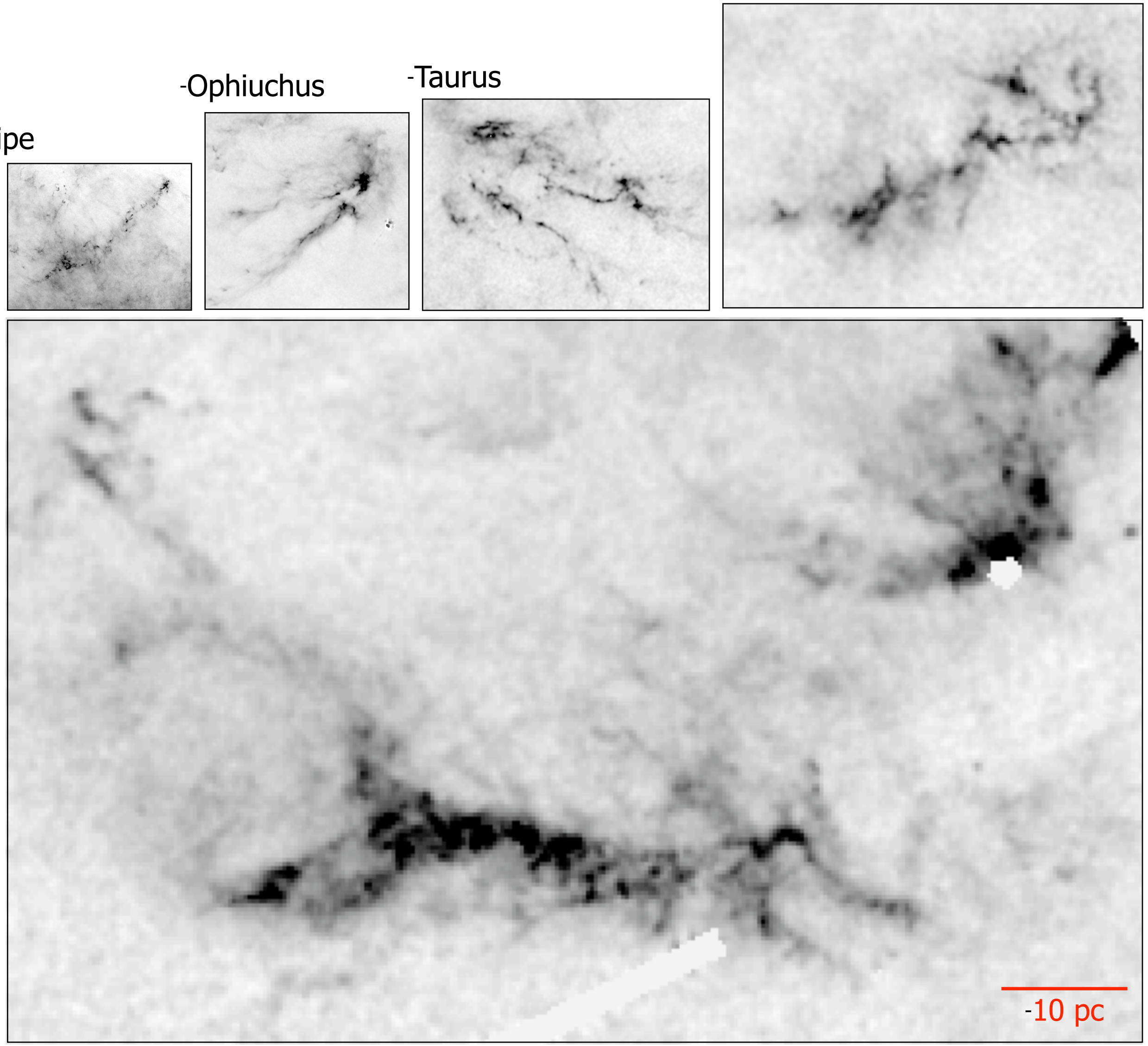

scales to same scale

(from A. Goodman)

nearby molecular clouds

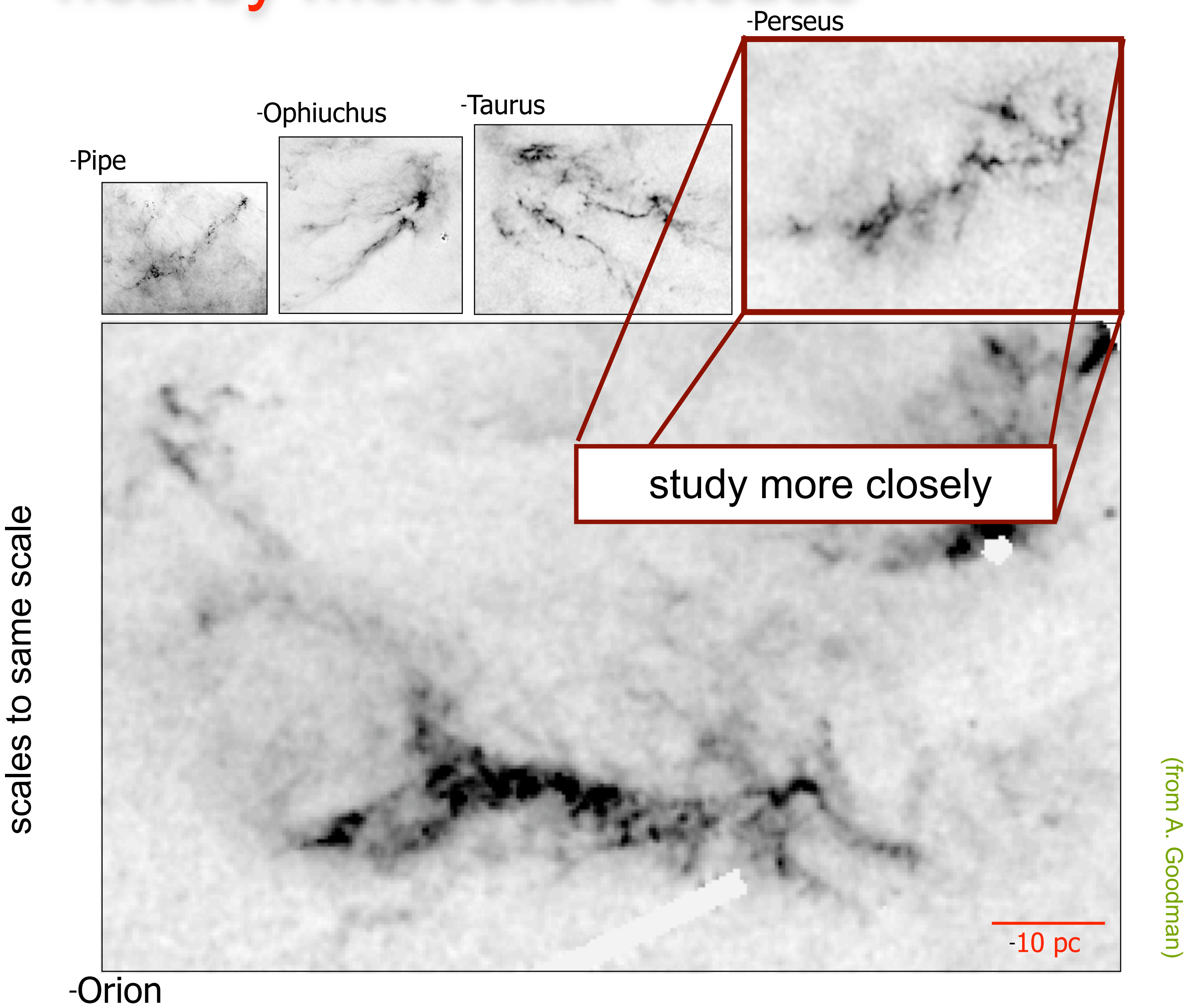

COMPLETE = COordinated Molecular Probe Line Extinction Thermal Emission Survey of Star-Forming Regions

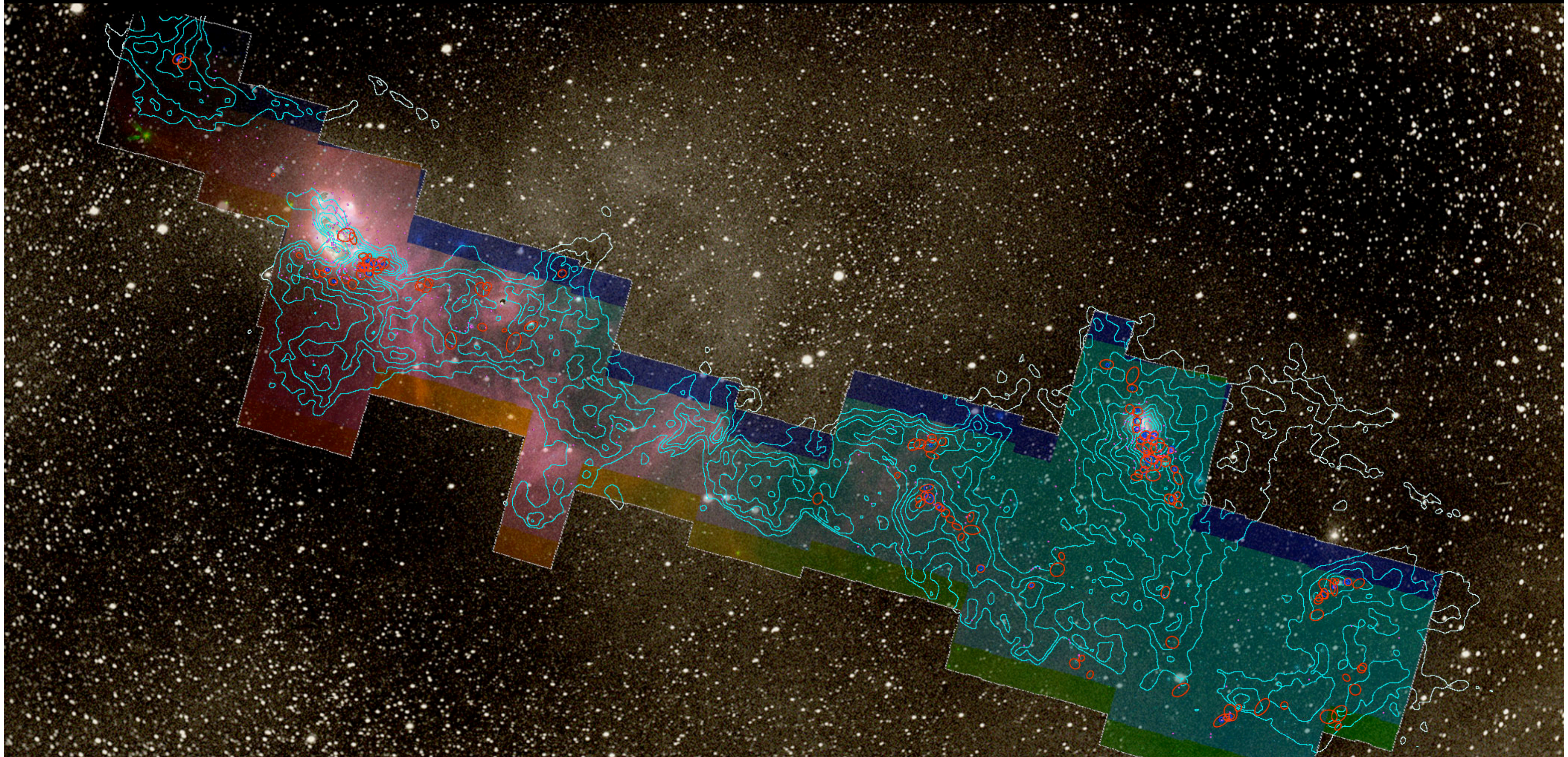

COMPLETE Collaborators, Summer 2008:

Alyssa A. Goodman (CfA/IIC)
João Alves (Calar Alto, Spain)
Héctor Arce (Yale)
Michelle Borkin (IIC)
Paola Caselli (Leeds, UK)
James DiFrancesco (HIA, Canada)
Jonathan Foster (CfA, PhD Student)
Katherine Guenthner (CfA/Leipzig)
Mark Heyer (UMASS/FCRAO)
Doug Johnstone (HIA, Canada)
Jens Kauffmann (CfA/IIC)
Helen Kirk (HIA, Canada)
Di Li (JPL)
Jaime Pineda (CfA, PhD Student)
Erik Rosolowsky (UBC Okanagan)
Rahul Shetty (CfA)
Scott Schnee (Caltech)
Mario Tafalla (OAN, Spain)

molecular clouds

- high-density regions in the ISM
- consist mostly of H_2
- cold
- extremely complex velocity and density structure (turbulence, fractal dimension?)
- all stars form in molecular clouds
- mass spectrum $dN/dM \sim M^{-2}$

molecular cloud formation

molecular cloud formation

- star formation on galactic scales
  → requires understanding of
  formation of molecular clouds
- questions
  - *where* and *when* do molecular clouds form?
  - *what* are their properties?
  - *how* do stars form in their interior?
  - global correlations? → *Schmidt law*

molecular cloud formation

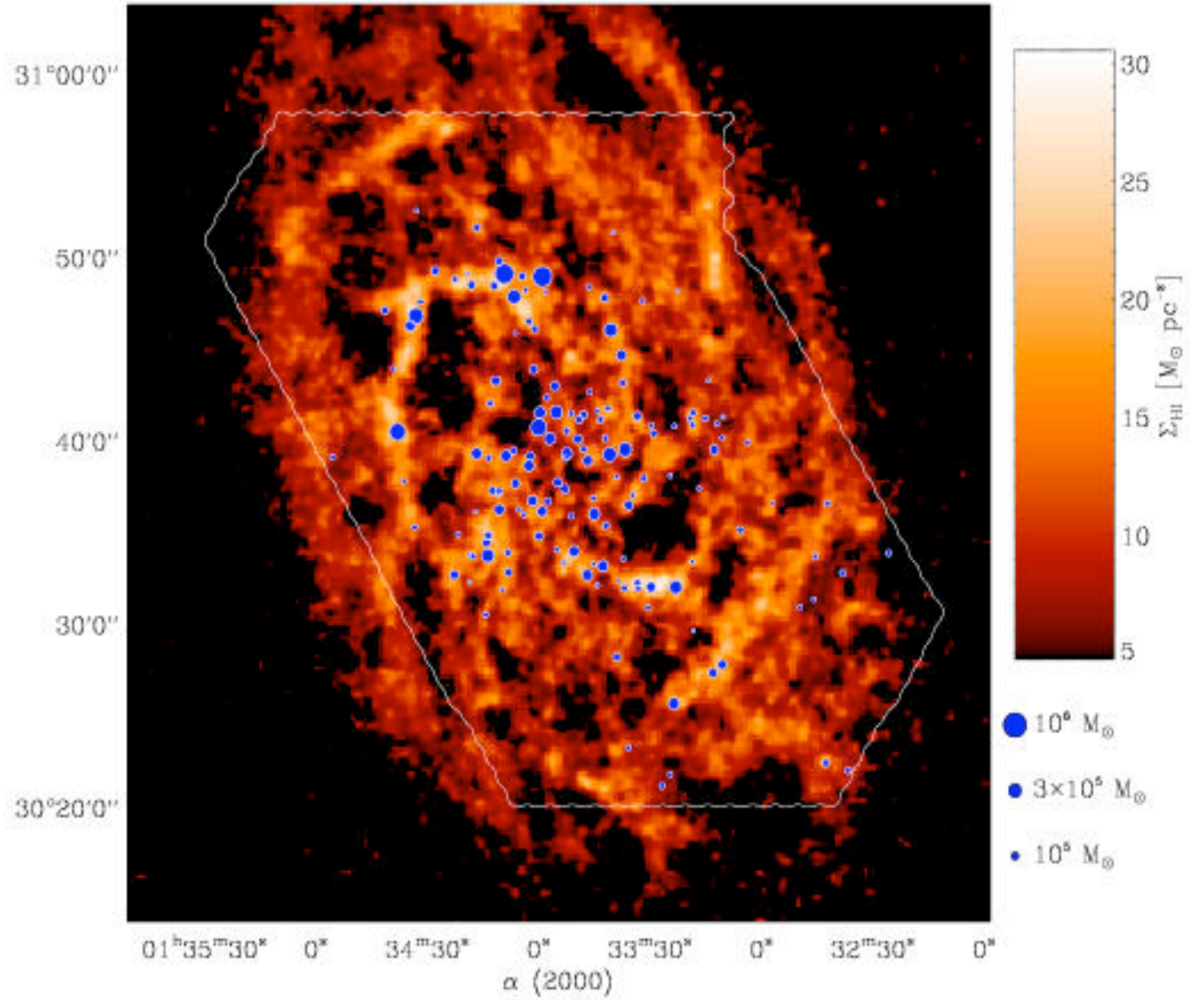

Thesis:

Molecular clouds form at *stagnation points* of large-scale convergent flows, mostly triggered by global (or external) perturbations.

(Deul & van der Hulst 1987, Blitz et al. 2004)

correlation with large-scale perturbations

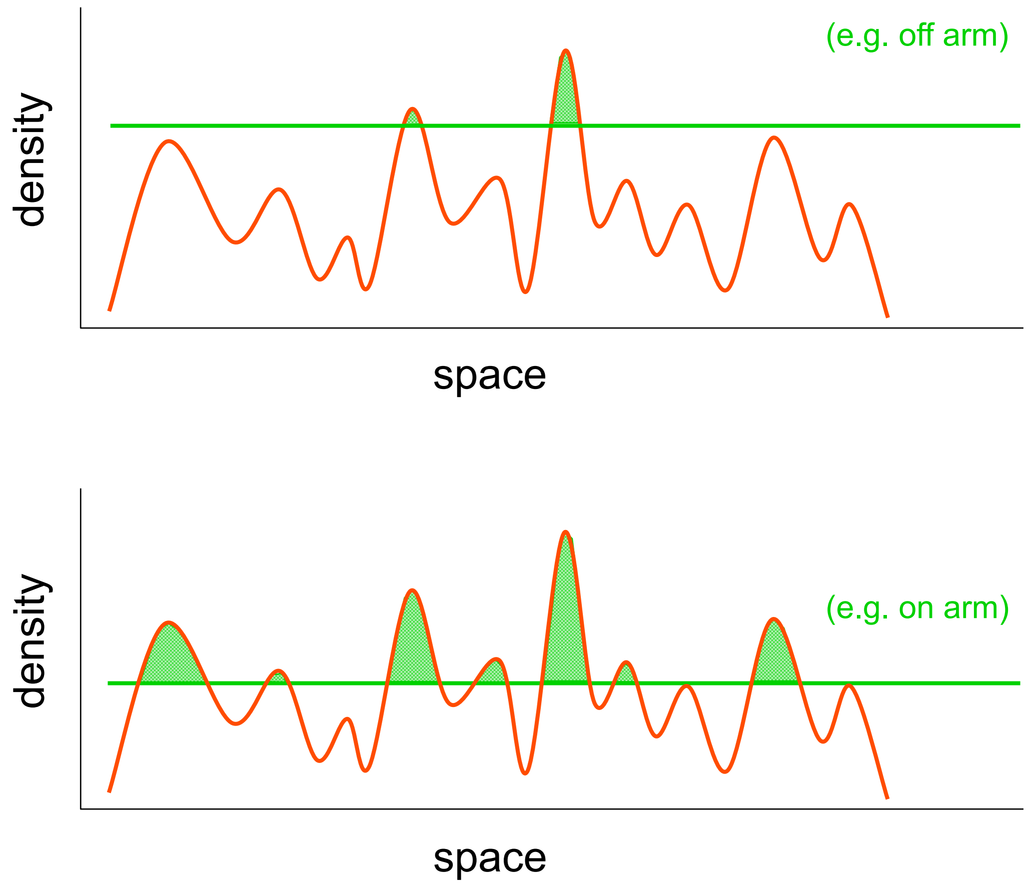

density/temperature fluctuations in warm atomar ISM are caused by *thermal/ gravitational instability* and/ or *supersonic turbulence*

some fluctuations are *dense* enough to *form H_2* within "*reasonable time*"
→ *molecular cloud*

external perturbuations (i.e. potential changes) *increase* likelihood

star formation on *global* scales

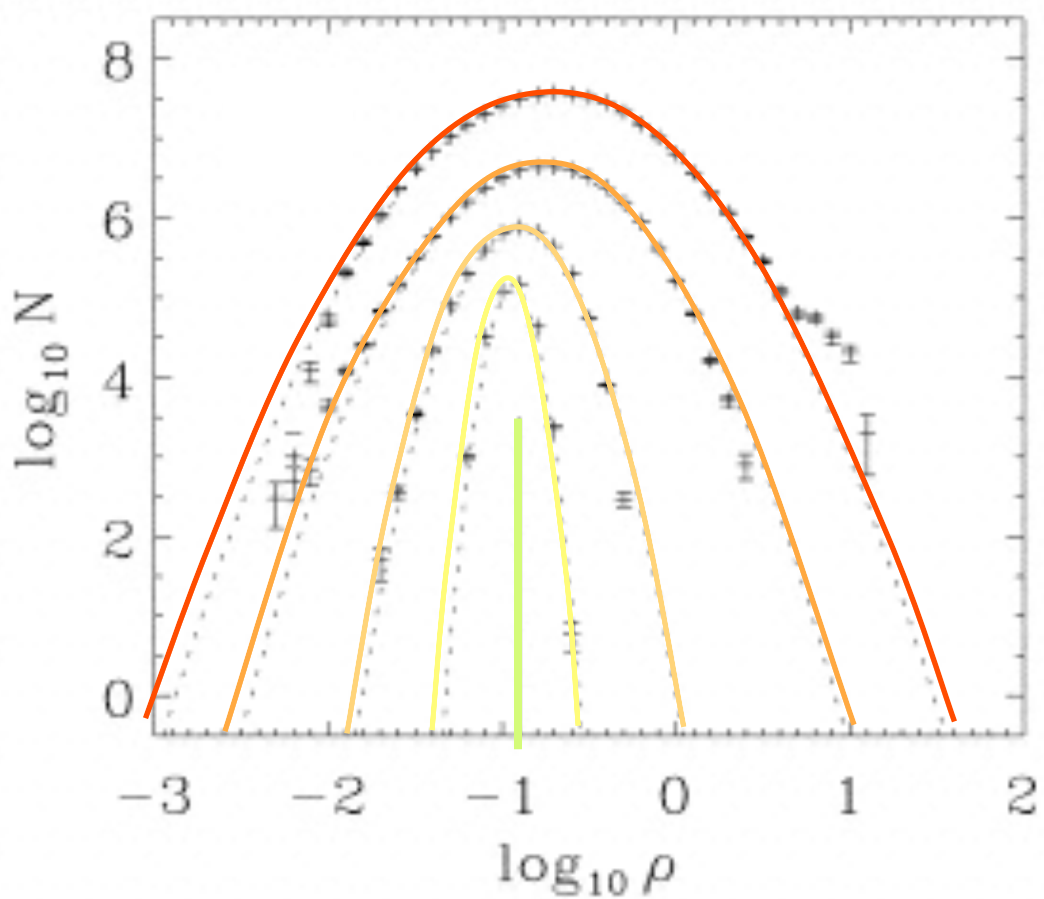

probability distribution function of the density (*ρ-pdf)*

varying rms Mach numbers:

M1 > M2 > M3 > M4 > 0

mass weighted ρ-pdf, each shifted by ΔlogN=1

(from Klessen, 2001; also Gazol et al. 2005, Krumholz & McKee 2005, Glover & Mac Low 2007ab)

star formation on *global* scales

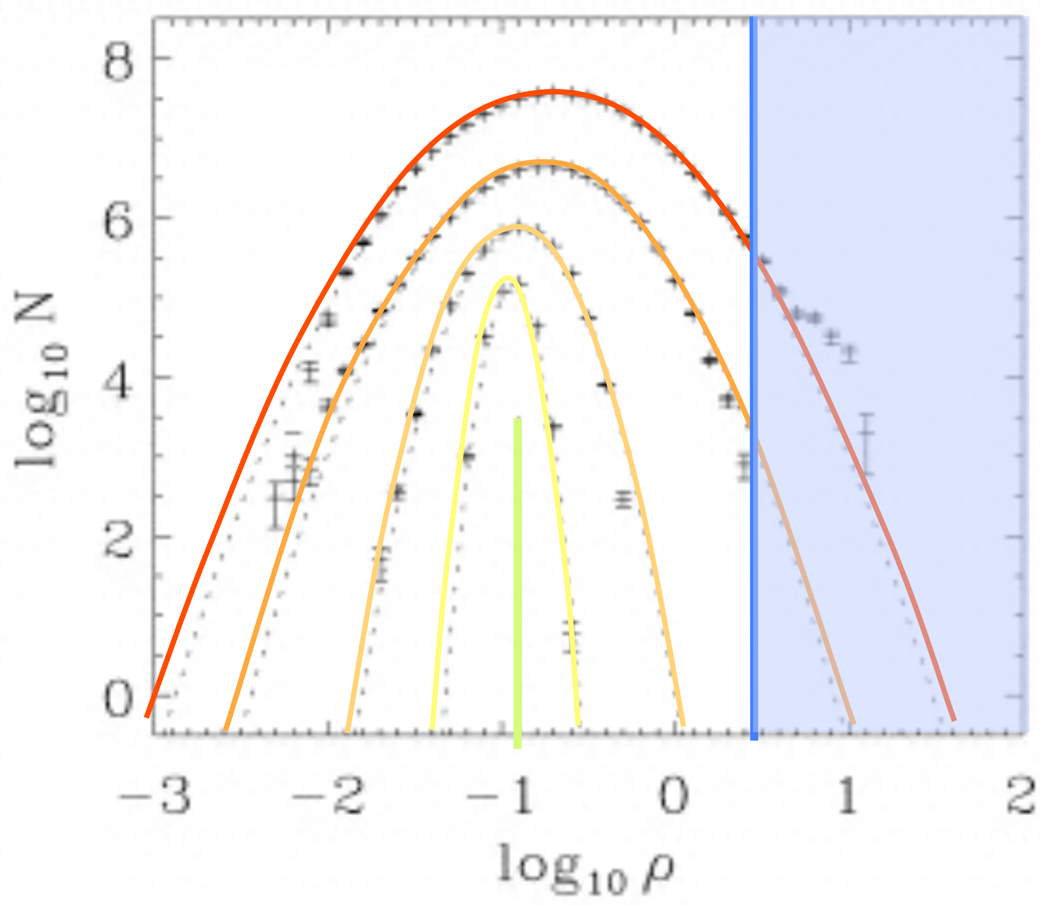

mass weighted ρ-pdf, each shifted by ΔlogN=1

(rate from Hollenback, Werner, & Salpeter 1971)

H_2 formation rate:

$$\tau_{H_2} \approx \frac{1.5\,\mathrm{Gyr}}{n_H / 1\mathrm{cm}^{-3}}$$

for $n_H \geq 100$ cm^{-3}, H_2 forms within 10 Myr, this is about the lifetime of typical MC's.

in turbulent gas, the H_2 fraction can become very high on short timescale

(for models with coupling between cloud dynamics and time-dependent chemistry, see Glover & Mac Low 2007a,b)

star formation on *global* scales

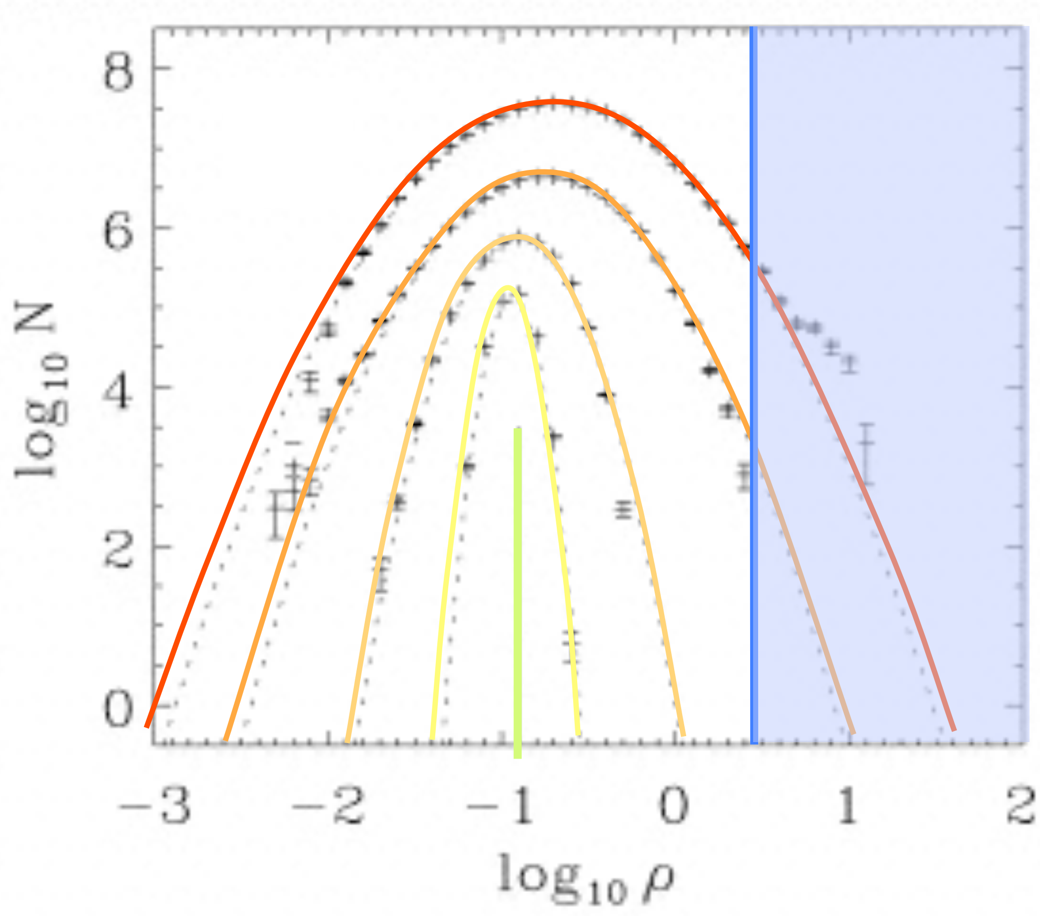

mass weighted ρ-pdf, each shifted by ΔlogN=1

(rate from Hollenback, Werner, & Salpeter 1971)

BUT: *it doesn't work* (at least not so easy):

Chemistry has a memory effect!

H2 forms more quickly in high-density regions as it gets destroyed in low-density parts.

(for models with coupling between cloud dynamics and time-dependent chemistry, see Glover & Mac Low 2007a,b)

modeling galactic SF

SPH calculations of self-gravitating disks of stars and (isothermal) gas in dark-matter potential, sink particles measure local collapse --> star formation

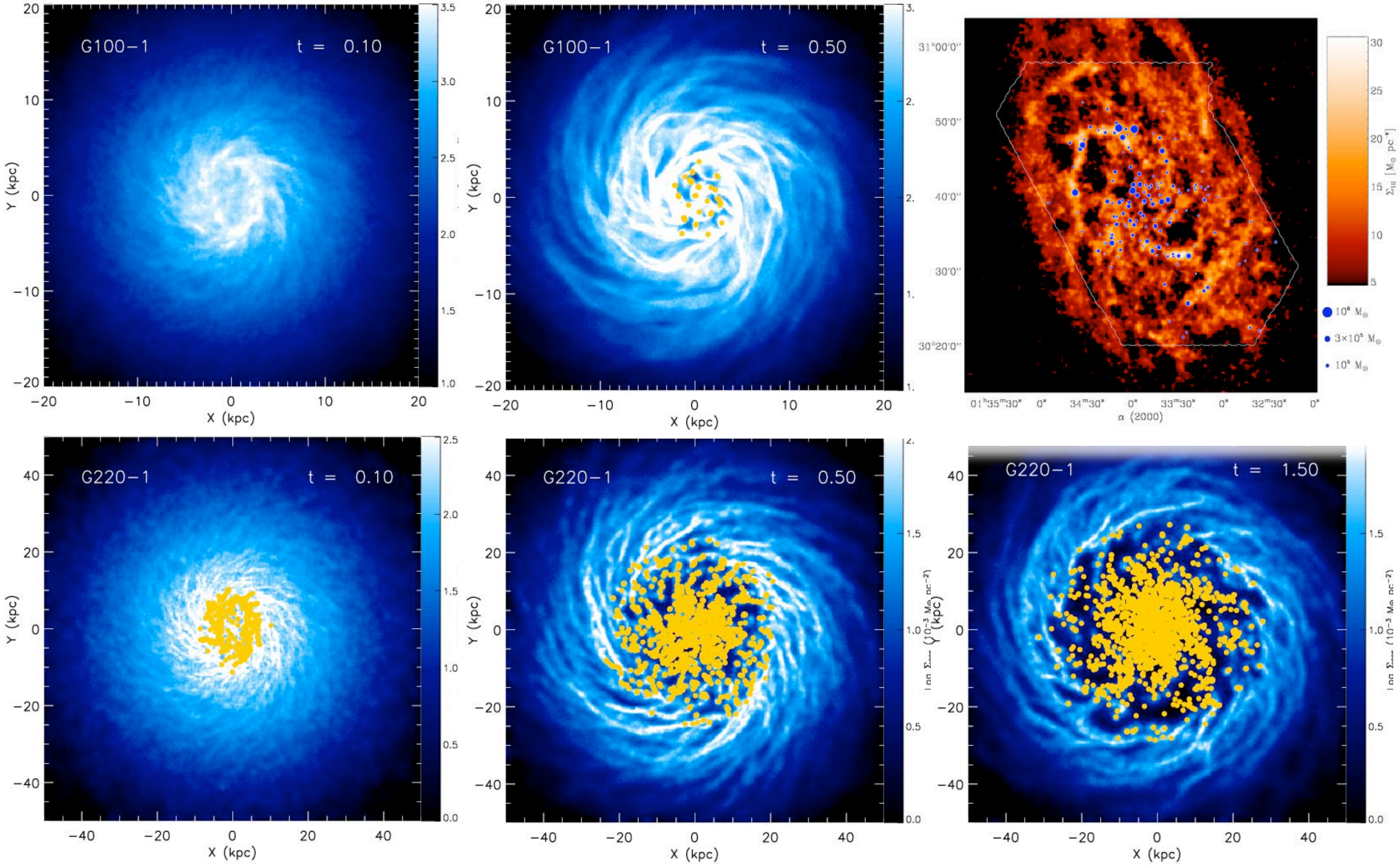

(Li, Mac Low, & Klessen, 2005, ApJ, 620,L19 - L22)

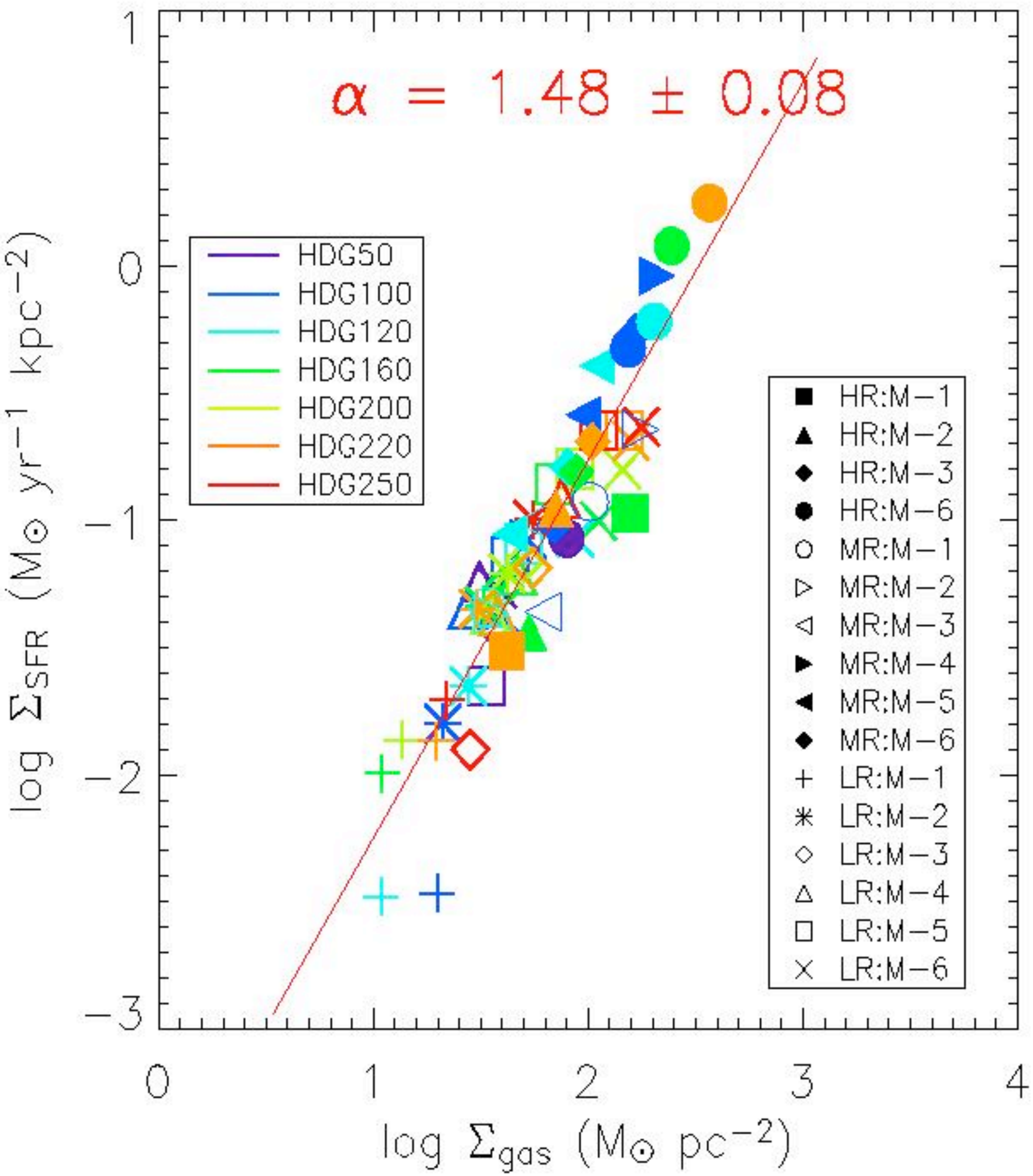

(Li, Mac Low, & Klessen, 2005, ApJ, 620, L19 - L22)

We find correlation between *star formation rate* and *gas surface density:*

$$\Sigma_{\mathrm{SFR}} \propto \Sigma_{\mathrm{gas}}^{1.5}$$

global Schmidt law

observed Schmidt law

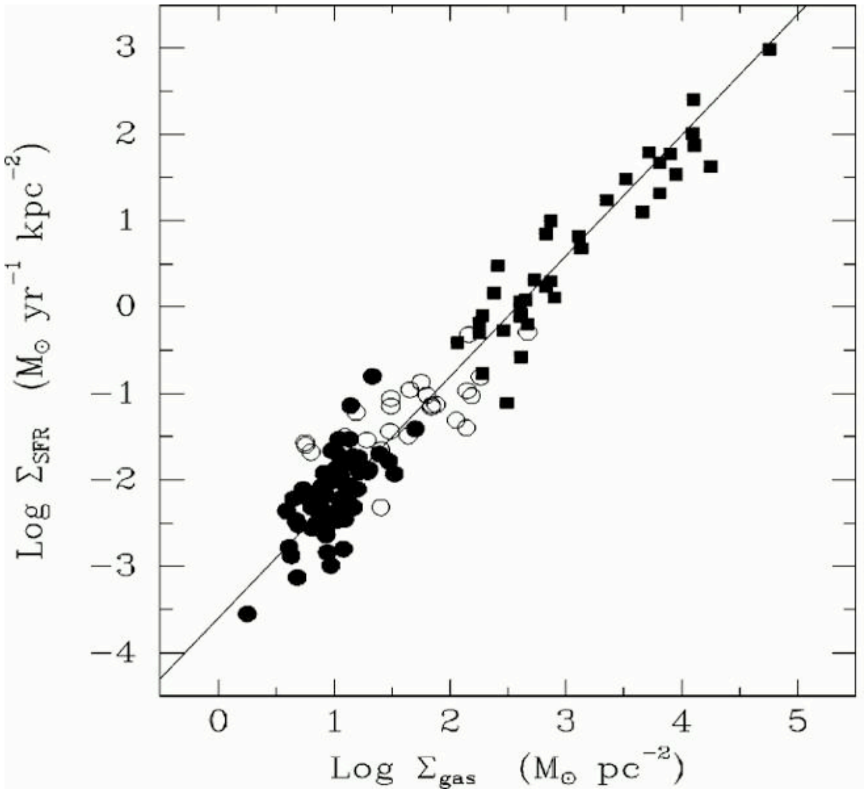

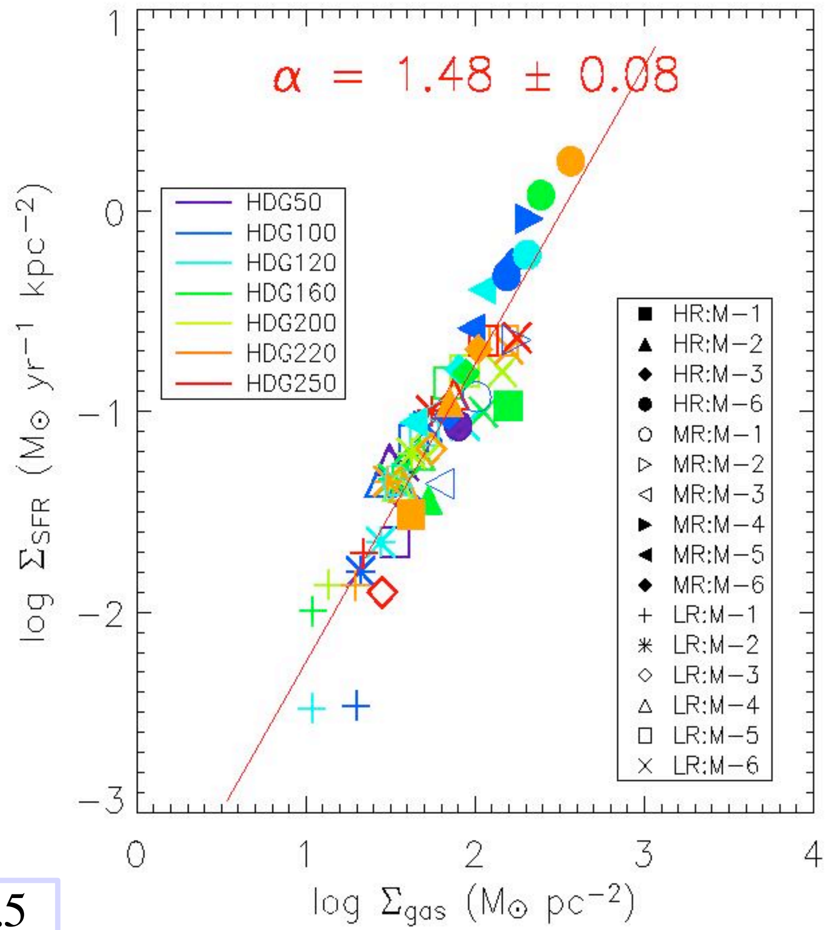

in both cases: $\Sigma_{SFR} \propto \Sigma_{gas}^{1.5}$

(from Kennicutt 1998)

local Schmidt law

Gravity only:
Local Schmidt law exhibits downturn!
Global one does not.

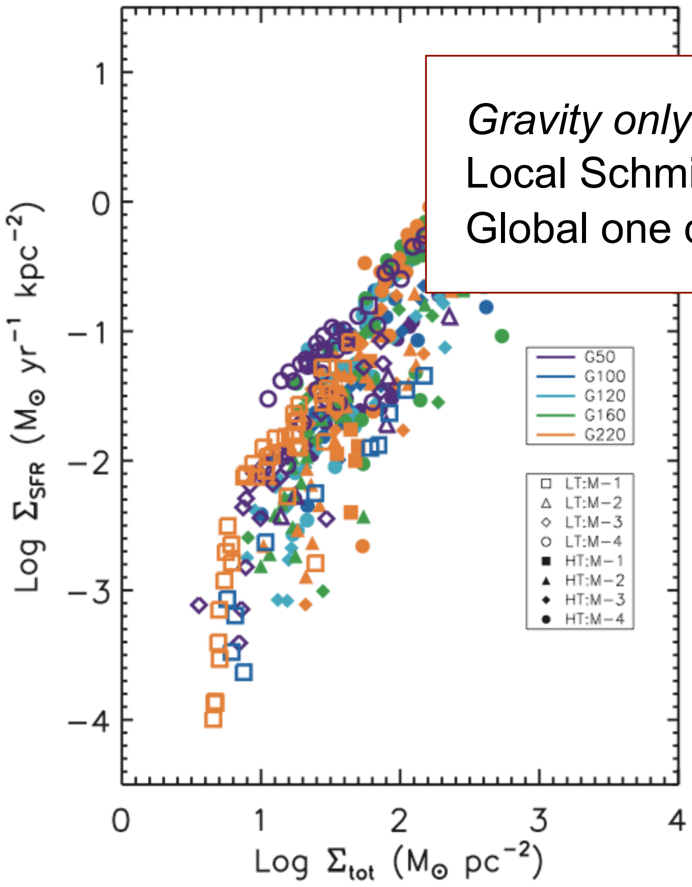

FIG. 11.—Local Schmidt laws of all models with $\tau_{SF} < 3$ Gyr. The legends are the same as in Fig. 5: the color of the symbol indicates the rotational velocity for each model as given in Table 1, the shape indicates the submodel classified by gas fraction, and open and filled symbols represent low- and high-T models, respectively.

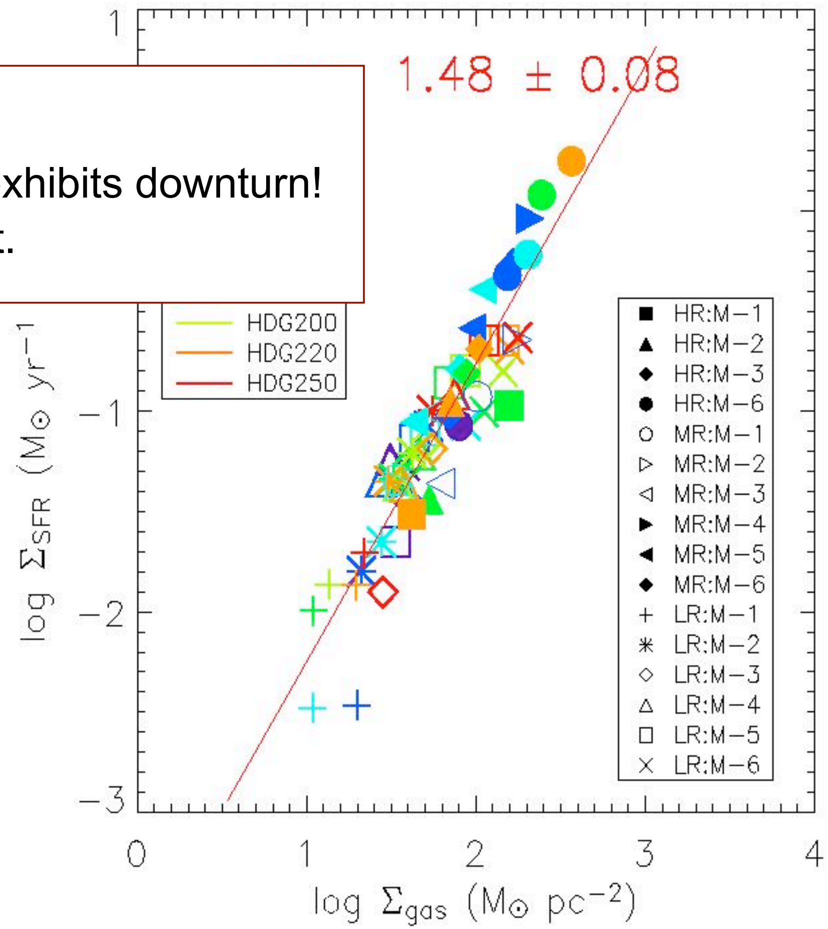

(Li et al. 2006)

molecular cloud formation

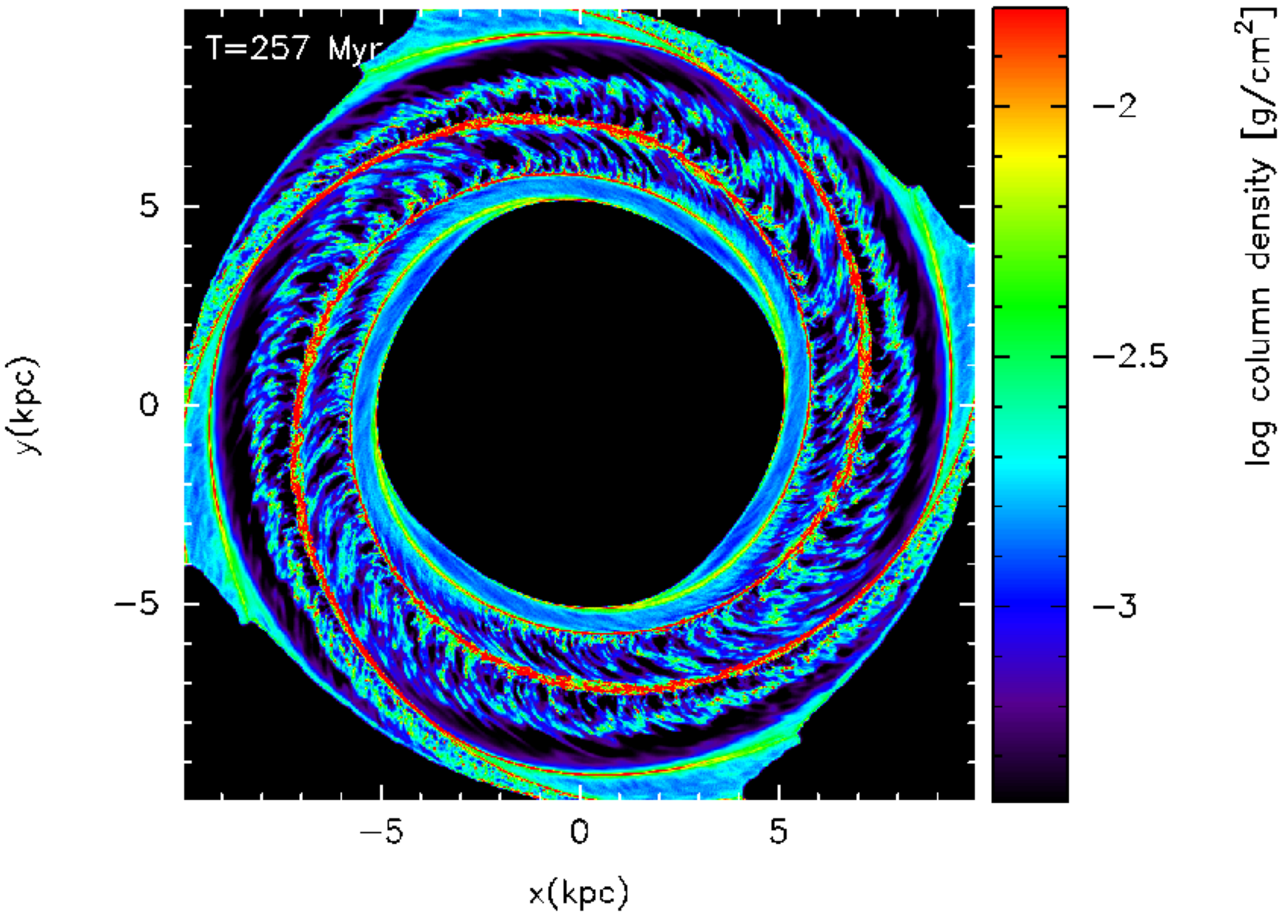

(from Dobbs et al. 2008)

molecular cloud formation

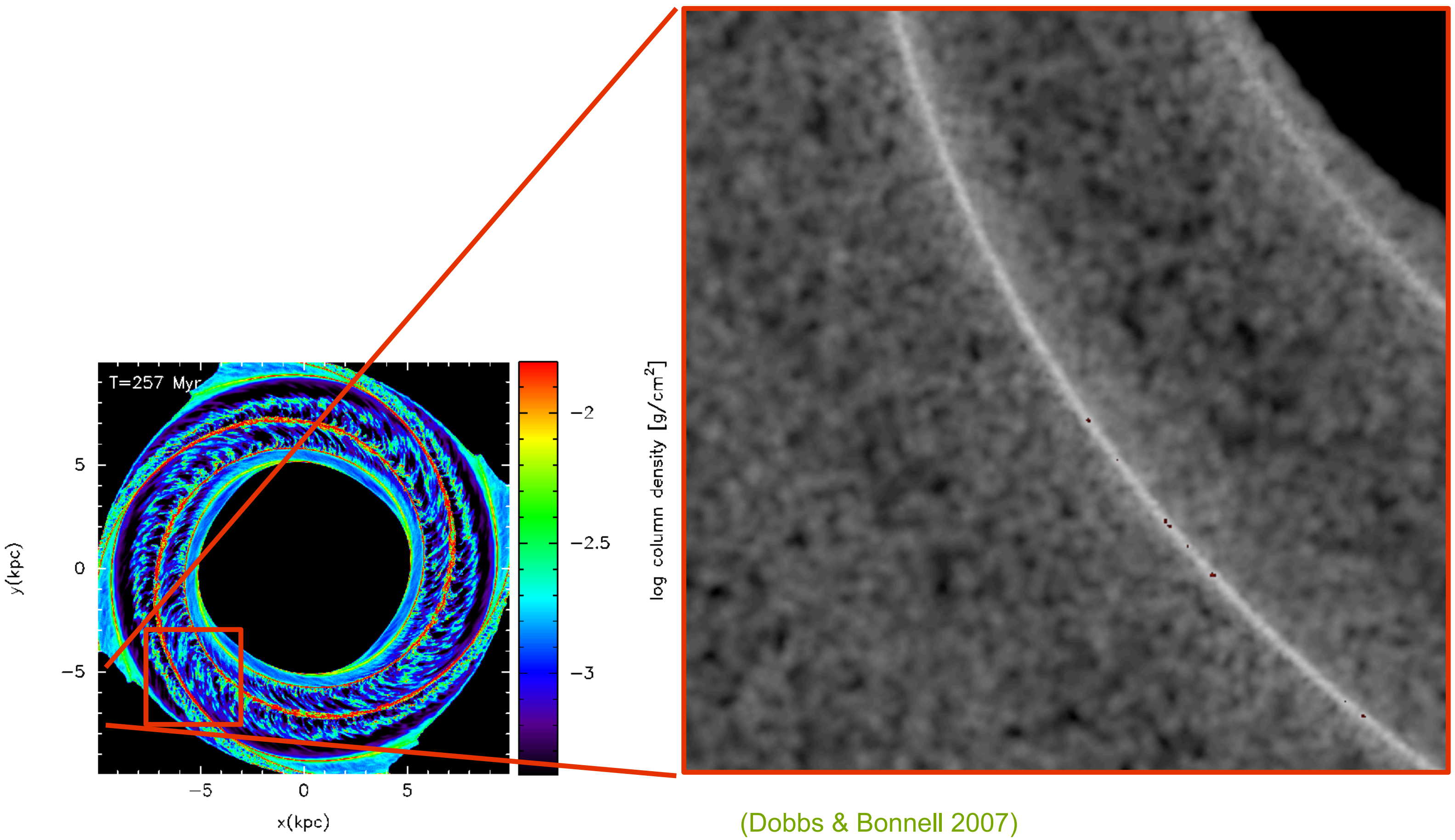

(Dobbs & Bonnell 2007)

molecular cloud formation

molecular gas fraction as function of time

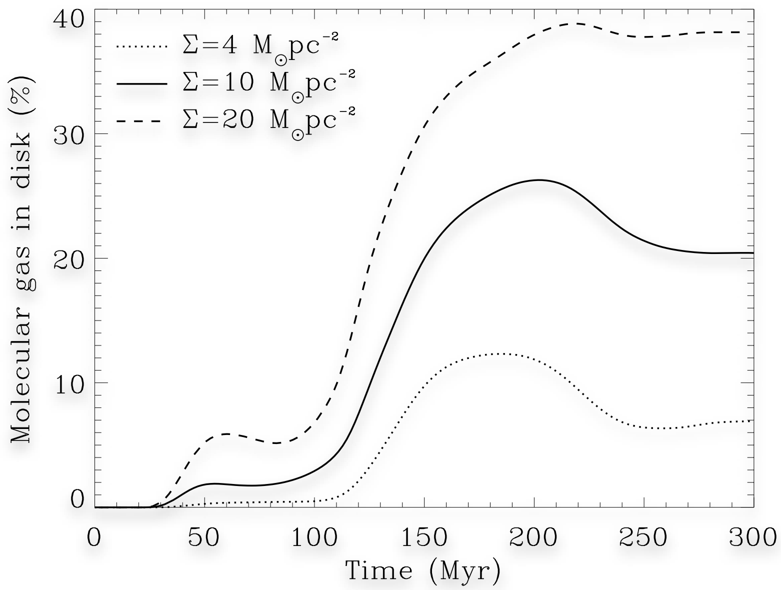

molecular gas fraction as function of density

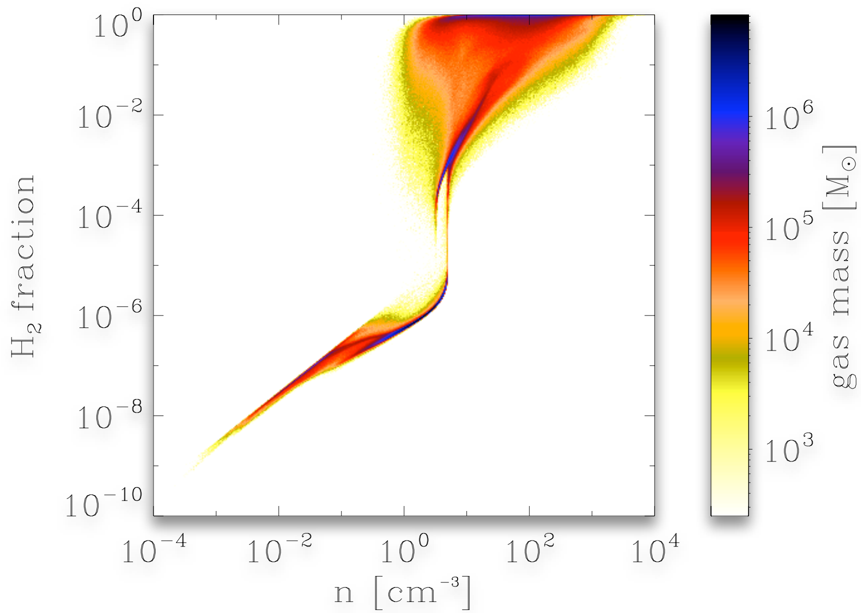

(Dobbs et al. 2008)

molecular cloud formation

molecular gas fraction of fluid element as function of time

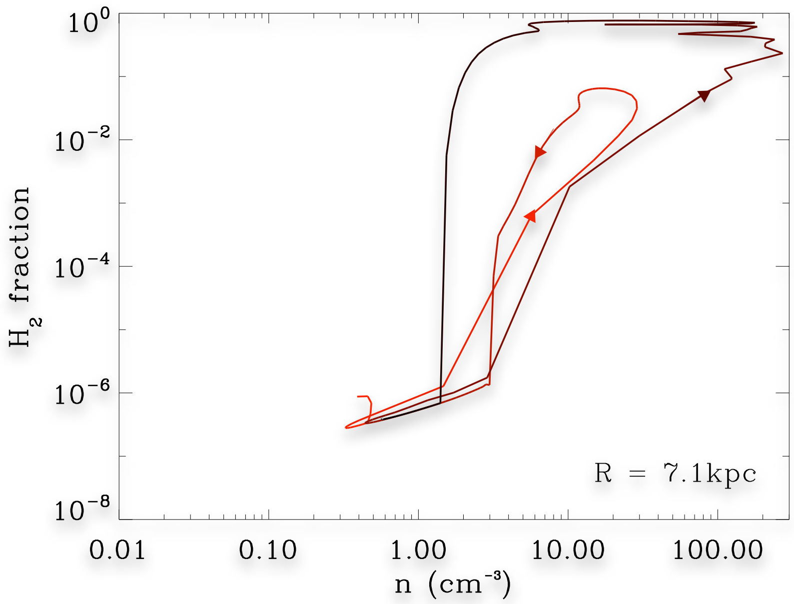

molecular gas fraction as function of density

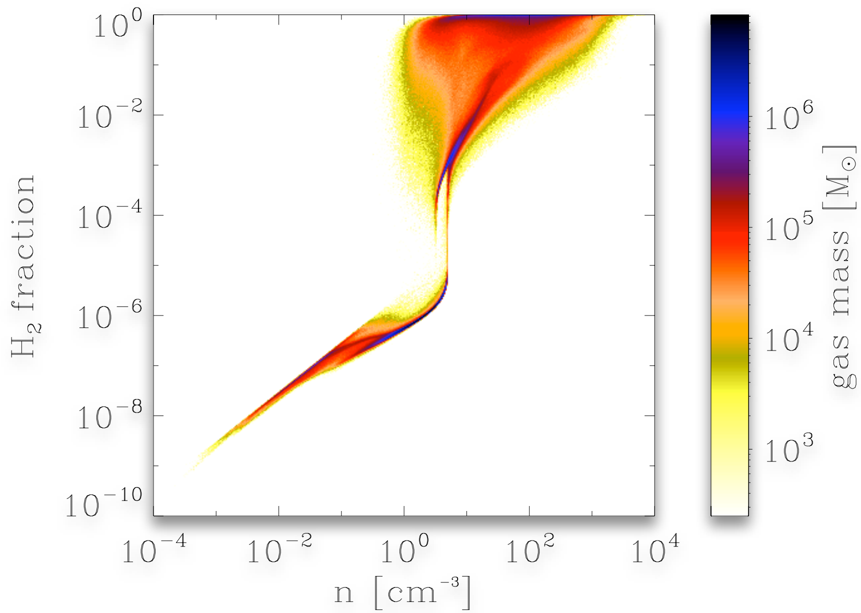

(Dobbs et al. 2008)

observed timescales

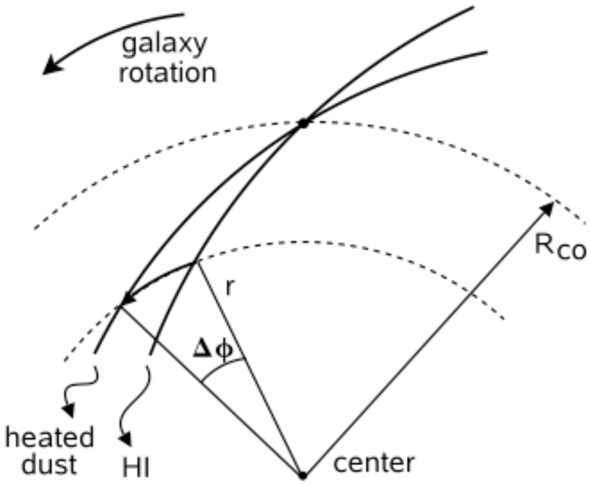

Tamburro et al. (2008)

Fig. 1.— NGC 5194: the 24 μm band image is plotted in color scale; the H I emission map is overlayed with green contours.

observed timescales

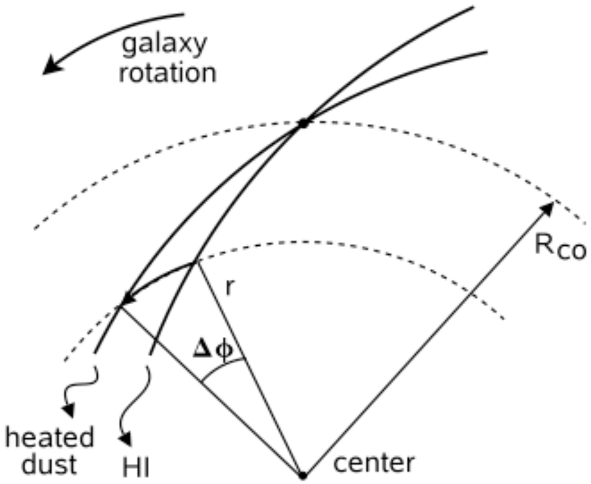

Tamburro et al. (2008)

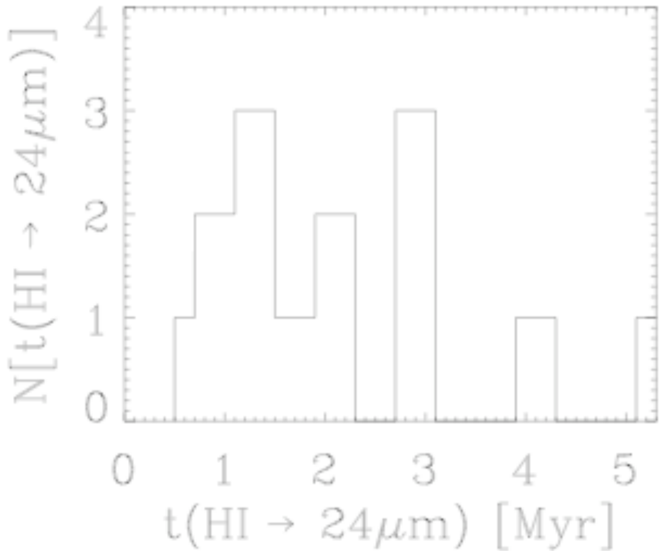

Fig. 5.— Histogram of the time scales $t_{\mathrm{HI}\mapsto 24\,\mu\mathrm{m}}$ derived from the fits in Figure 4 and listed in Table. 2 for the 14 sample galaxies listed in Table. 1. The timescales range between 1 and 4 Myr for almost all galaxies.

calculated timescales

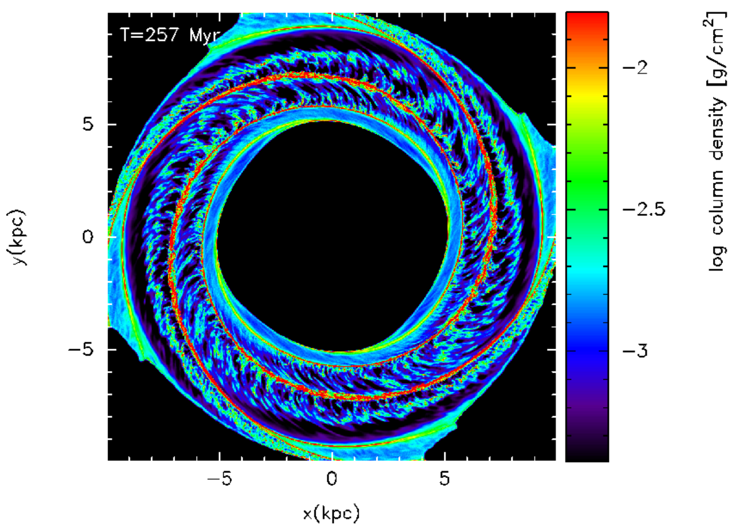

Dobbs et al. (2008)

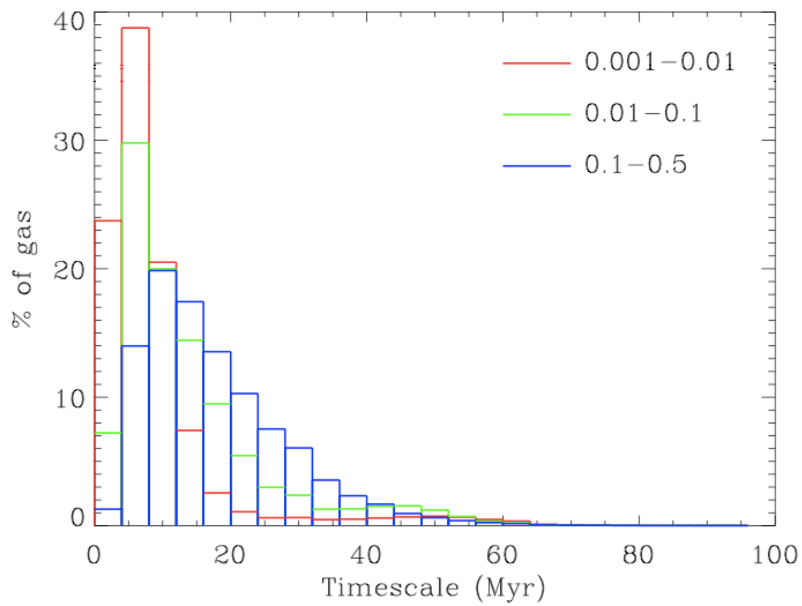

Figure 16. This histogram gives the distribution of timescales over which the gas reaches certain molecular gas fractions. The timescales denote the time for the H_2 fraction of a particle to increase from 0.001 to 0.01, 0.01 to 0.1 and 0.1 to 0.5, as indicated.

models with B-fields

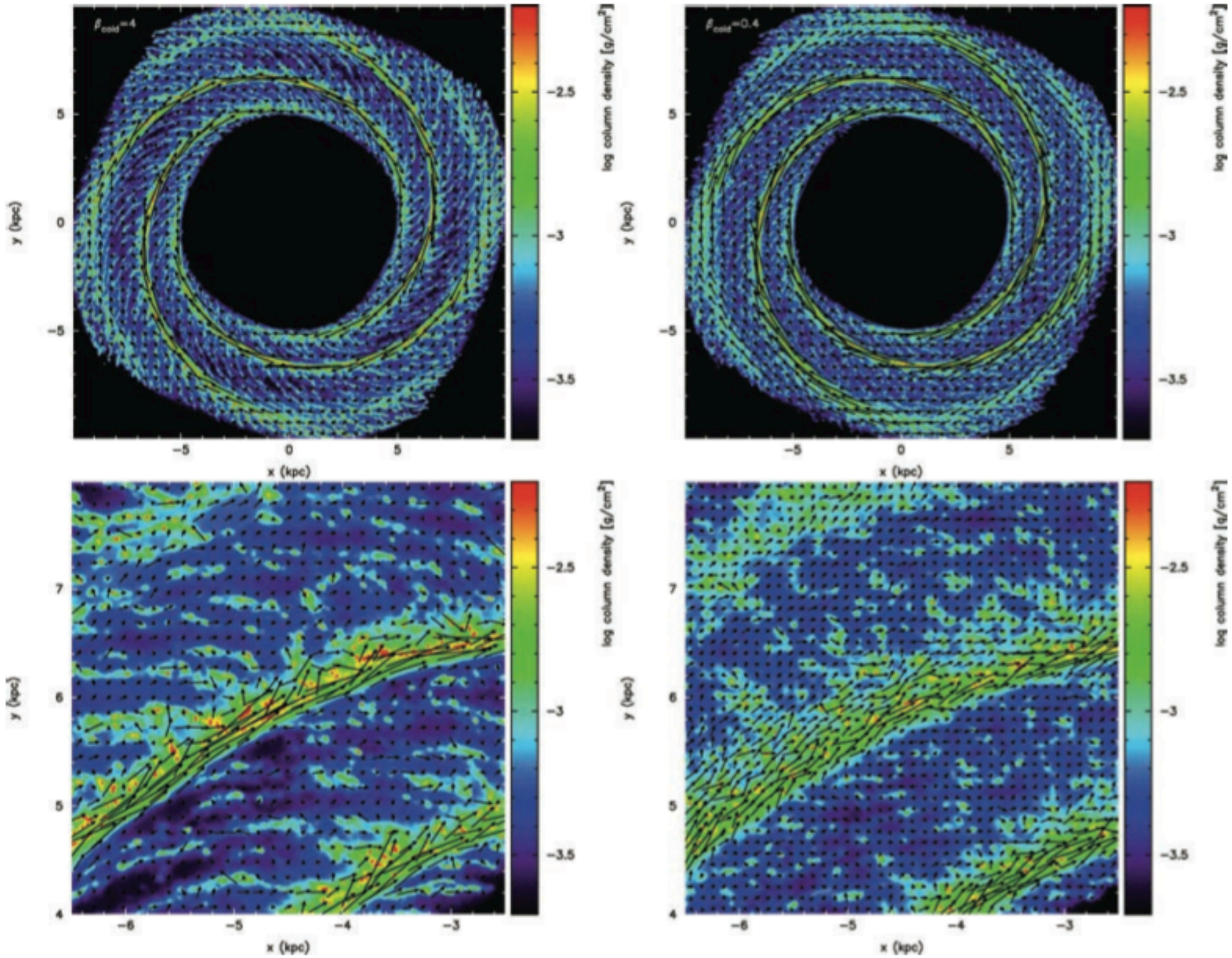

Figure 9. The column density is shown for the two-phase simulations after 250 Myr, for the whole disc (top panel) and a 4 × 4 kpc subsection (bottom panel). The left-hand panels show the case where $\beta_{\rm cold} = 4$ and the right-hand panels where $\beta_{\rm cold} = 0.4$. Both the cold and warm phases are shown in the plots, but we show them separately for the case where $\beta_{\rm cold} = 4$ in Fig. 12. There is more structure in the cold gas when the magnetic field is weaker ($\beta_{\rm cold} = 4$). The vectors show the magnetic field smoothed over a particular grid size. There is more detailed structure on smaller scales, particularly in the spiral arms which are better resolved.

obbs & Price (2008), Shetty & Ostriker (2007, 2008)

modeling chemistry

experimental set-up

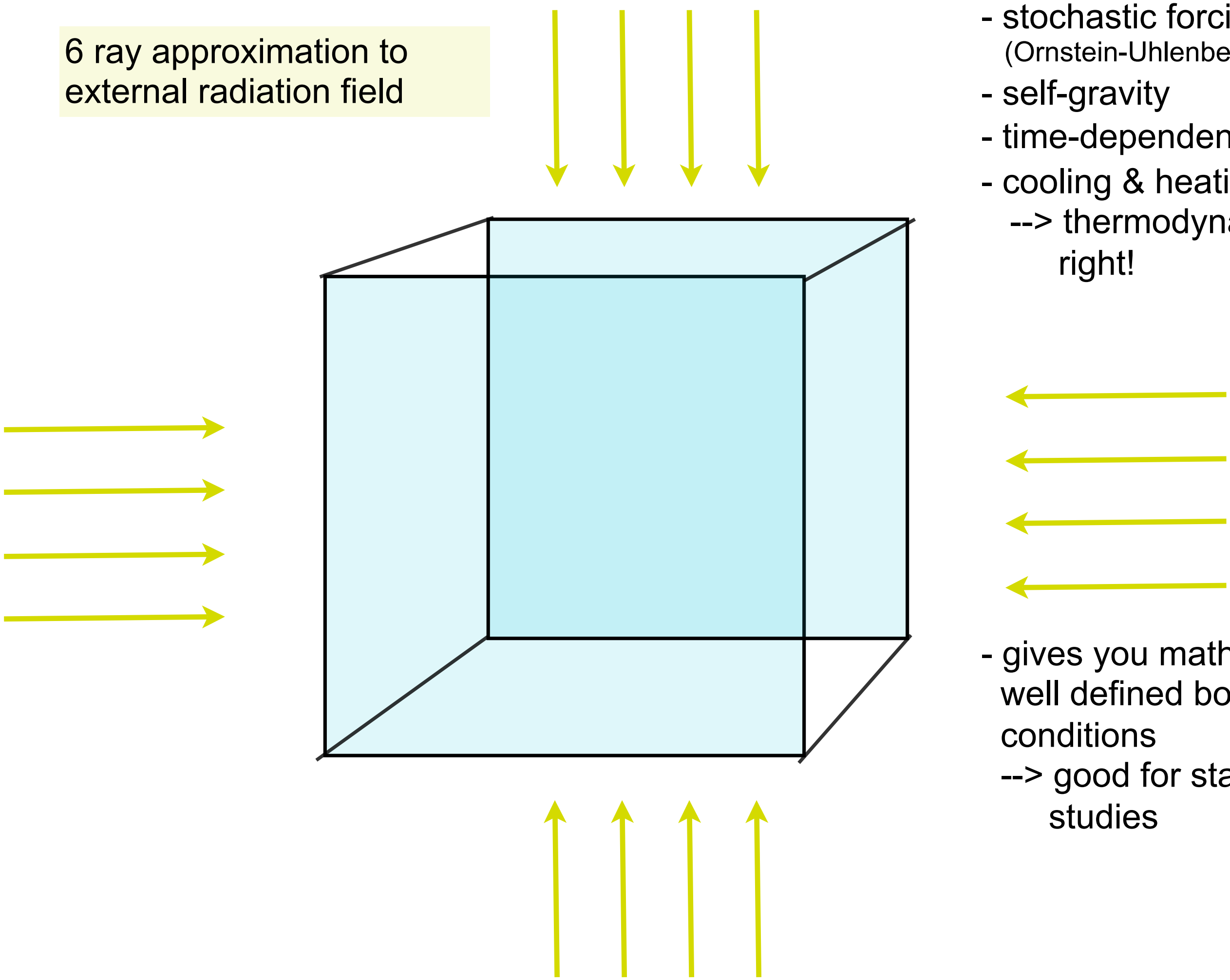

- AMR MHD (B = 2 muG)
- stochastic forcing
  (Ornstein-Uhlenbeck)
- self-gravity
- time-dependent chemistry
- cooling & heating processes
  --> thermodynamics done right!

- gives you mathematically well defined boundary conditions
  --> good for statistical studies

chemical model 0

- 32 chemical species
  - 17 in instantaneous equilibrium:

H^-, H_2^+, H_3^+, CH^+, CH_2^+, OH^+, H_2O^+, H_3O^+, CO^+, HOC^+, O^-, C^- and O_2^+

  - 19 full non-equilibrium evolution

e^-, H^+, H, H_2, He, He^+, C, C^+, O, O^+, OH, H_2O, CO,

C_2, O_2, HCO^+, CH, CH_2 and CH_3^+

- 218 reactions
- various heating and cooling processes

(Glover, Federrath, Mac Low, Klessen, 2010, MNRAS, 404, 2)

chemical model 1

Process	Reference(s)
Cooling:	
C fine structure lines	Atomic data – Silva & Viegas (2002)
	Collisional rates (H) – Abrahamsson, Krems & Dalgarno (2007)
	Collisional rates (H_2) – Schroder et al. (1991)
	Collisional rates (e^-) – Johnson et al. (1987)
	Collisional rates (H^+) – Roueff & Le Bourlot (1990)
C^+ fine structure lines	Atomic data – Silva & Viegas (2002)
	Collisional rates (H_2) – Flower & Launay (1977)
	Collisional rates (H, $T < 2000$ K) – Hollenbach & McKee (1989)
	Collisional rates (H, $T > 2000$ K) – Keenan et al. (1986)
	Collisional rates (e^-) – Wilson & Bell (2002)
O fine structure lines	Atomic data – Silva & Viegas (2002)
	Collisional rates (H) – Abrahamsson, Krems & Dalgarno (2007)
	Collisional rates (H_2) – see Glover & Jappsen (2007)
	Collisional rates (e^-) – Bell, Berrington & Thomas (1998)
	Collisional rates (H^+) – Pequignot (1990, 1996)
H_2 rovibrational lines	Le Bourlot, Pineau des Forêts & Flower (1999)
CO and H_2O rovibrational lines	Neufeld & Kaufman (1993); Neufeld, Lepp & Melnick (1995)
OH rotational lines	Pavlovski et al. (2002)
Gas-grain energy transfer	Hollenbach & McKee (1989)
Recombination on grains	Wolfire et al. (2003)
Atomic resonance lines	Sutherland & Dopita (1993)
H collisional ionization	Abel et al. (1997)
H_2 collisional dissociation	See Table B1
Compton cooling	Cen (1992)
Heating:	
Photoelectric effect	Bakes & Tielens (1994); Wolfire et al. (2003)
H_2 photodissociation	Black & Dalgarno (1977)
UV pumping of H_2	Burton, Hollenbach & Tielens (1990)
H_2 formation on dust grains	Hollenbach & McKee (1989)
Cosmic ray ionization	Goldsmith & Langer (1978)

(Glover, Federrath, Mac Low, Klessen, 2010, MNRS, 404, 2)

chemical model 2

Table B1. List of collisional gas-phase reactions included in our chemical model.

No.	Reaction	Rate coefficient (cm^3 s^{-1})	Notes	Ref.
1	$H + e^- \rightarrow H^- + \gamma$	$k_1 = \mathrm{dex}[-17.845 + 0.762 \log T + 0.1523(\log T)^2$		1
		$- 0.03274(\log T)^3]$	$T \leqslant 6000$ K	
		$= \mathrm{dex}[-16.420 + 0.1998(\log T)^2$		
		$- 5.447 \times 10^{-3}(\log T)^4$		
		$+ 4.0415 \times 10^{-5}(\log T)^6]$	$T > 6000$ K	
2	$H^- + H \rightarrow H_2 + e^-$	$k_2 = 1.5 \times 10^{-9}$	$T \leqslant 300$ K	2
		$= 4.0 \times 10^{-9} T^{-0.17}$	$T > 300$ K	
3	$H + H^+ \rightarrow H_2^+ + \gamma$	$k_3 = \mathrm{dex}[-19.38 - 1.523 \log T$		3
		$+ 1.118(\log T)^2 - 0.1269(\log T)^3]$		
4	$H + H_2^+ \rightarrow H_2 + H^+$	$k_4 = 6.4 \times 10^{-10}$		4
5	$H^- + H^+ \rightarrow H + H$	$k_5 = 2.4 \times 10^{-6} T^{-1/2}(1.0 + T/20000)$		5
6	$H_2^+ + e^- \rightarrow H + H$	$k_6 = 1.0 \times 10^{-8}$	$T \leqslant 617$ K	6
		$= 1.32 \times 10^{-6} T^{-0.76}$	$T > 617$ K	
7	$H_2 + H^+ \rightarrow H_2^+ + H$	$k_7 = [-3.3232183 \times 10^{-7}$		7
		$+ 3.3735382 \times 10^{-7} \ln T$		
		$- 1.4491368 \times 10^{-7}(\ln T)^2$		
		$+ 3.4172805 \times 10^{-8}(\ln T)^3$		
		$- 4.7813720 \times 10^{-9}(\ln T)^4$		
		$+ 3.9731542 \times 10^{-10}(\ln T)^5$		
		$- 1.8171411 \times 10^{-11}(\ln T)^6$		
		$+ 3.5311932 \times 10^{-13}(\ln T)^7]$		
		$\times \exp\left(\frac{-21237.15}{T}\right)$		
8	$H_2 + e^- \rightarrow H + H + e^-$	$k_8 = 3.73 \times 10^{-9} T^{0.1121} \exp\left(\frac{-99430}{T}\right)$		8
9	$H_2 + H \rightarrow H + H + H$	$k_{9,l} = 6.67 \times 10^{-12} T^{1/2} \exp\left[-(1 + \frac{63590}{T})\right]$		9
		$k_{9,h} = 3.52 \times 10^{-9} \exp\left(-\frac{43900}{T}\right)$		10
		$n_{cr,H} = \mathrm{dex}\left[3.0 - 0.416 \log\left(\frac{T}{10000}\right) - 0.327 \left\{\log\left(\frac{T}{10000}\right)\right\}^2\right]$		10
10	$H_2 + H_2 \rightarrow H_2 + H + H$	$k_{10,l} = \frac{5.996 \times 10^{-30} T^{4.1881}}{(1.0 + 6.761 \times 10^{-6} T)^{5.6881}} \exp\left(-\frac{54657.4}{T}\right)$		11
		$k_{10,h} = 1.3 \times 10^{-9} \exp\left(-\frac{53300}{T}\right)$		12
		$n_{cr,H_2} = \mathrm{dex}\left[4.845 - 1.3 \log\left(\frac{T}{10000}\right) + 1.62 \left\{\log\left(\frac{T}{10000}\right)\right\}^2\right]$		12
11	$H + e^- \rightarrow H^+ + e^- + e^-$	$k_{11} = \exp[-3.271396786 \times 10^1$		13
		$+ 1.35365560 \times 10^1 \ln T_e$		
		$- 5.73932875 \times 10^0 (\ln T_e)^2$		
		$+ 1.56315498 \times 10^0 (\ln T_e)^3$		
		$- 2.87705600 \times 10^{-1}(\ln T_e)^4$		
		$+ 3.48255977 \times 10^{-2}(\ln T_e)^5$		
		$- 2.63197617 \times 10^{-3}(\ln T_e)^6$		
		$+ 1.11954395 \times 10^{-4}(\ln T_e)^7$		
		$- 2.03914985 \times 10^{-6}(\ln T_e)^8]$		
12	$H^+ + e^- \rightarrow H + \gamma$	$k_{12,A} = 1.269 \times 10^{-13} \left(\frac{315614}{T}\right)^{1.503}$	Case A	14
		$\times [1.0 + \left(\frac{604625}{T}\right)^{0.470}]^{-1.923}$		
		$k_{12,B} = 2.753 \times 10^{-14} \left(\frac{315614}{T}\right)^{1.500}$	Case B	14
		$\times [1.0 + \left(\frac{115188}{T}\right)^{0.407}]^{-2.242}$		
13	$H^- + e^- \rightarrow H + e^- + e^-$	$k_{13} = \exp[-1.801849334 \times 10^1$		13
		$+ 2.36085220 \times 10^0 \ln T_e$		
		$- 2.82744300 \times 10^{-1}(\ln T_e)^2$		
		$+ 1.62331664 \times 10^{-2}(\ln T_e)^3$		
		$- 3.36501203 \times 10^{-2}(\ln T_e)^4$		
		$+ 1.17832978 \times 10^{-2}(\ln T_e)^5$		
		$- 1.65619470 \times 10^{-3}(\ln T_e)^6$		
		$+ 1.06827520 \times 10^{-4}(\ln T_e)^7$		
		$- 2.63128581 \times 10^{-6}(\ln T_e)^8]$		

(Glover, Federrath, Mac Low, Klessen, 2010, MNRS, 404, 2)

chemical model 2

Table B1.

No.	Reaction	Rate coefficient	Notes	Ref.
14	$H^- + H \rightarrow H + H + e^-$	$k_{14} = 2.5634 \times 10^{-9} T_e^{1.78186}$	$T_e \leqslant 0.1$ eV	13
		$= \exp[-2.0372609 \times 10^{1}$		
		$+ 1.13944933 \times 10^{0} \ln T_e$		
		$- 1.4210135 \times 10^{-1} (\ln T_e)^2$		
		$+ 8.4644554 \times 10^{-3} (\ln T_e)^3$		
		$-$ [illegible] $\times 10^{-3} (\ln T_e)^4$		
		$+$ [illegible] $\times 10^{-4} (\ln T_e)^5$		
		$+ 8.6639632 \times 10^{-5} (\ln T_e)^6$		
		$- 2.5850097 \times 10^{-5} (\ln T_e)^7$		
		$+ 2.4555012 \times 10^{-6} (\ln T_e)^8$		
		$- 8.0683825 \times 10^{-8} (\ln T_e)^9]$	$T_e > 0.1$ eV	
15	$H^- + H^+ \rightarrow H_2^+ + e^-$	$k_{15} = 6.9 \times 10^{-9} T^{-0.35}$	$T \leqslant 8000$ K	15
		$= 9.6 \times 10^{-7} T^{-0.90}$	$T > 8000$ K	
16	$He + e^- \rightarrow He^+ + e^- + e^-$	$k_{16} = \exp[-4.409864886 \times 10^{1}$		13
		$+ 2.391596563 \times 10^{1} \ln T_e$		
		$- 1.07532302 \times 10^{1} (\ln T_e)^2$		
		$+ 3.05803875 \times 10^{0} (\ln T_e)^3$		
		$- 5.6851189 \times 10^{-1} (\ln T_e)^4$		
		$+ 6.79539123 \times 10^{-2} (\ln T_e)^5$		
		$- 5.0090561 \times 10^{-3} (\ln T_e)^6$		
		$+ 2.06723616 \times 10^{-4} (\ln T_e)^7$		
		$- 3.64916141 \times 10^{-6} (\ln T_e)^8]$		
17	$He^+ + e^- \rightarrow He + \gamma$	$k_{17,rr,A} = 10^{-11} T^{-0.5} [12.72 - 1.615 \log T$	Case A	16
		$- 0.3162 (\log T)^2 + 0.0493 (\log T)^3]$		
		$k_{17,rr,B} = 10^{-11} T^{-0.5} [11.19 - 1.676 \log T$	Case B	16
		$- 0.2852 (\log T)^2 + 0.04433 (\log T)^3]$		
		$k_{17,di} = 1.9 \times 10^{-3} T^{-1.5} \exp\left(-\frac{473421}{T}\right)$		
		$\times \left[1.0 + 0.3 \exp\left(-\frac{94684}{T}\right)\right]$		17
18	$He^+ + H \rightarrow He + H^+$	$k_{18} = 1.25 \times 10^{-15} \left(\frac{T}{300}\right)^{0.25}$		18
19	$He + H^+ \rightarrow He^+ + H$	$k_{19} = 1.26 \times 10^{-9} T^{-0.75} \exp\left(-\frac{127500}{T}\right)$	$T \leqslant 10000$ K	19
		$= 4.0 \times 10^{-37} T^{4.74}$	$T > 10000$ K	
20	$C^+ + e^- \rightarrow C + \gamma$	$k_{20} = 4.67 \times 10^{-12} \left(\frac{T}{300}\right)^{-0.6}$	$T \leqslant 7950$ K	20
		$= 1.23 \times 10^{-17} \left(\frac{T}{300}\right)^{2.49} \exp\left(\frac{21845.6}{T}\right)$	$7950 \text{ K} < T \leqslant 21140$ K	
		$= 9.62 \times 10^{-8} \left(\frac{T}{300}\right)^{-1.37} \exp\left(\frac{-115786.2}{T}\right)$	$T > 21140$ K	
21	$O^+ + e^- \rightarrow O + \gamma$	$k_{21} = 1.30 \times 10^{-10} T^{-0.64}$	$T \leqslant 400$ K	21
		$= 1.41 \times 10^{-10} T^{-0.66} + 7.4 \times 10^{-4} T^{-1.5}$		
		$\times \exp\left(-\frac{175000}{T}\right) [1.0 + 0.062 \times \exp\left(-\frac{145000}{T}\right)]$	$T > 400$ K	
22	$C + e^- \rightarrow C^+ + e^- + e^-$	$k_{22} = 6.85 \times 10^{-8} (0.193 + u)^{-1} u^{0.25} e^{-u}$	$u = 11.26/T_e$	22
23	$O + e^- \rightarrow O^+ + e^- + e^-$	$k_{23} = 3.59 \times 10^{-8} (0.073 + u)^{-1} u^{0.34} e^{-u}$	$u = 13.6/T_e$	22
24	$O^+ + H \rightarrow O + H^+$	$k_{24} = 4.99 \times 10^{-11} T^{0.405} + 7.54 \times 10^{-10} T^{-0.458}$		23
25	$O + H^+ \rightarrow O^+ + H$	$k_{25} = [1.08 \times 10^{-11} T^{0.517}$		24
		$+ 4.00 \times 10^{-10} T^{0.00669}] \exp\left(-\frac{227}{T}\right)$		
26	$O + He^+ \rightarrow O^+ + He$	$k_{26} = 4.991 \times 10^{-15} \left(\frac{T}{10000}\right)^{0.3794} \exp\left(-\frac{T}{1121000}\right)$		25
		$+ 2.780 \times 10^{-15} \left(\frac{T}{10000}\right)^{-0.2163} \exp\left(\frac{T}{815800}\right)$		
27	$C + H^+ \rightarrow C^+ + H$	$k_{27} = 3.9 \times 10^{-16} T^{0.213}$		24
28	$C^+ + H \rightarrow C + H^+$	$k_{28} = 6.08 \times 10^{-14} \left(\frac{T}{10000}\right)^{1.96} \exp\left(-\frac{170000}{T}\right)$		24
29	$C + He^+ \rightarrow C^+ + He$	$k_{29} = 8.58 \times 10^{-17} T^{0.757}$	$T \leqslant 200$ K	26
		$= 3.25 \times 10^{-17} T^{0.968}$	$200 < T \leqslant 2000$ K	
		$= 2.77 \times 10^{-19} T^{1.597}$	$T > 2000$ K	
30	$H_2 + He \rightarrow H + H + He$	$k_{30,l} = \text{dex}[-27.029 + 3.801 \log(T) - 29487/T]$		27
		$k_{30,h} = \text{dex}[-2.729 - 1.75 \log(T) - 23474/T]$		
		$n_{cr,He} = \text{dex}\left[5.0792(1.0 - 1.23 \times 10^{-5}(T - 2000)\right]$		27
31	$OH + H \rightarrow O + H + H$	$k_{31} = 6.0 \times 10^{-9} \exp\left(-\frac{50900}{T}\right)$		28
32	$HOC^+ + H_2 \rightarrow HCO^+ + H_2$	$k_{32} = 3.8 \times 10^{-10}$		29
33	$HOC^+ + CO \rightarrow HCO^+ + CO$	$k_{33} = 4.0 \times 10^{-10}$		30
34	$C + H_2 \rightarrow CH + H$	$k_{34} = 6.64 \times 10^{-10} \exp\left(-\frac{11700}{T}\right)$		31
35	$CH + H \rightarrow C + H_2$	$k_{35} = 1.31 \times 10^{-10} \exp\left(-\frac{80}{T}\right)$		32

(Glover, Federrath, Mac Low, Klessen, 2010, MNRS, 404, 2)

chemical model 2

(Glover, Federrath, Mac Low, Klessen, 2010, MNRS, 404, 2)

Table B1.

14	$H^- + H \rightarrow H + H + e^-$	$k_{14} = 2.5634 \times 10^{-9} T_e^{1.78186}$	$T_e \leqslant 0.1$ eV	13

36	$CH + H_2 \rightarrow CH_2 + H$	$k_{36} = 5.46 \times 10^{-10} \exp\left(-\frac{1943}{T}\right)$		33
37	$CH + C \rightarrow C_2 + H$	$k_{37} = 6.59 \times 10^{-11}$		34
38	CH + [illegible]	$k_{38} = 6.6 \times 10^{-11}$	T [illegible] 2000 K	35
		[illegible] $\times 10^{-10}$ [illegible]	[illegible] 2000 K	36
39	[illegible]	[illegible] $\times 10^{-11}$		37
40	$CH_2 + O \rightarrow CO + H + H$	$k_{40} = 1.33 \times 10^{-10}$		38
41	$CH_2 + O \rightarrow CO + H_2$	$k_{41} = 8.0 \times 10^{-11}$		39
42	$C_2 + O \rightarrow CO + C$	$k_{42} = 5.0 \times 10^{-11} \left(\frac{T}{300}\right)^{0.5}$	$T \leqslant 300$ K	40
		$= 5.0 \times 10^{-11} \left(\frac{T}{300}\right)^{0.757}$	$T > 300$ K	41
43	$O + H_2 \rightarrow OH + H$	$k_{43} = 3.14 \times 10^{-13} \left(\frac{T}{300}\right)^{2.7} \exp\left(-\frac{3150}{T}\right)$		42
44	$OH + H \rightarrow O + H_2$	$k_{44} = 6.99 \times 10^{-14} \left(\frac{T}{300}\right)^{2.8} \exp\left(-\frac{1950}{T}\right)$		43
45	$OH + H_2 \rightarrow H_2O + H$	$k_{45} = 2.05 \times 10^{-12} \left(\frac{T}{300}\right)^{1.52} \exp\left(-\frac{1736}{T}\right)$		44
46	$OH + C \rightarrow CO + H$	$k_{46} = 1.0 \times 10^{-10}$		34
47	$OH + O \rightarrow O_2 + H$	$k_{47} = 3.50 \times 10^{-11}$	$T \leqslant 261$ K	45
		$= 1.77 \times 10^{-11} \exp\left(\frac{178}{T}\right)$	$T > 261$ K	33
48	$OH + OH \rightarrow H_2O + H$	$k_{48} = 1.65 \times 10^{-12} \left(\frac{T}{300}\right)^{1.14} \exp\left(-\frac{50}{T}\right)$		34
49	$H_2O + H \rightarrow H_2 + OH$	$k_{49} = 1.59 \times 10^{-11} \left(\frac{T}{300}\right)^{1.2} \exp\left(-\frac{9610}{T}\right)$		46
50	$O_2 + H \rightarrow OH + O$	$k_{50} = 2.61 \times 10^{-10} \exp\left(-\frac{8156}{T}\right)$		33
51	$O_2 + H_2 \rightarrow OH + OH$	$k_{51} = 3.16 \times 10^{-10} \exp\left(-\frac{21890}{T}\right)$		47
52	$O_2 + C \rightarrow CO + O$	$k_{52} = 4.7 \times 10^{-11} \left(\frac{T}{300}\right)^{-0.34}$	$T \leqslant 295$ K	34
		$= 2.48 \times 10^{-12} \left(\frac{T}{300}\right)^{1.54} \exp\left(\frac{613}{T}\right)$	$T > 295$ K	33
53	$CO + H \rightarrow C + OH$	$k_{53} = 1.1 \times 10^{-10} \left(\frac{T}{300}\right)^{0.5} \exp\left(-\frac{77700}{T}\right)$		28
54	$H_2^+ + H_2 \rightarrow H_3^+ + H$	$k_{54} = 2.24 \times 10^{-9} \left(\frac{T}{300}\right)^{0.042} \exp\left(-\frac{T}{46600}\right)$		48
55	$H_3^+ + H \rightarrow H_2^+ + H_2$	$k_{55} = 7.7 \times 10^{-9} \exp\left(-\frac{17560}{T}\right)$		49
56	$C + H_2^+ \rightarrow CH^+ + H$	$k_{56} = 2.4 \times 10^{-9}$		28
57	$C + H_3^+ \rightarrow CH^+ + H_2$	$k_{57} = 2.0 \times 10^{-9}$		28
58	$C^+ + H_2 \rightarrow CH^+ + H$	$k_{58} = 1.0 \times 10^{-10} \exp\left(-\frac{4640}{T}\right)$		50
59	$CH^+ + H \rightarrow C^+ + H_2$	$k_{59} = 7.5 \times 10^{-10}$		51
60	$CH^+ + H_2 \rightarrow CH_2^+ + H$	$k_{60} = 1.2 \times 10^{-9}$		51
61	$CH^+ + O \rightarrow CO^+ + H$	$k_{61} = 3.5 \times 10^{-10}$		52
62	$CH_2 + H^+ \rightarrow CH^+ + H_2$	$k_{62} = 1.4 \times 10^{-9}$		28
63	$CH_2^+ + H \rightarrow CH^+ + H_2$	$k_{63} = 1.0 \times 10^{-9} \exp\left(-\frac{7080}{T}\right)$		28
64	$CH_2^+ + H_2 \rightarrow CH_3^+ + H$	$k_{64} = 1.6 \times 10^{-9}$		53
65	$CH_2^+ + O \rightarrow HCO^+ + H$	$k_{65} = 7.5 \times 10^{-10}$		28
66	$CH_3^+ + H \rightarrow CH_2^+ + H_2$	$k_{66} = 7.0 \times 10^{-10} \exp\left(-\frac{10560}{T}\right)$		28
67	$CH_3^+ + O \rightarrow HCO^+ + H_2$	$k_{67} = 4.0 \times 10^{-10}$		54
68	$C_2 + O^+ \rightarrow CO^+ + C$	$k_{68} = 4.8 \times 10^{-10}$		28
69	$O^+ + H_2 \rightarrow OH^+ + H$	$k_{69} = 1.7 \times 10^{-9}$		55
70	$O + H_2^+ \rightarrow OH^+ + H$	$k_{70} = 1.5 \times 10^{-9}$		28
71	$O + H_3^+ \rightarrow OH^+ + H_2$	$k_{71} = 8.4 \times 10^{-10}$		56
72	$OH + H_3^+ \rightarrow H_2O^+ + H_2$	$k_{72} = 1.3 \times 10^{-9}$		28
73	$OH + C^+ \rightarrow CO^+ + H$	$k_{73} = 7.7 \times 10^{-10}$		28
74	$OH^+ + H_2 \rightarrow H_2O^+ + H$	$k_{74} = 1.01 \times 10^{-9}$		57
75	$H_2O^+ + H_2 \rightarrow H_3O^+ + H$	$k_{75} = 6.4 \times 10^{-10}$		58
76	$H_2O + H_3^+ \rightarrow H_3O^+ + H_2$	$k_{76} = 5.9 \times 10^{-9}$		59
77	$H_2O + C^+ \rightarrow HCO^+ + H$	$k_{77} = 9.0 \times 10^{-10}$		60
78	$H_2O + C^+ \rightarrow HOC^+ + H$	$k_{78} = 1.8 \times 10^{-9}$		60
79	$H_3O^+ + C \rightarrow HCO^+ + H_2$	$k_{79} = 1.0 \times 10^{-11}$		28
80	$O_2 + C^+ \rightarrow CO^+ + O$	$k_{80} = 3.8 \times 10^{-10}$		53
81	$O_2 + C^+ \rightarrow CO + O^+$	$k_{81} = 6.2 \times 10^{-10}$		53
82	$O_2 + CH_2^+ \rightarrow HCO^+ + OH$	$k_{82} = 9.1 \times 10^{-10}$		53
83	$O_2^+ + C \rightarrow CO^+ + O$	$k_{83} = 5.2 \times 10^{-11}$		28
84	$CO + H_3^+ \rightarrow HOC^+ + H_2$	$k_{84} = 2.7 \times 10^{-11}$		61
85	$CO + H_3^+ \rightarrow HCO^+ + H_2$	$k_{85} = 1.7 \times 10^{-9}$		61
86	$HCO^+ + C \rightarrow CO + CH^+$	$k_{86} = 1.1 \times 10^{-9}$		28
87	$HCO^+ + H_2O \rightarrow CO + H_3O^+$	$k_{87} = 2.5 \times 10^{-9}$		62

chemical model 2

87	$HCO^+ + H_2O \rightarrow CO + H_3O^+$	$k_{87} = 2.5 \times 10^{-9}$	62
88	$H_2 + He^+ \rightarrow He + H_2^+$	$k_{88} = 7.2 \times 10^{-15}$	63
89	$H_2 + He^+ \rightarrow He + H + H^+$	$k_{89} = 3.7 \times 10^{-14} \exp\left(\frac{35}{T}\right)$	63
90	$CH + H^+ \rightarrow CH^+ + H$	$k_{90} = 1.9 \times 10^{-9}$	28
91	$CH_2 + H^+ \rightarrow CH_2^+ + H$	$k_{91} = 1.4 \times 10^{-9}$	28
92	$CH_2 + He^+ \rightarrow C^+ + He + H_2$	k_{92} = [illegible]	28
93	$C_2 + He^+ \rightarrow C^+ + C + He$	k_{93} = [illegible]6×10^{-9}	28
94	$OH + H^+ \rightarrow OH^+ + H$	$k_{94} = 2.1 \times 10^{-9}$	28
95	$OH + He^+ \rightarrow O^+ + He + H$	$k_{95} = 1.1 \times 10^{-9}$	28
96	$H_2O + H^+ \rightarrow H_2O^+ + H$	$k_{96} = 6.9 \times 10^{-9}$	64
97	$H_2O + He^+ \rightarrow OH + He + H^+$	$k_{97} = 2.04 \times 10^{-10}$	65
98	$H_2O + He^+ \rightarrow OH^+ + He + H$	$k_{98} = 2.86 \times 10^{-10}$	65
99	$H_2O + He^+ \rightarrow H_2O^+ + He$	$k_{99} = 6.05 \times 10^{-11}$	65
100	$O_2 + H^+ \rightarrow O_2^+ + H$	$k_{100} = 2.0 \times 10^{-9}$	64
101	$O_2 + He^+ \rightarrow O_2^+ + He$	$k_{101} = 3.3 \times 10^{-11}$	66
102	$O_2 + He^+ \rightarrow O^+ + O + He$	$k_{102} = 1.1 \times 10^{-9}$	66
103	$O_2^+ + C \rightarrow O_2 + C^+$	$k_{103} = 5.2 \times 10^{-11}$	28
104	$CO + He^+ \rightarrow C^+ + O + He$	$k_{104} = 1.4 \times 10^{-9} \left(\frac{T}{300}\right)^{-0.5}$	67
105	$CO + He^+ \rightarrow C + O^+ + He$	$k_{105} = 1.4 \times 10^{-16} \left(\frac{T}{300}\right)^{-0.5}$	67
106	$CO^+ + H \rightarrow CO + H^+$	$k_{106} = 7.5 \times 10^{-10}$	68
107	$C^- + H^+ \rightarrow C + H$	$k_{107} = 2.3 \times 10^{-7} \left(\frac{T}{300}\right)^{-0.5}$	28
108	$O^- + H^+ \rightarrow O + H$	$k_{108} = 2.3 \times 10^{-7} \left(\frac{T}{300}\right)^{-0.5}$	28
109	$He^+ + H^- \rightarrow He + H$	$k_{109} = 2.32 \times 10^{-7} \left(\frac{T}{300}\right)^{-0.52} \exp\left(\frac{T}{22400}\right)$	69
110	$H_3^+ + e^- \rightarrow H_2 + H$	$k_{110} = 2.34 \times 10^{-8} \left(\frac{T}{300}\right)^{-0.52}$	70
111	$H_3^+ + e^- \rightarrow H + H + H$	$k_{111} = 4.36 \times 10^{-8} \left(\frac{T}{300}\right)^{-0.52}$	70
112	$CH^+ + e^- \rightarrow C + H$	$k_{112} = 7.0 \times 10^{-8} \left(\frac{T}{300}\right)^{-0.5}$	71
113	$CH_2^+ + e^- \rightarrow CH + H$	$k_{113} = 1.6 \times 10^{-7} \left(\frac{T}{300}\right)^{-0.6}$	72
114	$CH_2^+ + e^- \rightarrow C + H + H$	$k_{114} = 4.03 \times 10^{-7} \left(\frac{T}{300}\right)^{-0.6}$	72
115	$CH_2^+ + e^- \rightarrow C + H_2$	$k_{115} = 7.68 \times 10^{-8} \left(\frac{T}{300}\right)^{-0.6}$	72
116	$CH_3^+ + e^- \rightarrow CH_2 + H$	$k_{116} = 7.75 \times 10^{-8} \left(\frac{T}{300}\right)^{-0.5}$	73
117	$CH_3^+ + e^- \rightarrow CH + H_2$	$k_{117} = 1.95 \times 10^{-7} \left(\frac{T}{300}\right)^{-0.5}$	73
118	$CH_3^+ + e^- \rightarrow CH + H + H$	$k_{118} = 2.0 \times 10^{-7} \left(\frac{T}{300}\right)^{-0.4}$	28
119	$OH^+ + e^- \rightarrow O + H$	$k_{119} = 6.3 \times 10^{-9} \left(\frac{T}{300}\right)^{-0.48}$	74
120	$H_2O^+ + e^- \rightarrow O + H + H$	$k_{120} = 3.05 \times 10^{-7} \left(\frac{T}{300}\right)^{-0.5}$	75
121	$H_2O^+ + e^- \rightarrow O + H_2$	$k_{121} = 3.9 \times 10^{-8} \left(\frac{T}{300}\right)^{-0.5}$	75
122	$H_2O^+ + e^- \rightarrow OH + H$	$k_{122} = 8.6 \times 10^{-8} \left(\frac{T}{300}\right)^{-0.5}$	75
123	$H_3O^+ + e^- \rightarrow H + H_2O$	$k_{123} = 1.08 \times 10^{-7} \left(\frac{T}{300}\right)^{-0.5}$	76
124	$H_3O^+ + e^- \rightarrow OH + H_2$	$k_{124} = 6.02 \times 10^{-8} \left(\frac{T}{300}\right)^{-0.5}$	76
125	$H_3O^+ + e^- \rightarrow OH + H + H$	$k_{125} = 2.58 \times 10^{-7} \left(\frac{T}{300}\right)^{-0.5}$	76
126	$H_3O^+ + e^- \rightarrow O + H + H_2$	$k_{126} = 5.6 \times 10^{-9} \left(\frac{T}{300}\right)^{-0.5}$	76
127	$O_2^+ + e^- \rightarrow O + O$	$k_{127} = 1.95 \times 10^{-7} \left(\frac{T}{300}\right)^{-0.7}$	77
128	$CO^+ + e^- \rightarrow C + O$	$k_{128} = 2.75 \times 10^{-7} \left(\frac{T}{300}\right)^{-0.55}$	78
129	$HCO^+ + e^- \rightarrow CO + H$	$k_{129} = 2.76 \times 10^{-7} \left(\frac{T}{300}\right)^{-0.64}$	79
130	$HCO^+ + e^- \rightarrow OH + C$	$k_{130} = 2.4 \times 10^{-8} \left(\frac{T}{300}\right)^{-0.64}$	79
131	$HOC^+ + e^- \rightarrow CO + H$	$k_{131} = 1.1 \times 10^{-7} \left(\frac{T}{300}\right)^{-1.0}$	28
132	$H^- + C \rightarrow CH + e^-$	$k_{132} = 1.0 \times 10^{-9}$	28
133	$H^- + O \rightarrow OH + e^-$	$k_{133} = 1.0 \times 10^{-9}$	28
134	$H^- + OH \rightarrow H_2O + e^-$	$k_{134} = 1.0 \times 10^{-10}$	28
135	$C^- + H \rightarrow CH + e^-$	$k_{135} = 5.0 \times 10^{-10}$	28
136	$C^- + H_2 \rightarrow CH_2 + e^-$	$k_{136} = 1.0 \times 10^{-13}$	28
137	$C^- + O \rightarrow CO + e^-$	$k_{137} = 5.0 \times 10^{-10}$	28
138	$O^- + H \rightarrow OH + e^-$	$k_{138} = 5.0 \times 10^{-10}$	28
139	$O^- + H_2 \rightarrow H_2O + e^-$	$k_{139} = 7.0 \times 10^{-10}$	28
140	$O^- + C \rightarrow CO + e^-$	$k_{140} = 5.0 \times 10^{-10}$	28

(Glover, Federrath, Mac Low, Klessen, 2010, MNRS, 404, 2)

chemical model 2

142	$C + e^- \rightarrow C^- + \gamma$	$k_{142} = 2.25 \times 10^{-15}$		81
143	$C + H \rightarrow CH + \gamma$	$k_{143} = 1.0 \times 10^{-17}$		82
144	$C + H_2 \rightarrow CH_2 + \gamma$	$k_{144} = 1.0 \times 10^{-17}$		82
145	$C + C \rightarrow C_2 + \gamma$	$k_{145} = 4.36 \times 10^{-18} \left(\frac{T}{300}\right)^{0.35} \exp\left(-\frac{161.3}{T}\right)$		83
146	$C + O \rightarrow CO + \gamma$	$k_{146} = 2.1 \times 10^{-19}$	$T \leqslant 300$ K	84
		$= 3.09 \times 10^{-17} \left(\frac{T}{300}\right)^{0.33} \exp\left(-\frac{1629}{T}\right)$	$T > 300$ K	85
147	$C^+ + H \rightarrow CH^+ + \gamma$	$k_{147} = 4.46 \times 10^{-16} T^{-0.5} \exp\left(-\frac{4.93}{T^{2/3}}\right)$		86
148	$C^+ + H_2 \rightarrow CH_2^+ + \gamma$	$k_{148} = 4.0 \times 10^{-16} \left(\frac{T}{300}\right)^{-0.2}$		87
149	$C^+ + O \rightarrow CO^+ + \gamma$	$k_{149} = 2.5 \times 10^{-18}$	$T \leqslant 300$ K	84
		$= 3.14 \times 10^{-18} \left(\frac{T}{300}\right)^{-0.15} \exp\left(\frac{68}{T}\right)$	$T > 300$ K	
150	$O + e^- \rightarrow O^- + \gamma$	$k_{150} = 1.5 \times 10^{-15}$		28
151	$O + H \rightarrow OH + \gamma$	$k_{151} = 9.9 \times 10^{-19} \left(\frac{T}{300}\right)^{-0.38}$		28
152	$O + O \rightarrow O_2 + \gamma$	$k_{152} = 4.9 \times 10^{-20} \left(\frac{T}{300}\right)^{1.58}$		82
153	$OH + H \rightarrow H_2O + \gamma$	$k_{153} = 5.26 \times 10^{-18} \left(\frac{T}{300}\right)^{-5.22} \exp\left(-\frac{90}{T}\right)$		88
154	$H + H + H \rightarrow H_2 + H$	$k_{154} = 1.32 \times 10^{-32} \left(\frac{T}{300}\right)^{-0.38}$	$T \leqslant 300$ K	89
		$= 1.32 \times 10^{-32} \left(\frac{T}{300}\right)^{-1.0}$	$T > 300$ K	90
155	$H + H + H_2 \rightarrow H_2 + H_2$	$k_{155} = 2.8 \times 10^{-31} T^{-0.6}$		91
156	$H + H + He \rightarrow H_2 + He$	$k_{156} = 6.9 \times 10^{-32} T^{-0.4}$		92
157	$C + C + M \rightarrow C_2 + M$	$k_{157} = 5.99 \times 10^{-33} \left(\frac{T}{5000}\right)^{-1.6}$	$T \leqslant 5000$ K	93
		$= 5.99 \times 10^{-33} \left(\frac{T}{5000}\right)^{-0.64} \exp\left(\frac{5255}{T}\right)$	$T > 5000$ K	94
158	$C + O + M \rightarrow CO + M$	$k_{158} = 6.16 \times 10^{-29} \left(\frac{T}{300}\right)^{-3.08}$	$T \leqslant 2000$ K	35
		$= 2.14 \times 10^{-29} \left(\frac{T}{300}\right)^{-3.08} \exp\left(\frac{2114}{T}\right)$	$T > 2000$ K	67
159	$C^+ + O + M \rightarrow CO^+ + M$	$k_{159} = 100 \times k_{210}$		67
160	$C + O^+ + M \rightarrow CO^+ + M$	$k_{160} = 100 \times k_{210}$		67
161	$O + H + M \rightarrow OH + M$	$k_{161} = 4.33 \times 10^{-32} \left(\frac{T}{300}\right)^{-1.0}$		43
162	$OH + H + M \rightarrow H_2O + M$	$k_{162} = 2.56 \times 10^{-31} \left(\frac{T}{300}\right)^{-2.0}$		35
163	$O + O + M \rightarrow O_2 + M$	$k_{163} = 9.2 \times 10^{-34} \left(\frac{T}{300}\right)^{-1.0}$		37
164	$O + CH \rightarrow HCO^+ + e^-$	$k_{164} = 2.0 \times 10^{-11} \left(\frac{T}{300}\right)^{0.44}$		95
165	$H + H(s) \rightarrow H_2$	$k_{165} = 3.0 \times 10^{-18} T^{0.5} f_A [1.0 + 0.04(T + T_d)^{0.5} + 0.002\,T + 8 \times 10^{-6} T^2]^{-1}$	$f_A = \left[1.0 + 10^4 \exp\left(-\frac{600}{T_d}\right)\right]^{-1}$	96

(Glover, Federrath, Mac Low, Klessen, 2010, MNRS, 404, 2)

chemical model 2

Table B2. List of photochemical reactions included in our chemical model

No.	Reaction	Optically thin rate (s^{-1})	γ	Ref.
166	$H^- + \gamma \rightarrow H + e^-$	$R_{166} = 7.1 \times 10^{-7}$	0.5	1
167	$H_2^+ + \gamma \rightarrow H + H^+$	$R_{167} = 1.1 \times 10^{-9}$	1.9	2
168	$H_2 + \gamma \rightarrow H + H$	$R_{168} = 5.6 \times 10^{-11}$	See §2.2	3
169	$H_3^+ + \gamma \rightarrow H_2 + H^+$	$R_{169} = 4.9 \times 10^{-13}$	1.8	4
170	$H_3^+ + \gamma \rightarrow H_2^+ + H$	$R_{170} = 4.9 \times 10^{-13}$	2.3	4
171	$C + \gamma \rightarrow C^+ + e^-$	$R_{171} = 3.1 \times 10^{-10}$	3.0	5
172	$C^- + \gamma \rightarrow C + e^-$	$R_{172} = 2.4 \times 10^{-7}$	0.9	6
173	$CH + \gamma \rightarrow C + H$	$R_{173} = 8.7 \times 10^{-10}$	1.2	7
174	$CH + \gamma \rightarrow CH^+ + e^-$	$R_{174} = 7.7 \times 10^{-10}$	2.8	8
175	$CH^+ + \gamma \rightarrow C + H^+$	$R_{175} = 2.6 \times 10^{-10}$	2.5	7
176	$CH_2 + \gamma \rightarrow CH + H$	$R_{176} = 7.1 \times 10^{-10}$	1.7	7
177	$CH_2 + \gamma \rightarrow CH_2^+ + e^-$	$R_{177} = 5.9 \times 10^{-10}$	2.3	6
178	$CH_2^+ + \gamma \rightarrow CH^+ + H$	$R_{178} = 4.6 \times 10^{-10}$	1.7	9
179	$CH_3^+ + \gamma \rightarrow CH_2^+ + H$	$R_{179} = 1.0 \times 10^{-9}$	1.7	6
180	$CH_3^+ + \gamma \rightarrow CH^+ + H_2$	$R_{180} = 1.0 \times 10^{-9}$	1.7	6
181	$C_2 + \gamma \rightarrow C + C$	$R_{181} = 1.5 \times 10^{-10}$	2.1	7
182	$O^- + \gamma \rightarrow O + e^-$	$R_{182} = 2.4 \times 10^{-7}$	0.5	6
183	$OH + \gamma \rightarrow O + H$	$R_{183} = 3.7 \times 10^{-10}$	1.7	10
184	$OH + \gamma \rightarrow OH^+ + e^-$	$R_{184} = 1.6 \times 10^{-12}$	3.1	6
185	$OH^+ + \gamma \rightarrow O + H^+$	$R_{185} = 1.0 \times 10^{-12}$	1.8	4
186	$H_2O + \gamma \rightarrow OH + H$	$R_{186} = 6.0 \times 10^{-10}$	1.7	11
187	$H_2O + \gamma \rightarrow H_2O^+ + e^-$	$R_{187} = 3.2 \times 10^{-11}$	3.9	8
188	$H_2O^+ + \gamma \rightarrow H_2^+ + O$	$R_{188} = 5.0 \times 10^{-11}$	See §2.2	12
189	$H_2O^+ + \gamma \rightarrow H^+ + OH$	$R_{189} = 5.0 \times 10^{-11}$	See §2.2	12
190	$H_2O^+ + \gamma \rightarrow O^+ + H_2$	$R_{190} = 5.0 \times 10^{-11}$	See §2.2	12
191	$H_2O^+ + \gamma \rightarrow OH^+ + H$	$R_{191} = 1.5 \times 10^{-10}$	See §2.2	12
192	$H_3O^+ + \gamma \rightarrow H^+ + H_2O$	$R_{192} = 2.5 \times 10^{-11}$	See §2.2	12
193	$H_3O^+ + \gamma \rightarrow H_2^+ + OH$	$R_{193} = 2.5 \times 10^{-11}$	See §2.2	12
194	$H_3O^+ + \gamma \rightarrow H_2O^+ + H$	$R_{194} = 7.5 \times 10^{-12}$	See §2.2	12
195	$H_3O^+ + \gamma \rightarrow OH^+ + H_2$	$R_{195} = 2.5 \times 10^{-11}$	See §2.2	12
196	$O_2 + \gamma \rightarrow O_2^+ + e^-$	$R_{196} = 5.6 \times 10^{-11}$	3.7	7
197	$O_2 + \gamma \rightarrow O + O$	$R_{197} = 7.0 \times 10^{-10}$	1.8	7
198	$CO + \gamma \rightarrow C + O$	$R_{198} = 2.0 \times 10^{-10}$	See §2.2	13

(Glover, Federrath, Mac Low, Klessen, 2010, MNRS, 404, 2)

chemical model 2

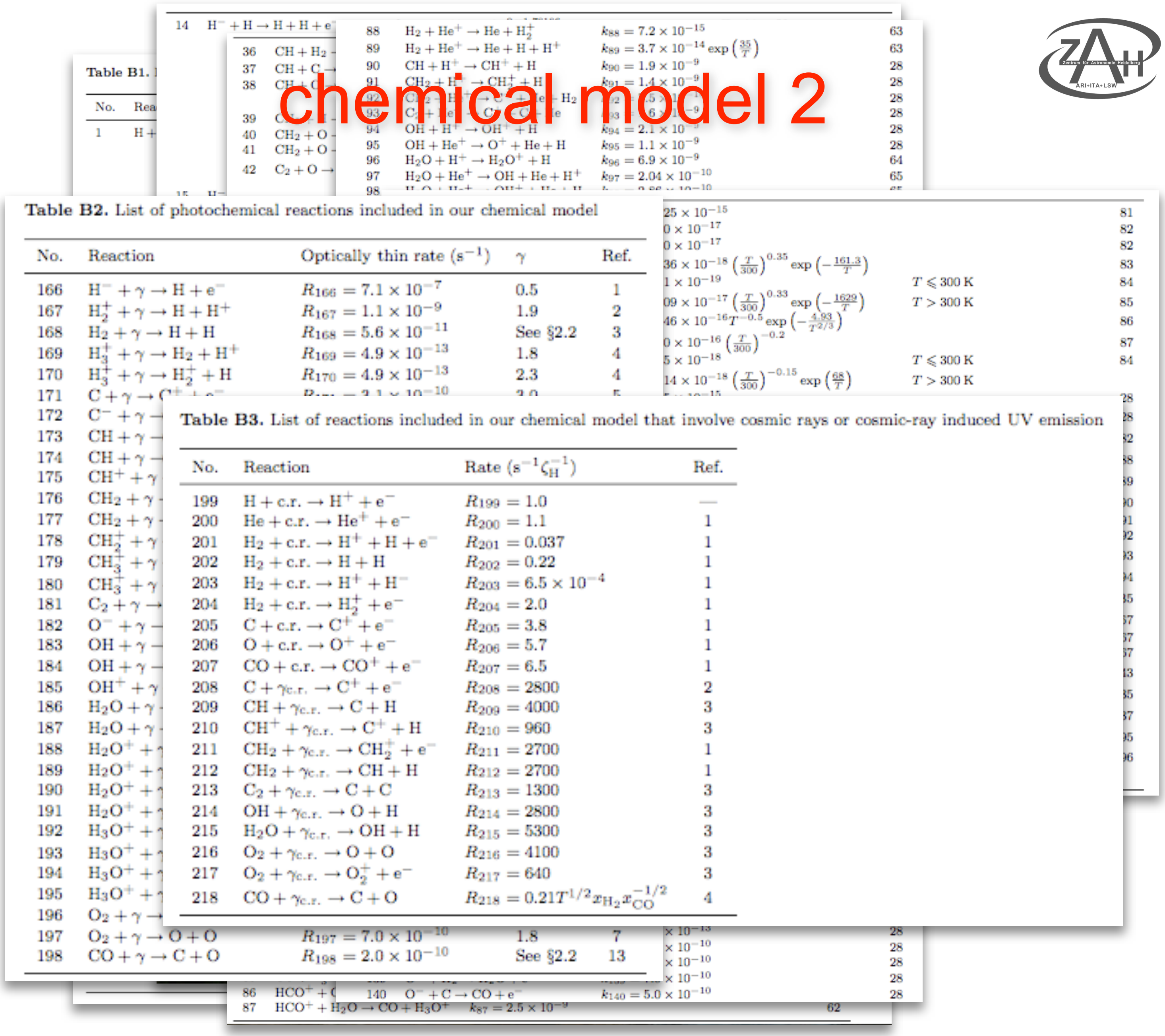

Table B2. List of photochemical reactions included in our chemical model

No.	Reaction	Optically thin rate (s^{-1})	γ	Ref.
166	$H^- + \gamma \rightarrow H + e^-$	$R_{166} = 7.1 \times 10^{-7}$	0.5	1
167	$H_2^+ + \gamma \rightarrow H + H^+$	$R_{167} = 1.1 \times 10^{-9}$	1.9	2
168	$H_2 + \gamma \rightarrow H + H$	$R_{168} = 5.6 \times 10^{-11}$	See §2.2	3
169	$H_3^+ + \gamma \rightarrow H_2 + H^+$	$R_{169} = 4.9 \times 10^{-13}$	1.8	4
170	$H_3^+ + \gamma \rightarrow H_2^+ + H$	$R_{170} = 4.9 \times 10^{-13}$	2.3	4
197	$O_2 + \gamma \rightarrow O + O$	$R_{197} = 7.0 \times 10^{-10}$	1.8	7
198	$CO + \gamma \rightarrow C + O$	$R_{198} = 2.0 \times 10^{-10}$	See §2.2	13

Table B3. List of reactions included in our chemical model that involve cosmic rays or cosmic-ray induced UV emission

No.	Reaction	Rate ($s^{-1}\zeta_H^{-1}$)	Ref.
199	$H + c.r. \rightarrow H^+ + e^-$	$R_{199} = 1.0$	—
200	$He + c.r. \rightarrow He^+ + e^-$	$R_{200} = 1.1$	1
201	$H_2 + c.r. \rightarrow H^+ + H + e^-$	$R_{201} = 0.037$	1
202	$H_2 + c.r. \rightarrow H + H$	$R_{202} = 0.22$	1
203	$H_2 + c.r. \rightarrow H^+ + H^-$	$R_{203} = 6.5 \times 10^{-4}$	1
204	$H_2 + c.r. \rightarrow H_2^+ + e^-$	$R_{204} = 2.0$	1
205	$C + c.r. \rightarrow C^+ + e^-$	$R_{205} = 3.8$	1
206	$O + c.r. \rightarrow O^+ + e^-$	$R_{206} = 5.7$	1
207	$CO + c.r. \rightarrow CO^+ + e^-$	$R_{207} = 6.5$	1
208	$C + \gamma_{c.r.} \rightarrow C^+ + e^-$	$R_{208} = 2800$	2
209	$CH + \gamma_{c.r.} \rightarrow C + H$	$R_{209} = 4000$	3
210	$CH^+ + \gamma_{c.r.} \rightarrow C^+ + H$	$R_{210} = 960$	3
211	$CH_2 + \gamma_{c.r.} \rightarrow CH_2^+ + e^-$	$R_{211} = 2700$	1
212	$CH_2 + \gamma_{c.r.} \rightarrow CH + H$	$R_{212} = 2700$	1
213	$C_2 + \gamma_{c.r.} \rightarrow C + C$	$R_{213} = 1300$	3
214	$OH + \gamma_{c.r.} \rightarrow O + H$	$R_{214} = 2800$	3
215	$H_2O + \gamma_{c.r.} \rightarrow OH + H$	$R_{215} = 5300$	3
216	$O_2 + \gamma_{c.r.} \rightarrow O + O$	$R_{216} = 4100$	3
217	$O_2 + \gamma_{c.r.} \rightarrow O_2^+ + e^-$	$R_{217} = 640$	3
218	$CO + \gamma_{c.r.} \rightarrow C + O$	$R_{218} = 0.21 T^{1/2} x_{H_2} x_{CO}^{-1/2}$	4

(Glover, Federrath, Mac Low, Klessen, 2010, MNRS, 404, 2)

HI to H2 conversion rate

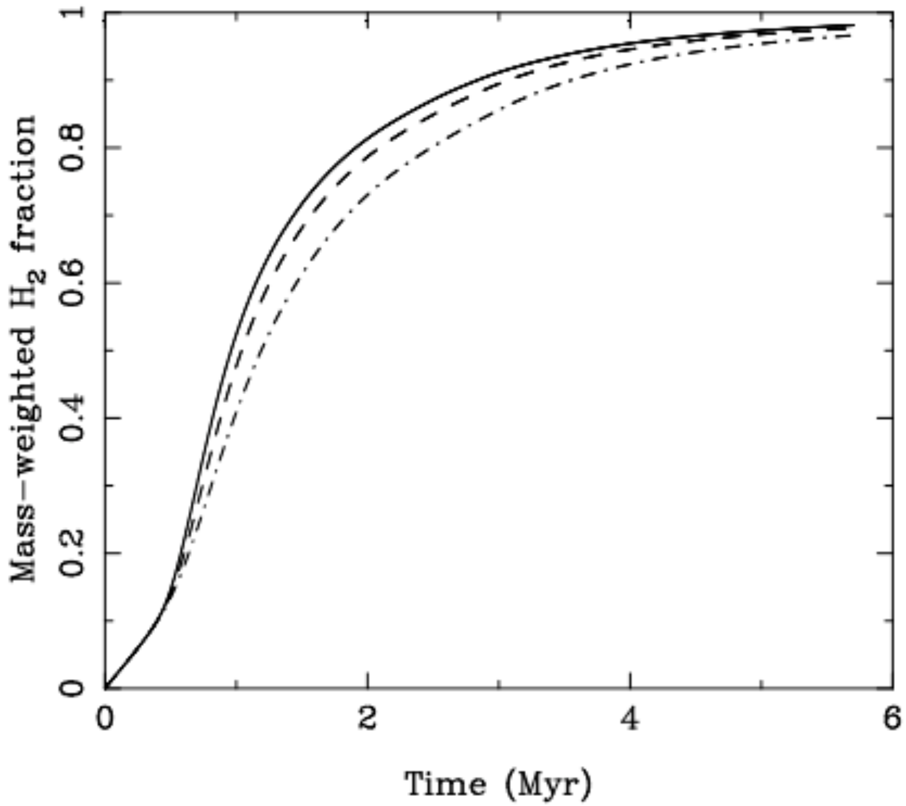

Figure 4. Time evolution of the mass-weighted H_2 abundance in simulations R1, R2 and R3, which have numerical resolutions of 64^3 zones (dot-dashed), 128^3 zones (dashed) and 256^3 zones (solid), respectively.

(Glover, Federrath, Mac Low, Klessen, 2010)

HI to H2 conversion rate

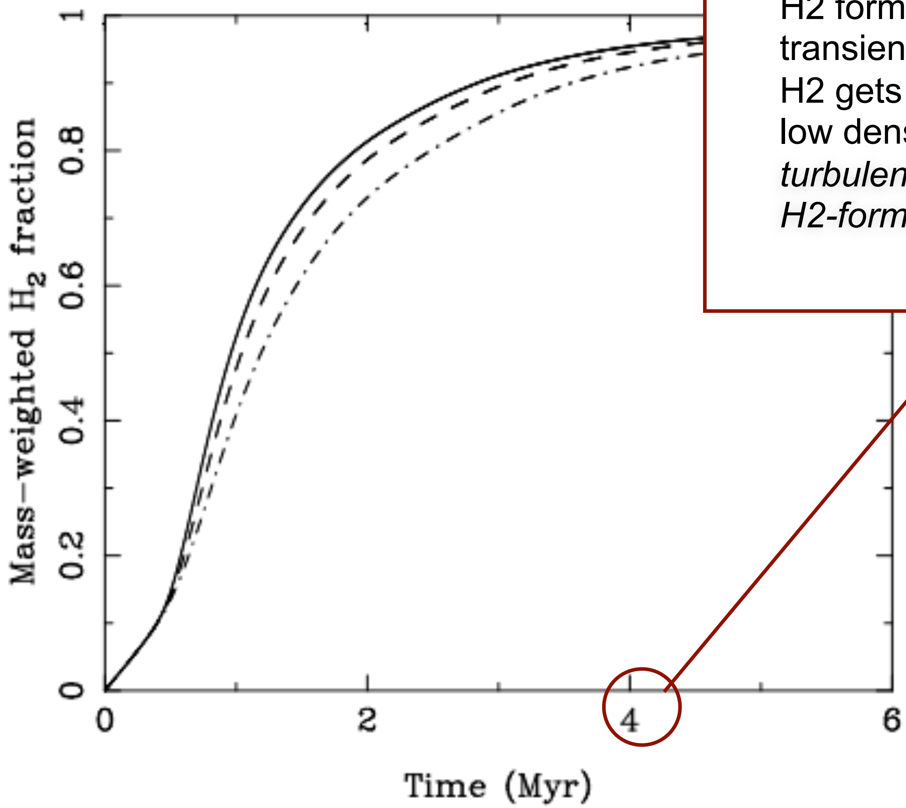

H2 forms rapidly in shocks / transient density fluctuations / H2 gets destroyed slowly in low density regions / *result: turbulence greatly enhances H2-formation rate*

Figure 4. Time evolution of the mass-weighted H_2 abundance in simulations R1, R2 and R3, which have numerical resolutions of 64^3 zones (dot-dashed), 128^3 zones (dashed) and 256^3 zones (solid), respectively.

(Glover, Federrath, Mac Low, Klessen, 2010)

HI to H2 conversion rate

compare to data from
Tamburro et al. (2008) study:

t_{form} ~ few x 10^6 years

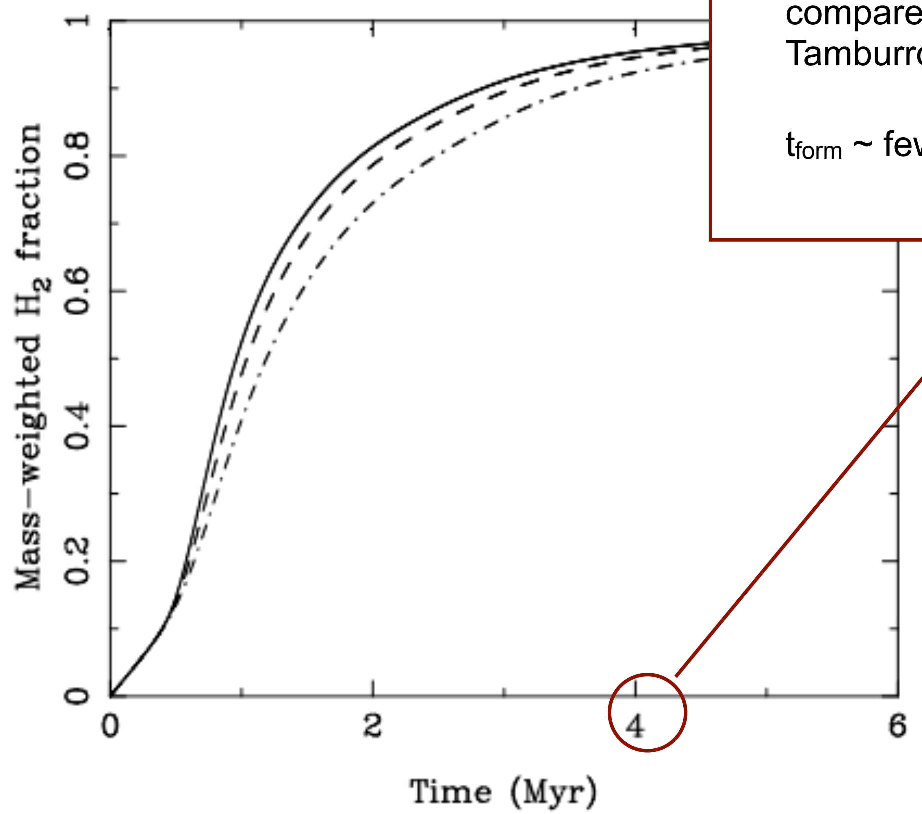

Figure 4. Time evolution of the mass-weighted H_2 abundance in simulations R1, R2 and R3, which have numerical resolutions of 64^3 zones (dot-dashed), 128^3 zones (dashed) and 256^3 zones (solid), respectively.

(Glover, Federrath, Mac Low, Klessen, 2010)

CO, C$^+$ formation rates

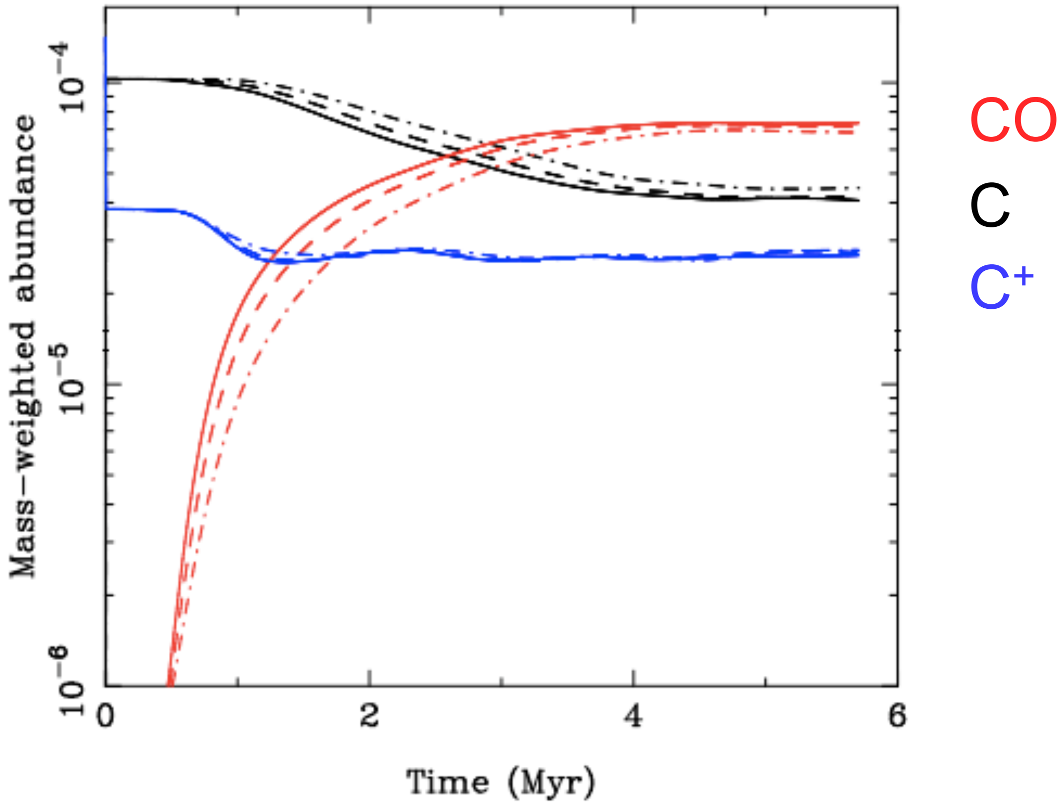

Figure 5. Time evolution of the mass-weighted abundances of atomic carbon (black lines), CO (red lines), and C$^+$ (blue lines) in simulations with numerical resolutions of 64^3 zones (dot-dashed), 128^3 zones (dashed) and 256^3 zones (solid).

(Glover, Federrath, Mac Low, Klessen, 2010)

effects of chemistry 1

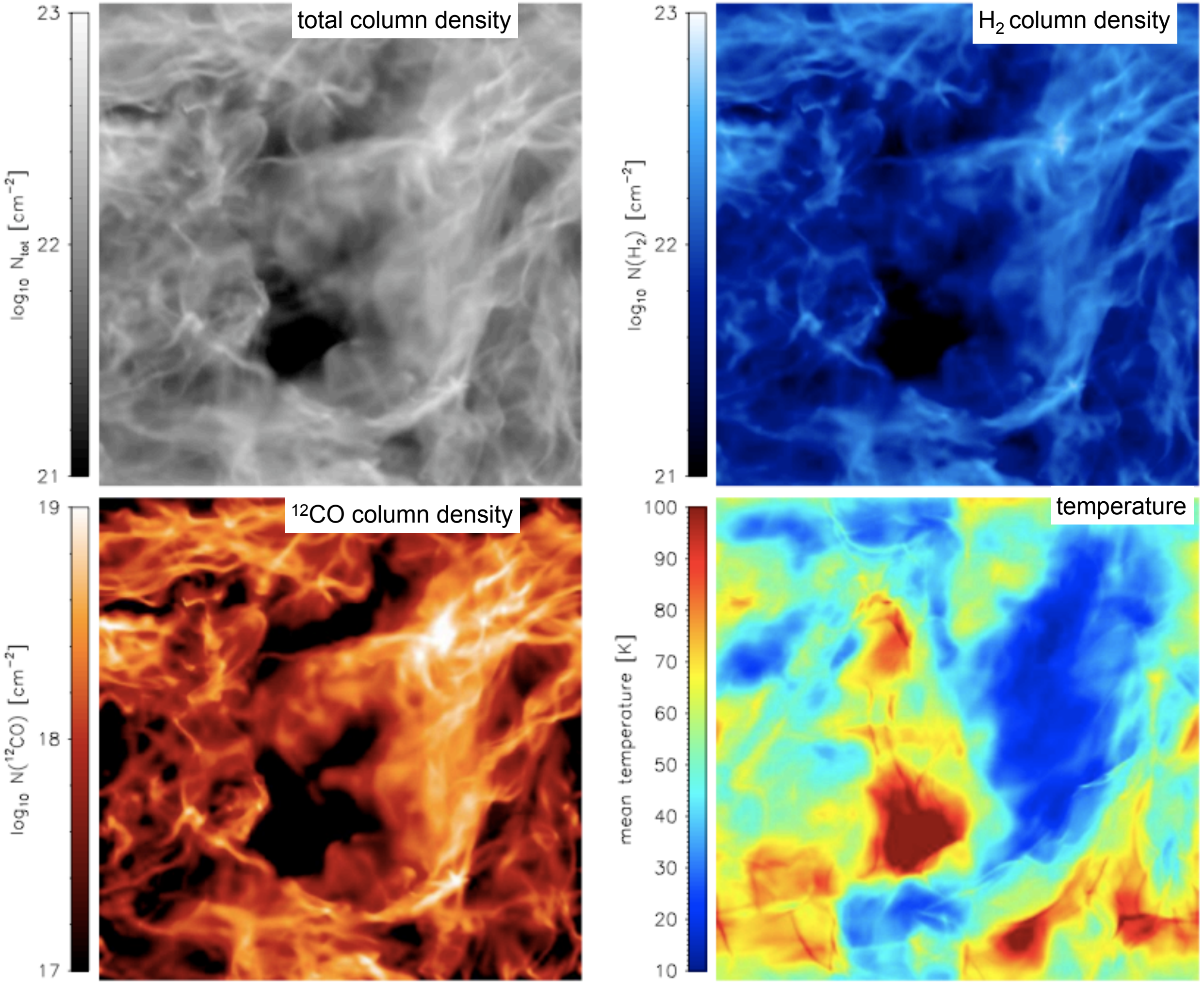

(Glover, Federrath, Mac Low, Klessen, 2010)

effects of chemistry 2

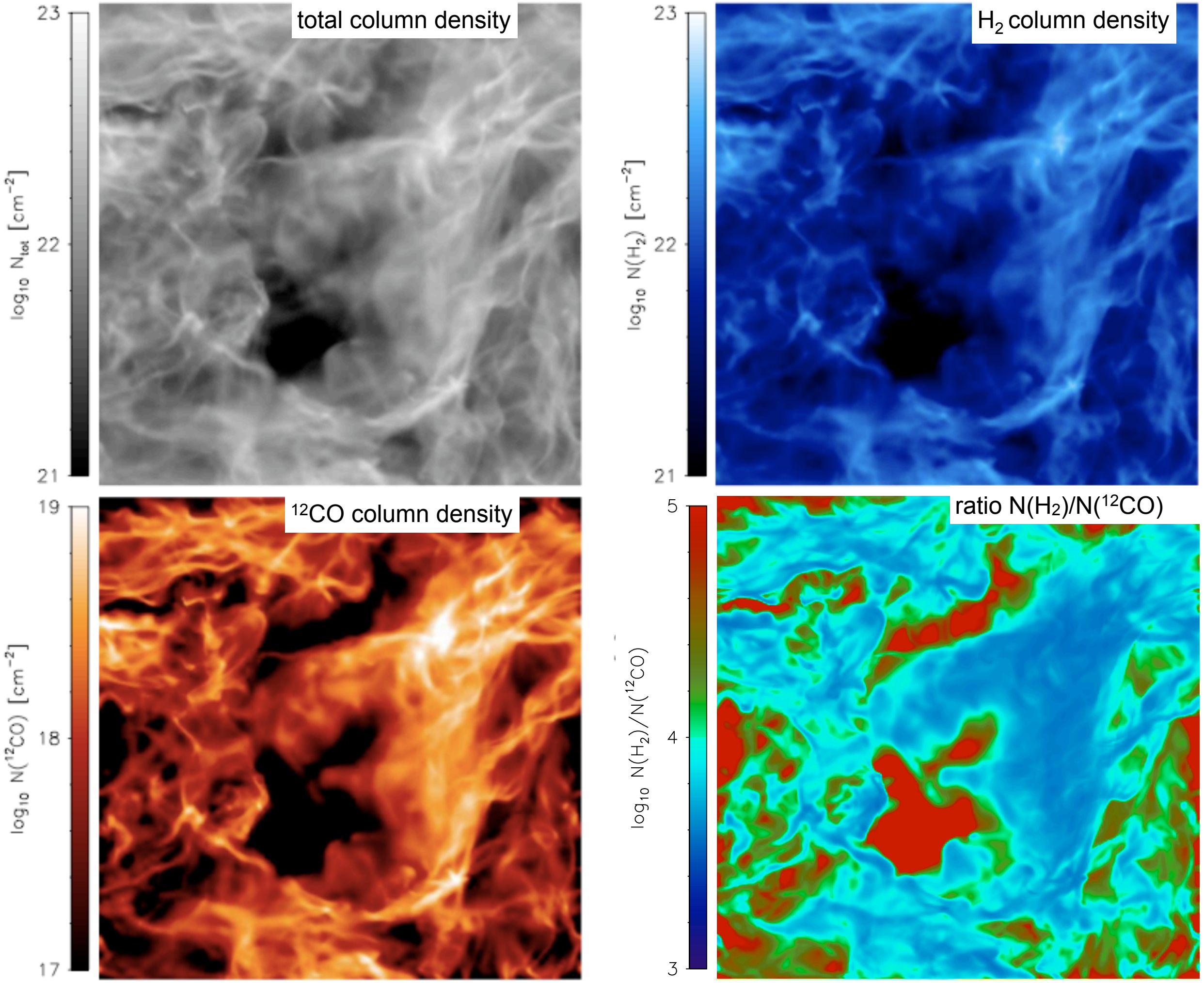

(Glover, Federrath, Mac Low, Klessen, 2010)

effects of chemistry 4

- deliverables / predictions:
  - x-factor estimates (as function of environmental conditions)
  - synthetic line emission maps (in combination with line transfer)
  - pdf's of density, velocity, emissivity / structure functions (to directly connect to observational regime)
  - *COMMENT:* density pdf is *NOT* lognormal!
    --> implications for analytical IMF theories

X-factor

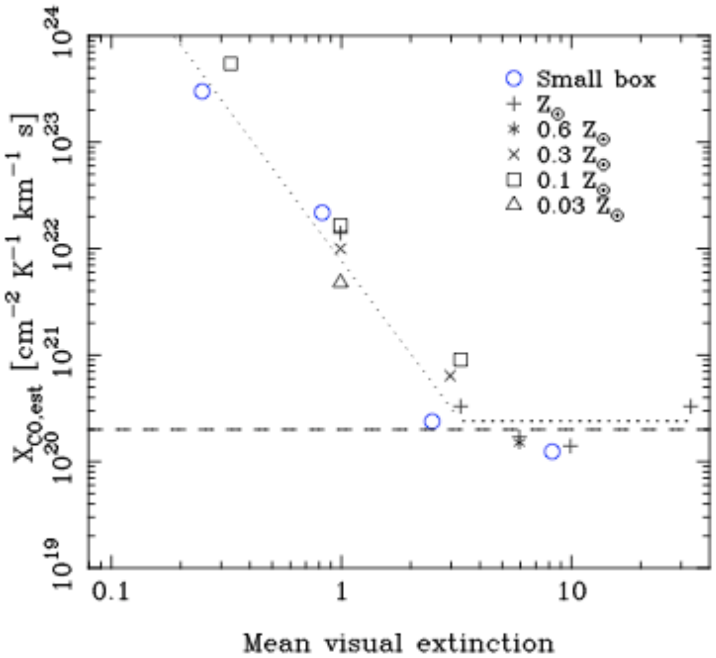

Figure 8. Estimate of the CO-to-H_2 conversion factor $X_{CO,est}$, plotted as a function of the mean visual extinction of the gas, $\langle A_V \rangle$. The simplifications made in our modelling mean that each value of $X_{CO,est}$ is uncertain by at least a factor of two. At $\langle A_V \rangle > 3$, the values we find are consistent with the value of $X_{CO} = 2 \times 10^{20} cm^{-2} K^{-1} km^{-1}$ s determined observationally for the Milky Way by Dame et al. (2001), indicated in the plot by the horizontal dashed line. At $\langle A_V \rangle < 3$, we find evidence for a strong dependence of $X_{CO,est}$ on $\langle A_V \rangle$. The empirical fit given by Equation 11 is indicated as the dotted line in the Figure, and demonstrates that at low $\langle A_V \rangle$, the CO-to-H_2 conversion factor increases roughly as $X_{CO,est} \propto A_V^{-2.8}$. It should also be noted that at any particular $\langle A_V \rangle$, the dependence of $X_{CO,est}$ on metallicity is relatively small. Previous claims of a strong metallicity dependence likely reflect the fact that there is a strong dependence on the mean extinction, which varies as $\langle A_V \rangle \propto Z$ given fixed mean cloud density and cloud size.

from Glover & Mac Low (2010, ApJ, submitted)

from atomic gas to molecular clouds

- importance of dynamics:
  - how does molecular cloud material form in convergent flows, e.g., as triggered by spiral density waves...?
  - do sequence of idealized numerical experiments
- questions
  - are molecular clouds truly “multi-phase” media?
  - turbulence? dynamical & morphological properties?
  - what is relation to initial & environmental conditions?
  - magnetic field structure?

convergent flows: set-up

numerical set-up

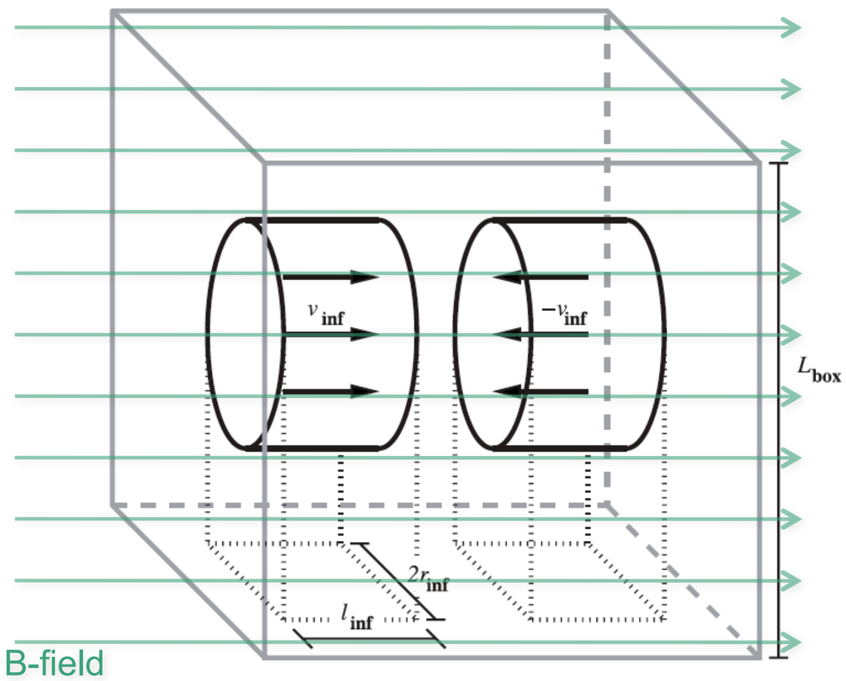

from Vazquez-Semadeni et al. (2007)

- convergent flow studies
  - atomic flows collide
  - cooling curve (soon chemistry)
  - gravity
  - magnetic fields
  - numerics: AMR, BGK, SPH

see studies by Banerjee et al., Heitsch et al., Hennebelle et al., Vazquez-Semadeni et al.

convergent flows: set-up

adopted cooling curve

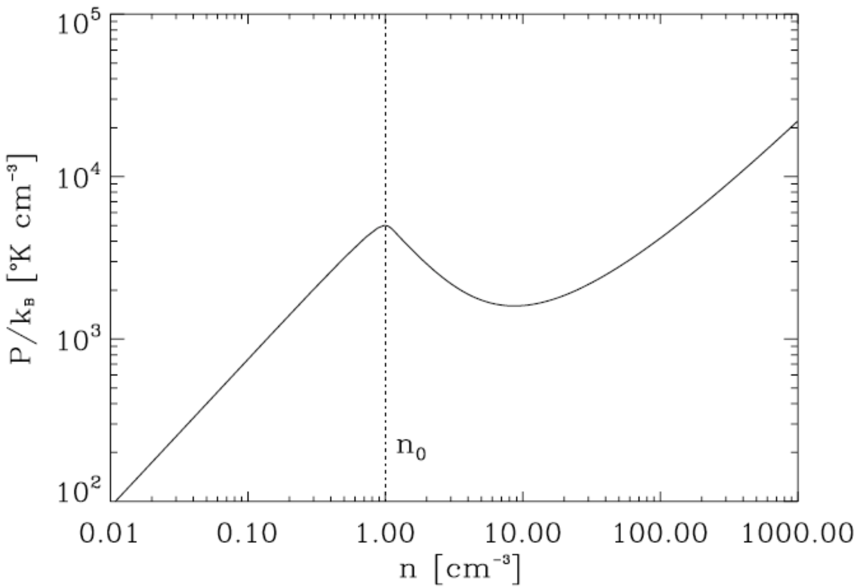

from Vazquez-Semadeni et al. (2007)

- convergent flow studies
  - atomic flows collide
  - cooling curve (soon chemistry)
  - gravity
  - magnetic fields
  - numerics: AMR, BGK, SPH

see studies by Banerjee et al., Heitsch et al., Hennebelle et al., Vazquez-Semadeni et al.

MC formation in convergent flows

thermal instability + gravity creates complex molecular cloud structure:

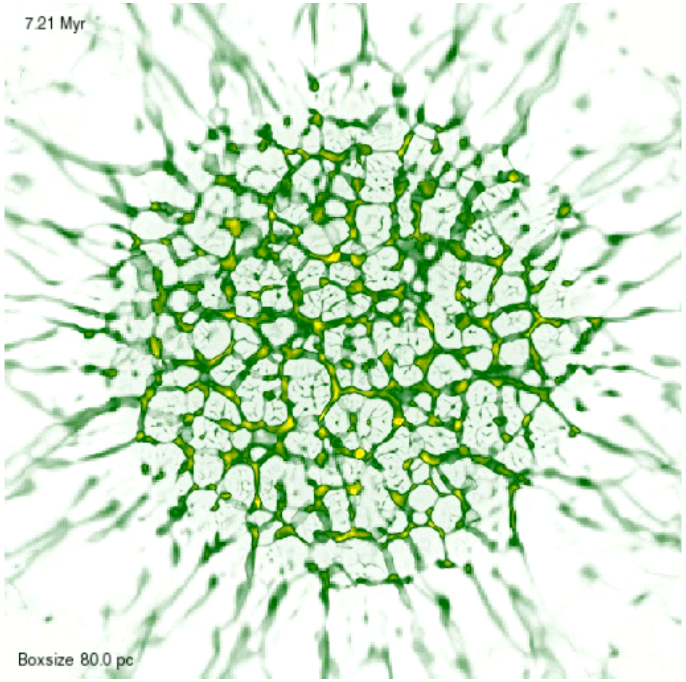

from Banerjee et al. (2008)
(see also studies by Hennebelle et al. and Vazquez-Semadeni et al. and Heitsch et al.)

MC formation in convergent flows

this simple set-up reproduces (and explains!) some of the main properties of MCs:

- highly patchy and clumpy
- high fraction of substructure
- cold dense molecular clumps coexist with warm atomic gas
- not a well bounded entity
- dynamical evolution (different star formation modes: from low mass to high mass SF?)

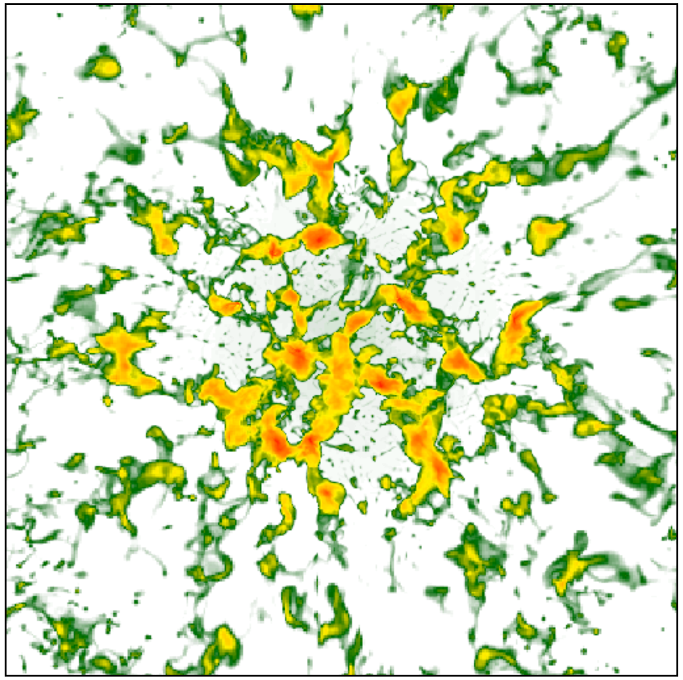

from Banerjee et al. (2008)
(see also studies by Hennebelle et al. and Vazquez-Semadeni et al. and Heitsch et al.)

MC formation in convergent flows

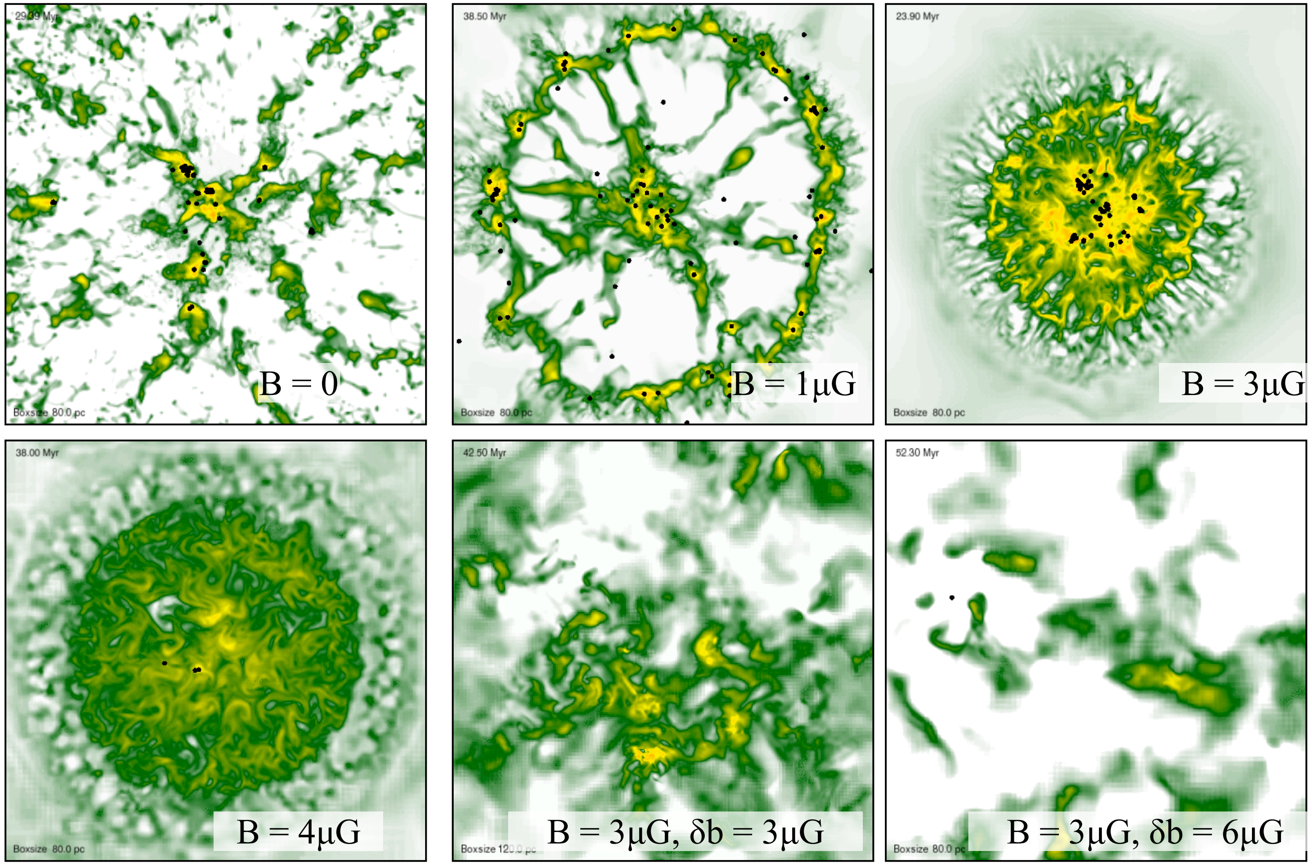

Morphology of the molecular cloud and star formation efficiency depends on the strength of the magnetic field

Banerjee et al. in prep.

MC formation in convergent flows

morphology and clump evolution

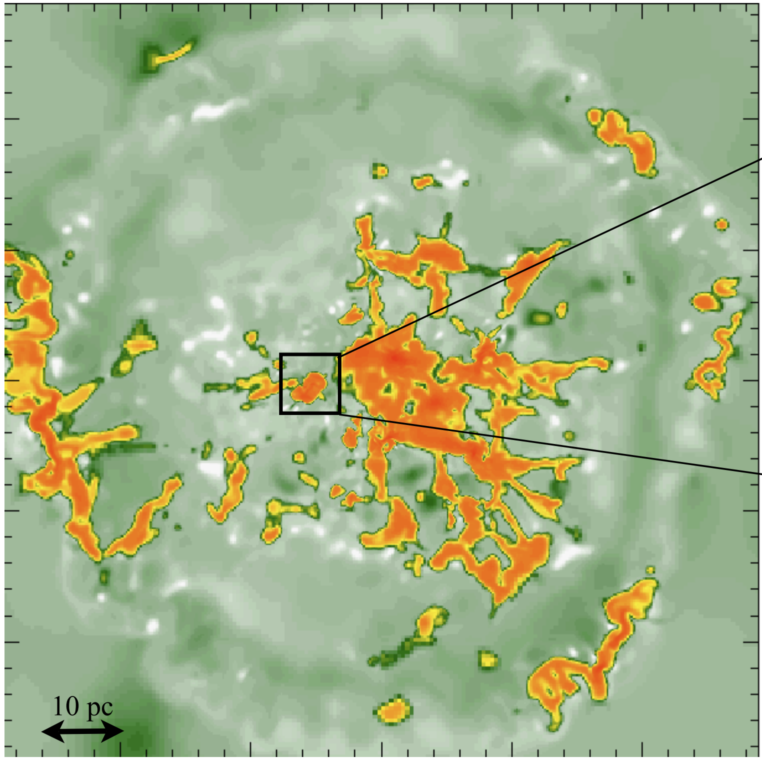

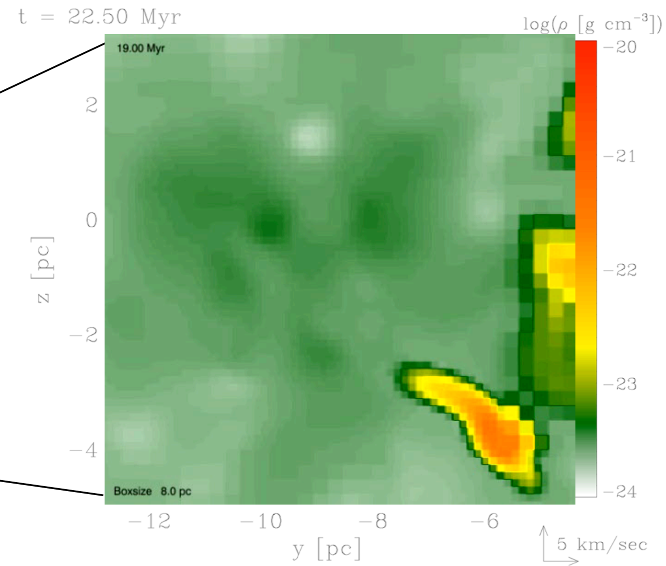

- MCs are inhomogeneous
- cold clumps embedded in warm atomic gas

- clumps growth by outward propagation of boundary layers and
- coalescence at later times

see studies by Banerjee et al., Heitsch et al., Hennebelle et al., Vazquez-Semadeni et al.

some results: growth of cores

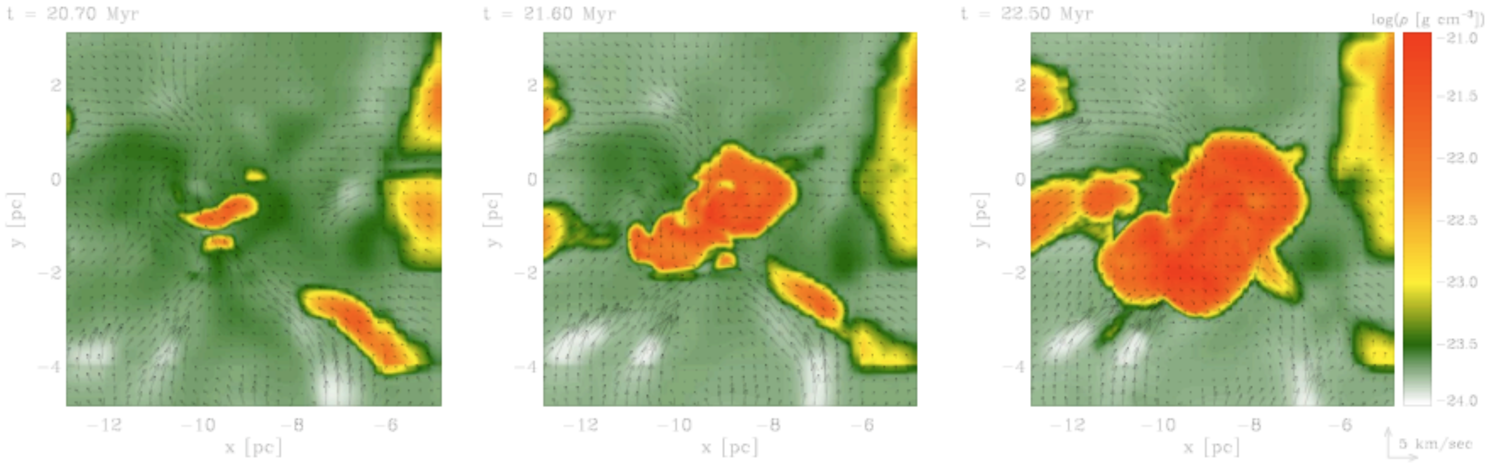

Figure 2. Shows the time evolution of a typical clump which initially develops out of the thermally unstable WNM in shock layers of turbulent flows. A small cold condensate grows by outward propagation of its boundary layer. Coalescence and merging with nearby clumps further increases the size and mass of these clumps. The global gravitational potential of the proto-cloud enhances the merging probability with time. The images show 2D slices of the density (logarithmic colour scale) and the gas velocity (indicated as arrows) in the plane perpendicular to the large scale flows.

two phases of core growth:
(1) by *outward propagation* of *boundary layer* → Jeans sub-critical phase
(2) *core mergers* → super-Jeans → gravitational collapse & star formation
example: *Pipe nebula* ???

from Banerjee et al. (2008)

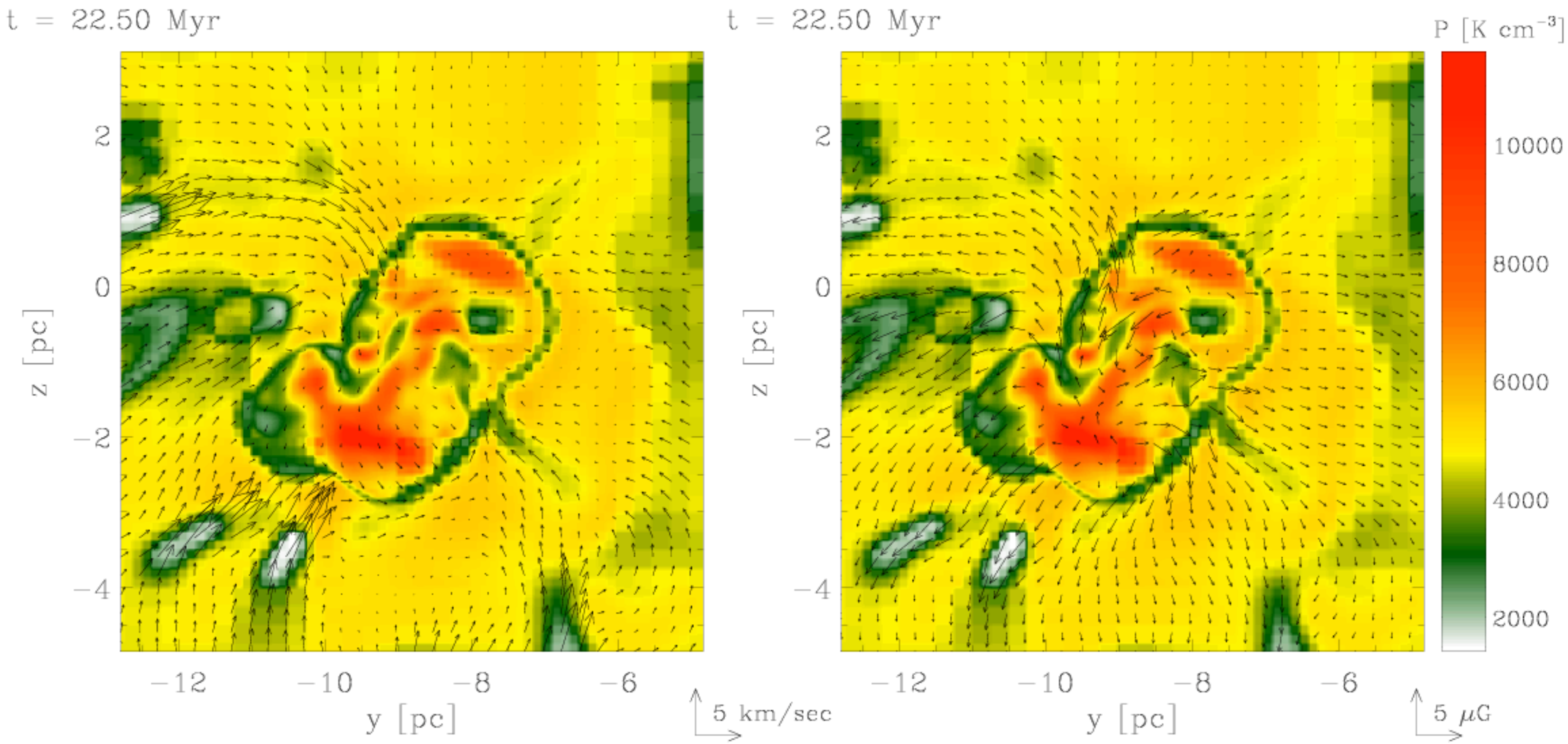

- cores roughly in pressure balance with surroudings
- relation between flow and magnetic field: mass flow mostly along field lines

from Banerjee et al. (2008)

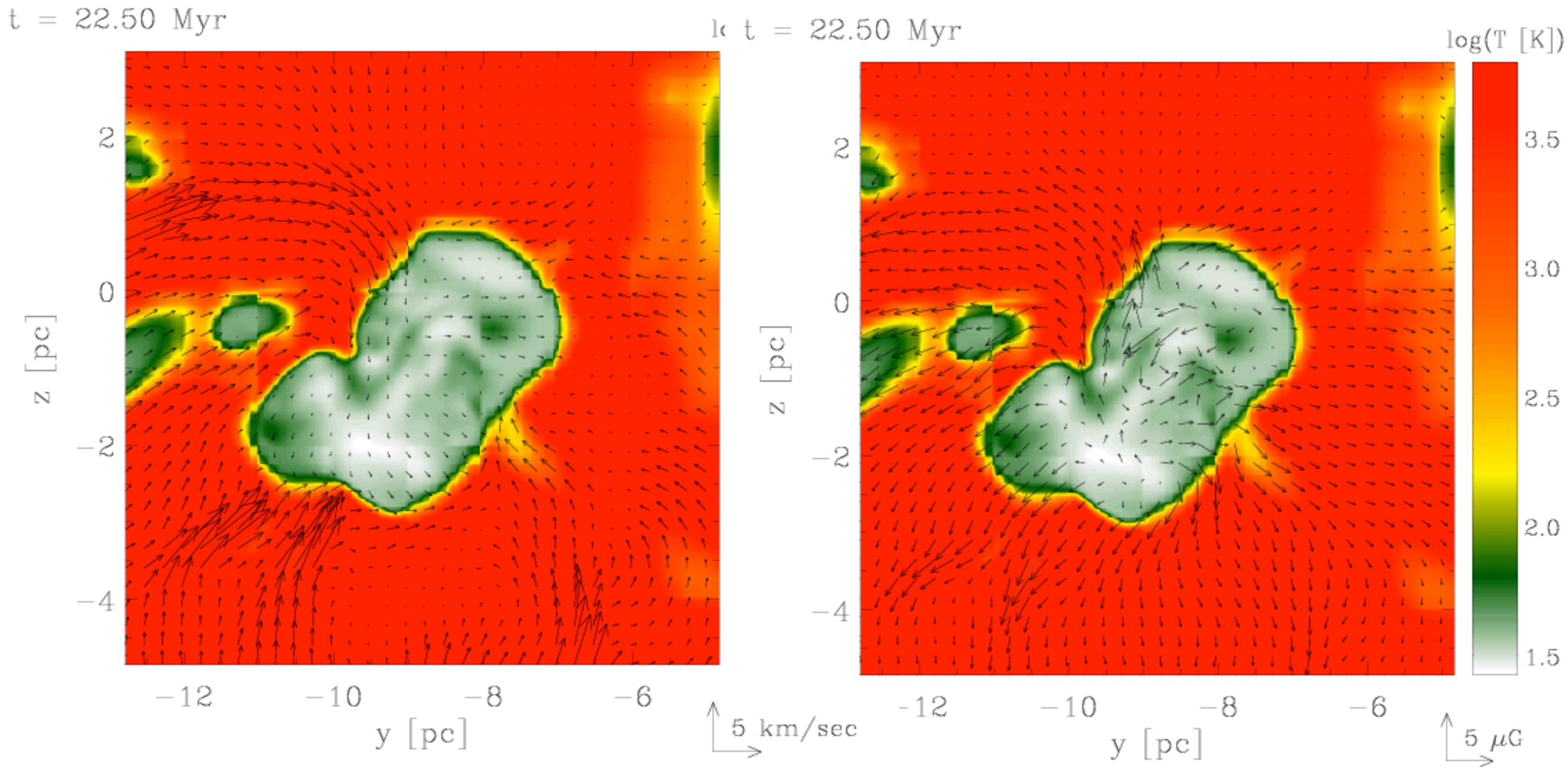

- typical core densities $n \sim 2 – 5 \times 10^3\ cm^{-3}$
- typical core temperatures $T \sim 30 – 50\ K$

from Banerjee et al. (2008)

some results: statistical correlations

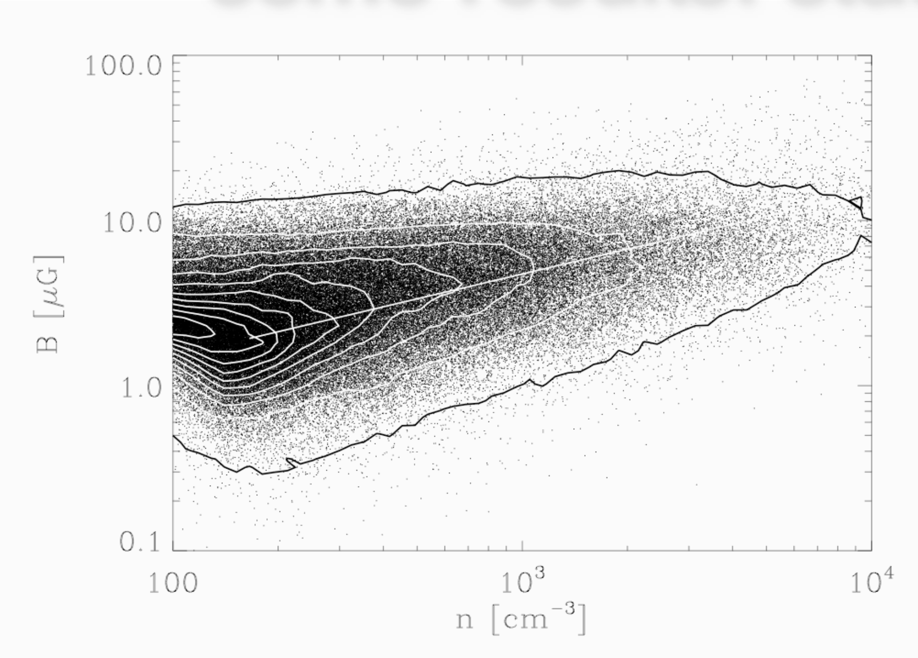

• strong correlation of gas streams and magnetic field lines

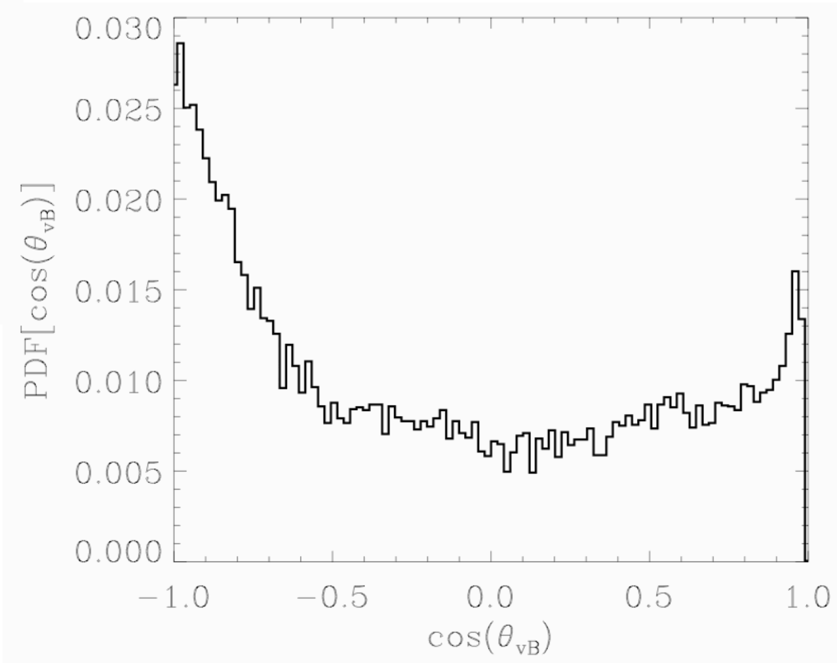

- large scatter of magnetic field strengths: sub- and super-critical cores exist
- median slope: $B \propto n^{0.5}$ (e.g. *Crutcher 1999*)

some results: loci of high-mass stars

global contraction phase

center of the cloud
→ birthplace for **massive stars**?
(eg. Zinnecker & Yorke 2007)

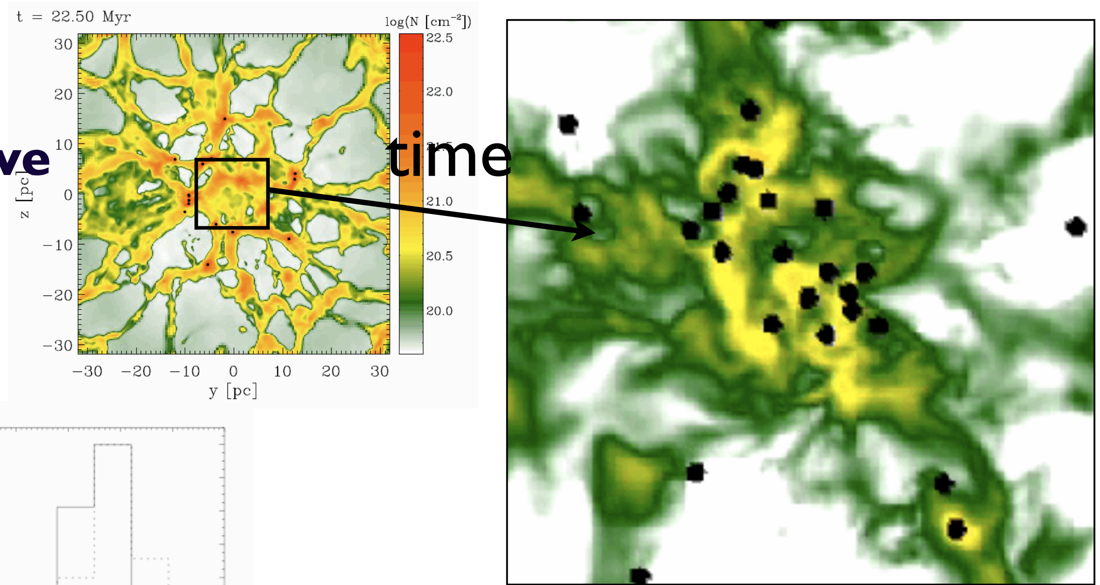

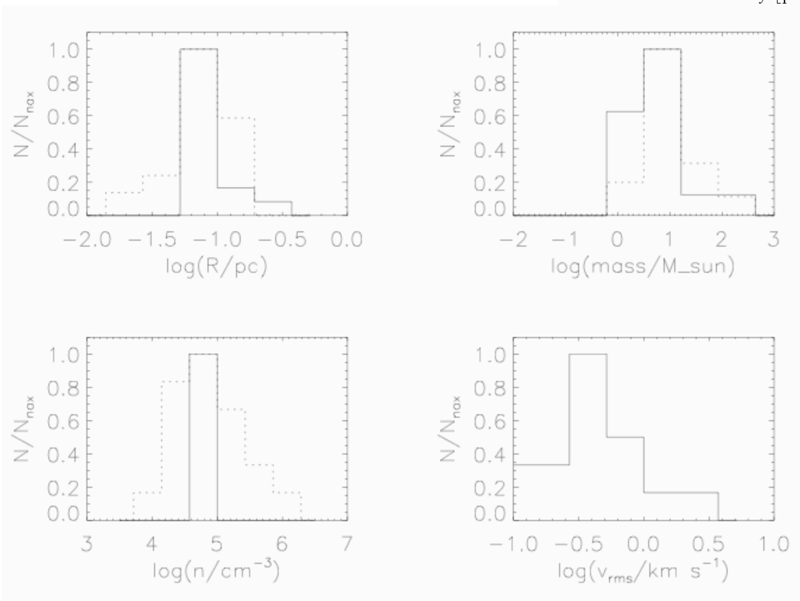

comparison of core properties with observation of Cygnus X by *Motte et al 2007*

Vazquez-Semadeni et al. 2008

dynamical SF in a nutshell

- interstellar gas is highly *inhomogeneous*
  - *gravitational instability*
  - *thermal instability*
  - *turbulent compression* (in shocks $\delta\rho/\rho \propto \mathcal{M}^2$; in atomic gas: $\mathcal{M} \approx 1...3$)

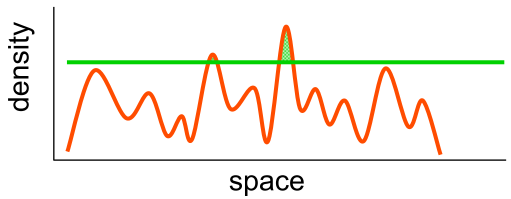

- cold *molecular clouds* can form rapidly in high-density regions at *stagnation points* of *convergent large-scale flows*
  - chemical *phase transition*: atomic → molecular
  - process is *modulated* by large-scale *dynamics* in the galaxy
- inside *cold clouds:* turbulence is highly supersonic ($\mathcal{M} \approx 1...20$)
  → *turbulence* creates large density contrast,
  gravity selects for collapse

  → ***GRAVOTUBULENT FRAGMENTATION***
- *turbulent cascade:* local compression *within* a cloud provokes collapse → formation of individual *stars* and *star clusters*

(e.g. Mac Low & Klessen, 2004, Rev. Mod. Phys., 76, 125-194)

turbulence

Turbulent cascade

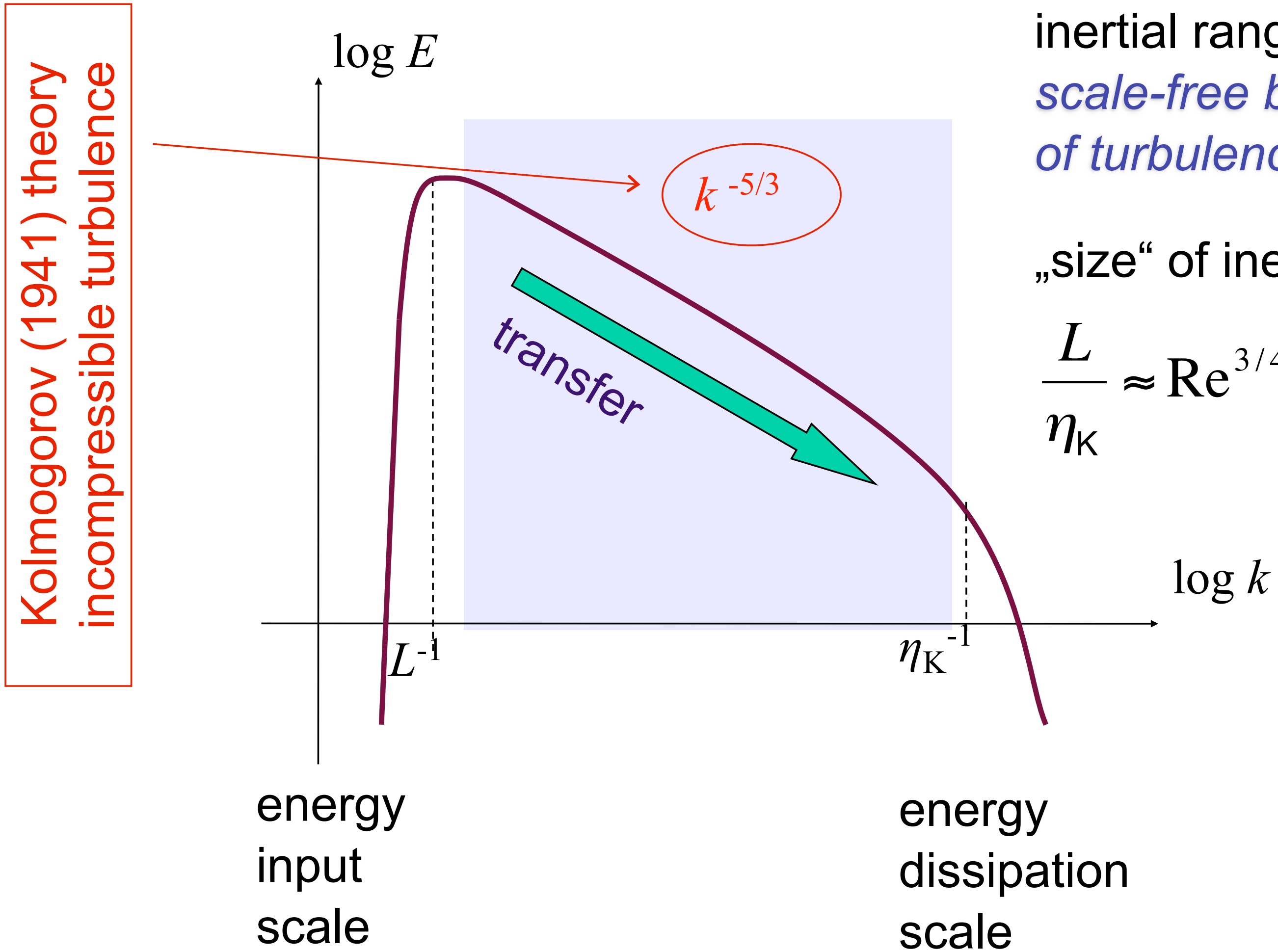

inertial range:
scale-free behavior of turbulence

„size“ of inertial range:

$$\frac{L}{\eta_K} \approx \mathrm{Re}^{3/4}$$

Turbulent cascade

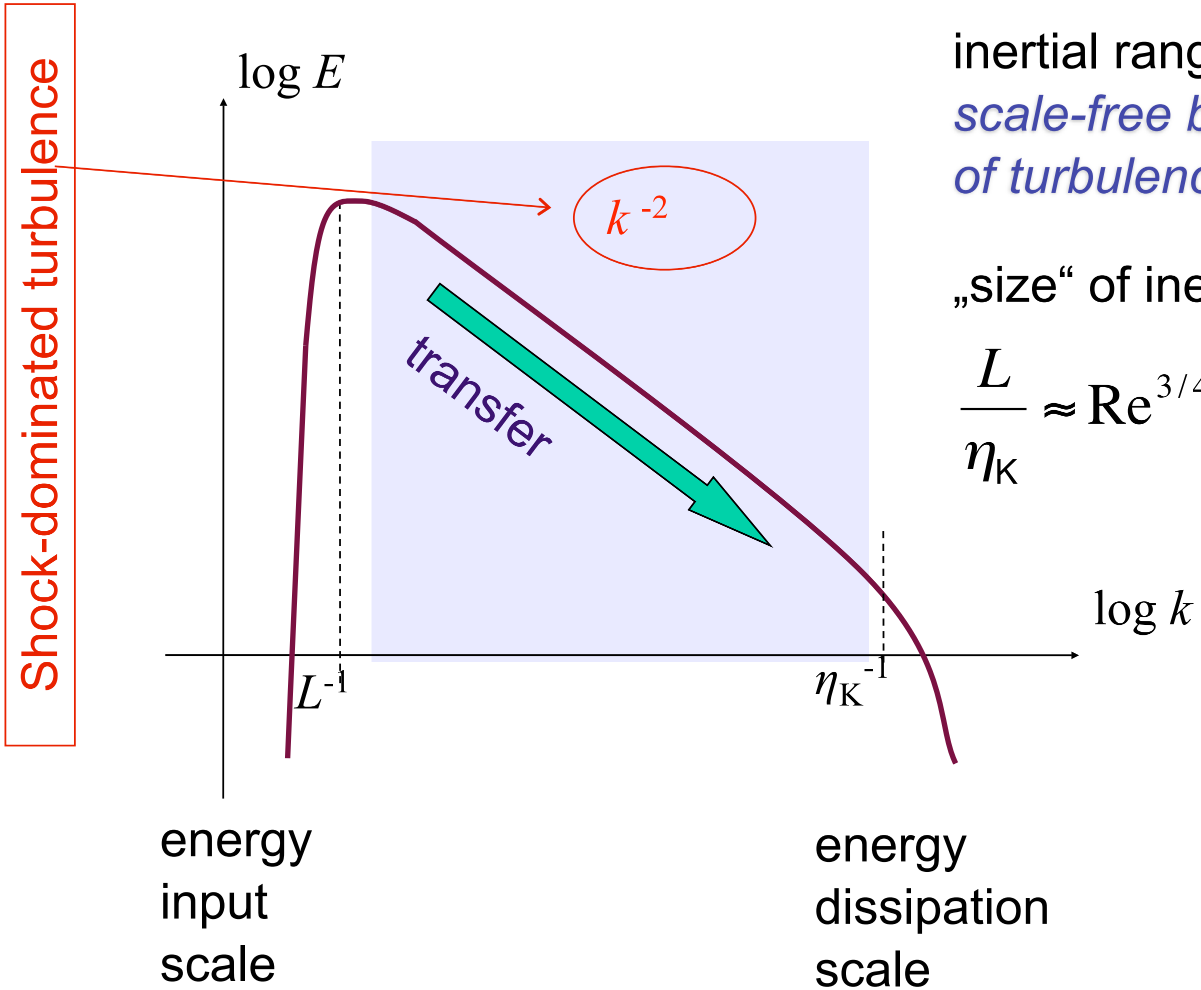

inertial range:
scale-free behavior
of turbulence

„size“ of inertial range:

$$\frac{L}{\eta_K} \approx \mathrm{Re}^{3/4}$$

Turbulent cascade in ISM

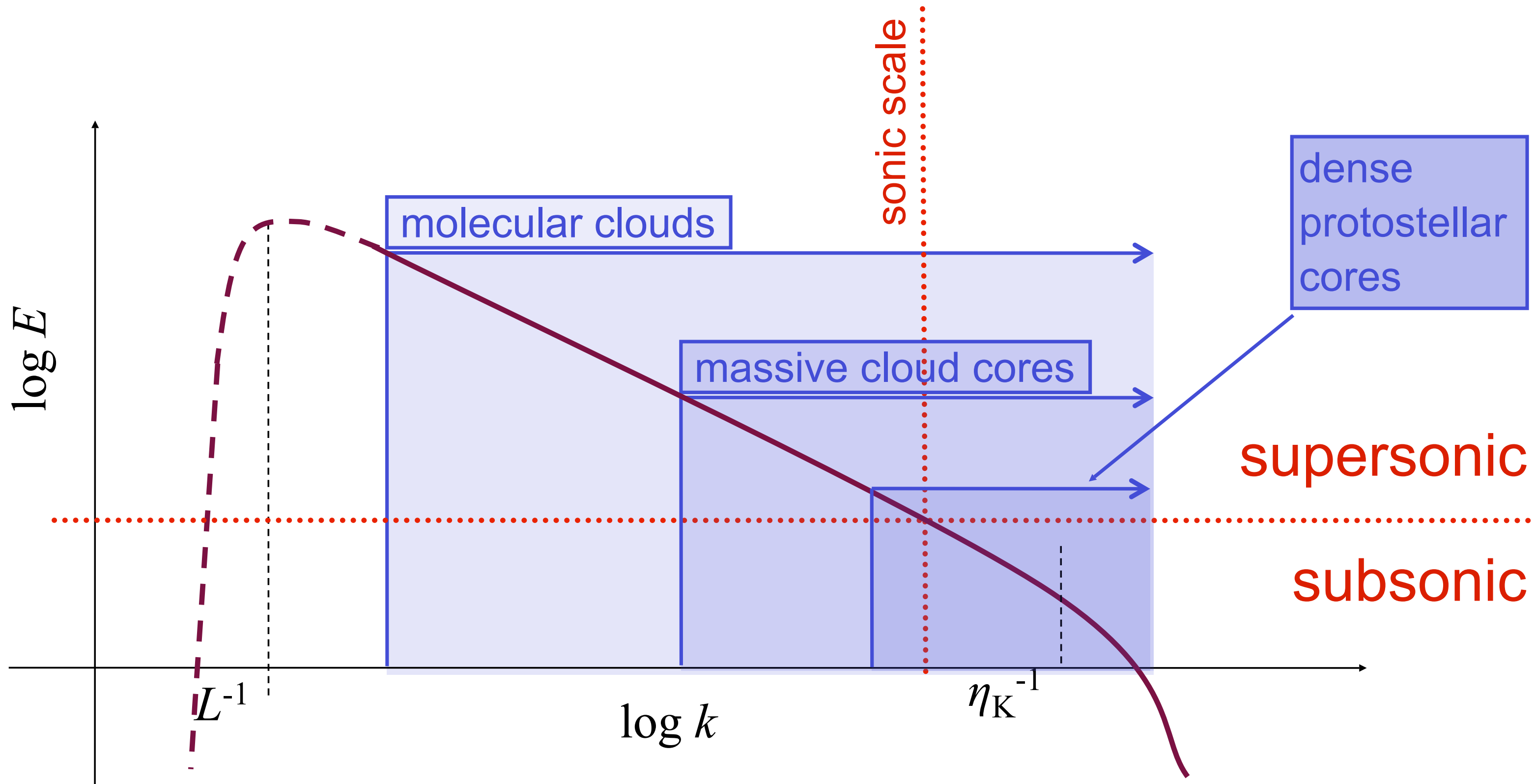

energy source & scale
NOT known
(supernovae, winds, spiral density waves?)

σ_{rms} << 1 km/s
$M_{rms} \leq 1$
L ≈ 0.1 pc

dissipation scale not known
(ambipolar diffusion, molecular diffusion?)

what drives ISM turbulence?

- seems to be driven on large scales, little difference between star-forming and non-SF clouds
  ---> rules out internal sources
- proposals in the literature
  - supernovae
  - expanding HII regions / stellar winds / outflows
  - spiral density waves
  - magneto-rotational instability
  - new idea: accretion onto disk

what drives ISM turbulence?

some energetic arguments...

energy decay by turbulent dissipation:

$$\dot{e} \simeq -(1/2)\rho v_{\rm rms}^3/L_{\rm d}$$
$$= -(3\times 10^{-27}\ {\rm erg\,cm^{-3}\,s^{-1}})\left(\frac{n}{1\ {\rm cm^{-3}}}\right)$$
$$\times\left(\frac{v_{\rm rms}}{10\ {\rm km\,s^{-1}}}\right)^3\left(\frac{L_{\rm d}}{100\ {\rm pc}}\right)^{-1},$$

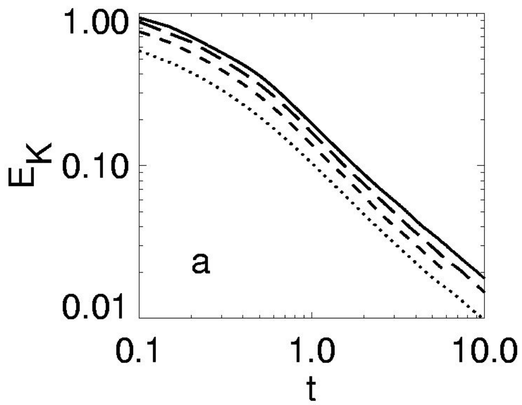

(Mac Low et al. 1999)

decay timescale:

$$\tau_{\rm d} = e/\dot{e} \simeq L_{\rm d}/v_{\rm rms}$$
$$= (9.8\ {\rm Myr})\left(\frac{L_{\rm d}}{100\ {\rm pc}}\right)\left(\frac{v_{\rm rms}}{10\ {\rm km\,s^{-1}}}\right)^{-1},$$

(from Mac Low & Klessen, 2004)

what drives ISM turbulence?

magneto-rotational instability:

$$\dot{e} = (3 \times 10^{-29}\ \mathrm{erg\,cm^{-3}\,s^{-1}}) \left(\frac{B}{3\,\mu\mathrm{G}}\right)^2 \left(\frac{\Omega}{(220\ \mathrm{Myr})^{-1}}\right).$$

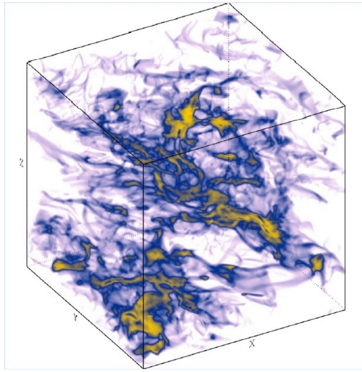

(from Piotek & Ostriker 2005)

gravitational instability (spiral waves)

$$\begin{aligned}\dot{e} &\simeq G(\Sigma_g/H)^2 \lambda^2 \Omega \\ &\simeq (4 \times 10^{-29}\ \mathrm{erg\,cm^{-3}\,s^{-1}}) \\ &\quad \times \left(\frac{\Sigma_g}{10 M_\odot\ \mathrm{pc}^{-2}}\right)^2 \left(\frac{H}{100\ \mathrm{pc}}\right)^{-2} \\ &\quad \times \left(\frac{\lambda}{100\ \mathrm{pc}}\right)^2 \left(\frac{\Omega}{(220\ \mathrm{Myr})^{-1}}\right),\end{aligned}$$

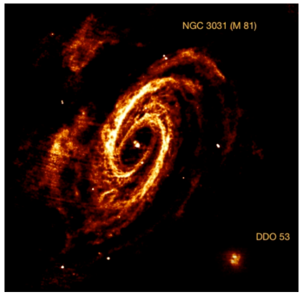

(from Walter et al. 2008)

(from Mac Low & Klessen, 2004)

what drives ISM turbulence?

protostellar outflows

$$\dot{e} = \frac{1}{2} f_{\rm w} \eta_{\rm w} \frac{\dot{\Sigma}_*}{H} v_{\rm w}^2$$
$$\simeq (2\times 10^{-28}\ {\rm erg\ cm^{-3}\ s^{-1}}) \left(\frac{H}{200\ {\rm pc}}\right)^{-1} \left(\frac{f_{\rm w}}{0.4}\right)$$
$$\times \left(\frac{v_{\rm w}}{200\ {\rm km\ s^{-1}}}\right) \left(\frac{v_{\rm rms}}{10\ {\rm km\ s^{-1}}}\right)$$
$$\times \left(\frac{\dot{\Sigma}_*}{4.5\times 10^{-9} M_\odot\ {\rm pc^{-2}\ yr^{-1}}}\right),$$

(Li & Nakamura 2006 vs. Banerjee et al. 2008)

expanding HII regions

$$\dot{e} = \frac{\langle \delta p \rangle \mathcal{N}(>1) v_i}{V t_i}$$
$$= (3\times 10^{-30}\ {\rm erg\ s}\ \ {}^{-3})$$
$$\times \left(\frac{N_{\rm H}}{1.5\times 10^{22}\ {\rm cm^{-2}}}\right)^{-3/14} \left(\frac{M_{cl}}{10^6 M_\odot}\right)^{1/14}$$
$$\times \left(\frac{\langle M_* \rangle}{440 M_\odot}\right) \left(\frac{\mathcal{N}(>1)}{650}\right) \left(\frac{v_i}{10\ {\rm km\ s^{-1}}}\right)$$
$$\times \left(\frac{H_c}{100\ {\rm pc}}\right)^{-1} \left(\frac{R_{sf}}{15\ {\rm kpc}}\right)^{-2} \left(\frac{t_i}{18.5\ {\rm Myr}}\right)^{-1}$$

(note: different numbers by Matzner 2002

(from Mac Low & Klessen, 2004)

what drives ISM turbulence?

supernovae

$$\dot{e} = \frac{\sigma_{SN}\eta_{SN}E_{SN}}{\pi R_{sf}^2 H_c}$$

$$= (3\times 10^{-26}\ \mathrm{erg\ s^{-1}\ cm^{-3}})\left(\frac{\eta_{SN}}{0.1}\right)\left(\frac{\sigma_{SN}}{1\ \mathrm{SNu}}\right)$$

$$\times\left(\frac{H_c}{100\ \mathrm{pc}}\right)^{-1}\left(\frac{R_{sf}}{15\ \mathrm{kpc}}\right)^{-2}\left(\frac{E_{SN}}{10^{51}\ \mathrm{erg}}\right).$$

in star-forming parts of the disk, clearly SN provide enough energy to compensate for the decay of ISM turbulence.
BUT: what is outside the disk?

(from Mac Low & Klessen, 2004)

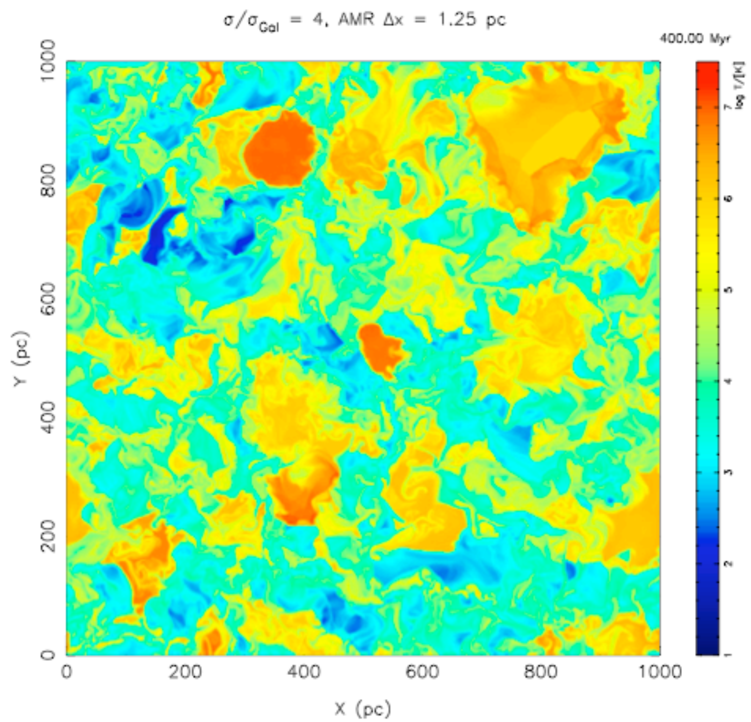

(distribution of temperature in SN driven disk turbulence, by de Avillez & Breitschwerdt 2004)

accretion driven turbulence

- thesis:
  - astrophysical objects *form* by *accretion* of ambient material
  - the *kinetic energy* associated with this process is a key agent *driving internal turbulence*.
  - this works on *ALL* scales:
    - galaxies
    - molecular clouds
    - protostellar accretion disks

Klessen & Hennebelle (2010, A&A, in press)

concept

- turbulence decays on a crossing time

$$\tau_{\rm d} \approx \frac{L_{\rm d}}{\sigma}$$

- energy decay rate

$$\dot{E}_{\rm decay} \approx \frac{E}{\tau_{\rm d}} = -\frac{1}{2}\frac{M\sigma^3}{L_{\rm d}}$$

- kinetic energy of infalling material

$$\dot{E}_{\rm in} = \frac{1}{2}\dot{M}_{\rm in} v_{\rm in}^2$$

- can both values match, modulo some efficiency?

$$\epsilon = \left|\frac{\dot{E}_{\rm decay}}{\dot{E}_{\rm in}}\right|$$

(Field et al.. 2008, MNRAS, 385, 181, Mac Low & Klessen 2004, RMP, 76, 125) some estimates from convergent flow studies

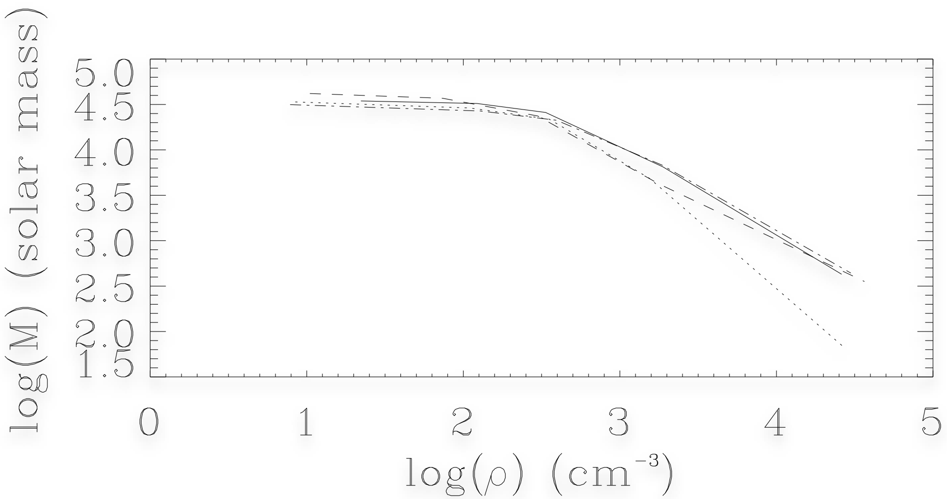

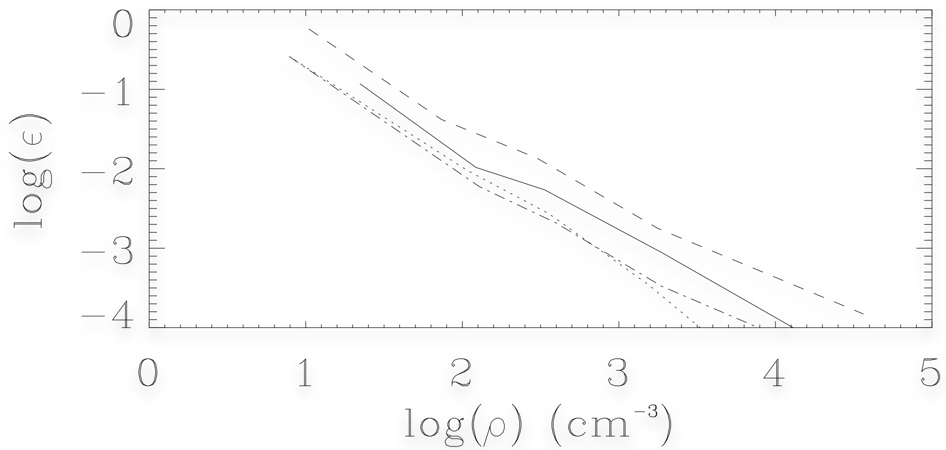

Klessen & Hennebelle (2010)

application to galaxies

- underlying assumption
  - galaxy is in steady state
    ---> accretion rate equals star formation rate
  - what is the required efficiency for the method to work?
- study Milky Way and 11 THINGS
  - excellent observational data in HI:
    velocity dispersion, column density, rotation curve

11 THINGS galaxies

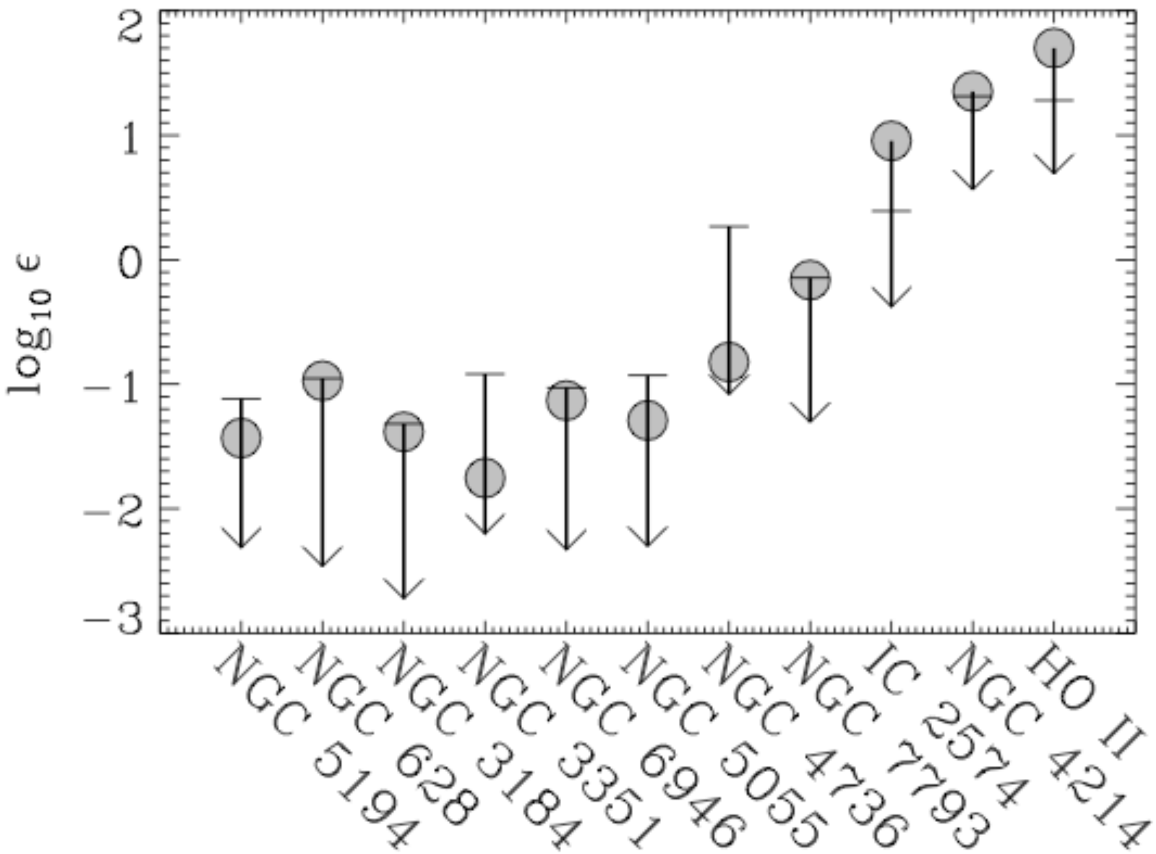

some further thoughts

- method works for Milky Way type galaxies:
  - required efficiencies are ~1% only!
- relevant for outer disks (extended HI disks)
  - there are not other sources of turbulence (certainly not stellar sources, maybe MRI)
- works well for molecular clouds
  - example clouds in the LMC (Fukui et al.)
- potentially interesting for TTS
  - model reproduces dM/dt - M relation (e.g Natta et al. 2006, Muzerolle et al. 2005, Muhanty et al. 2005, Calvet et al. 2004, etc.)

M83

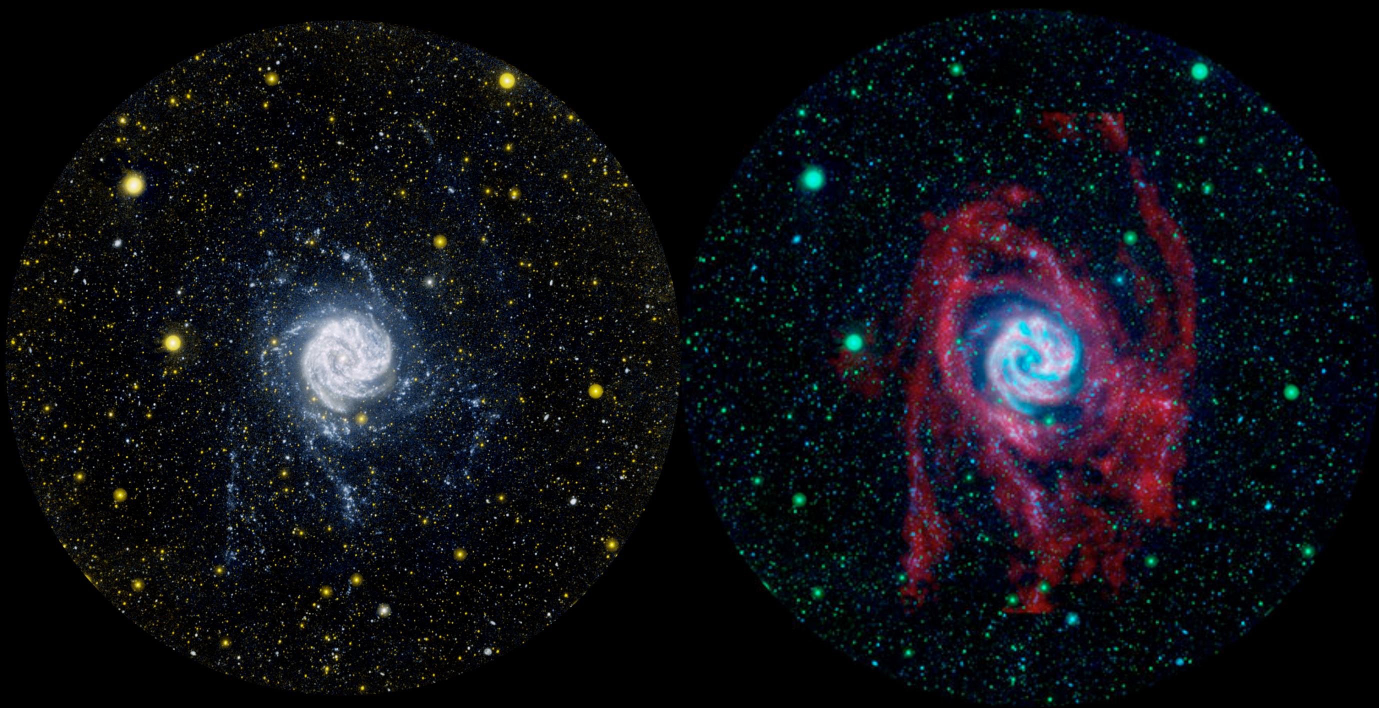

Do we actually see the flow through the disk?
ANSWER: Yes in M83!

M83

M83 HI column

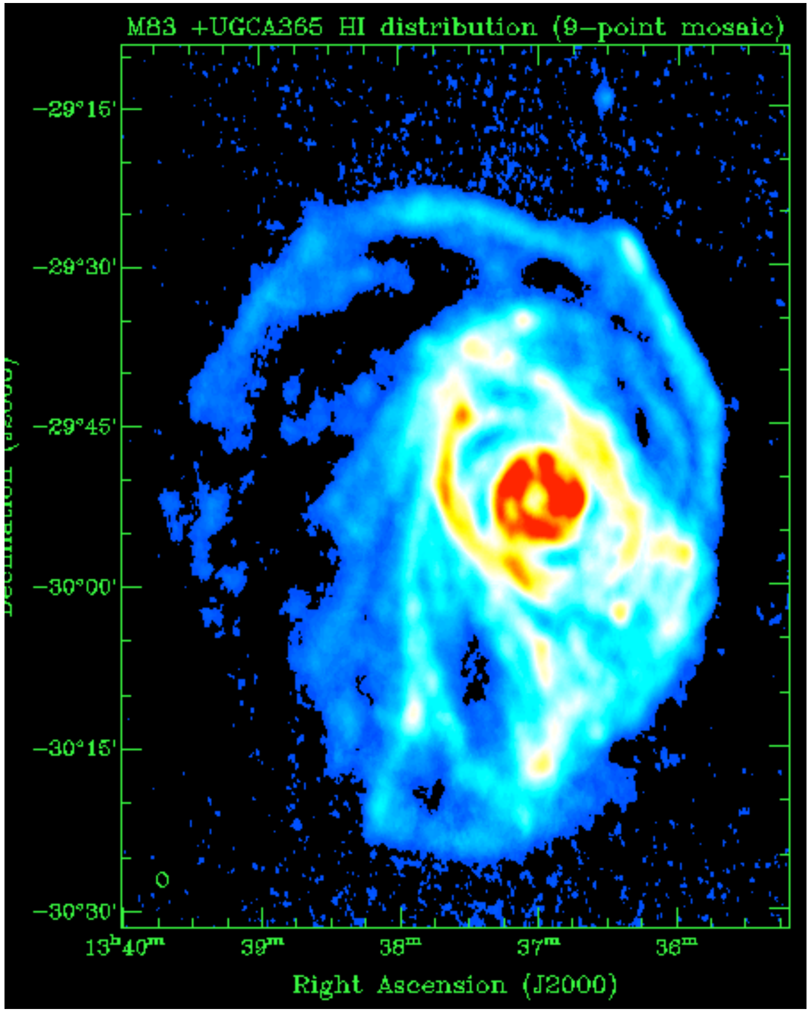

M83 HI velocity dispersion

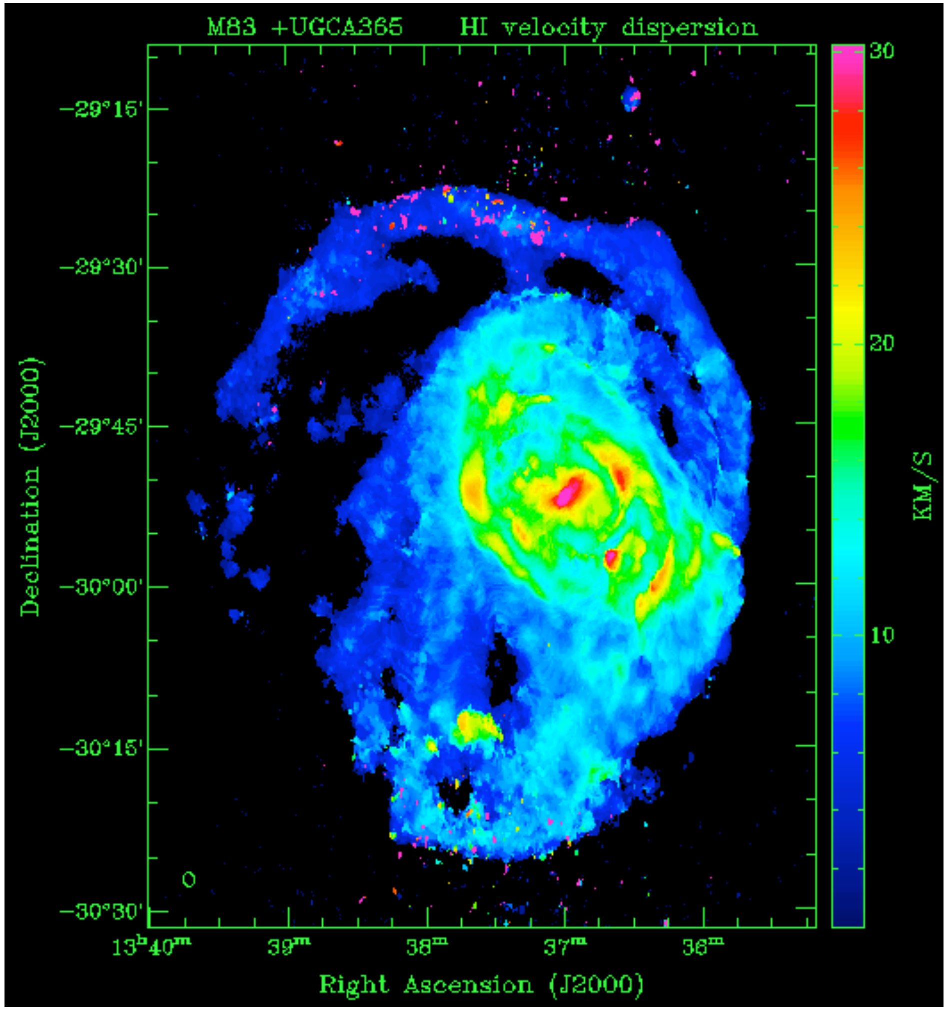

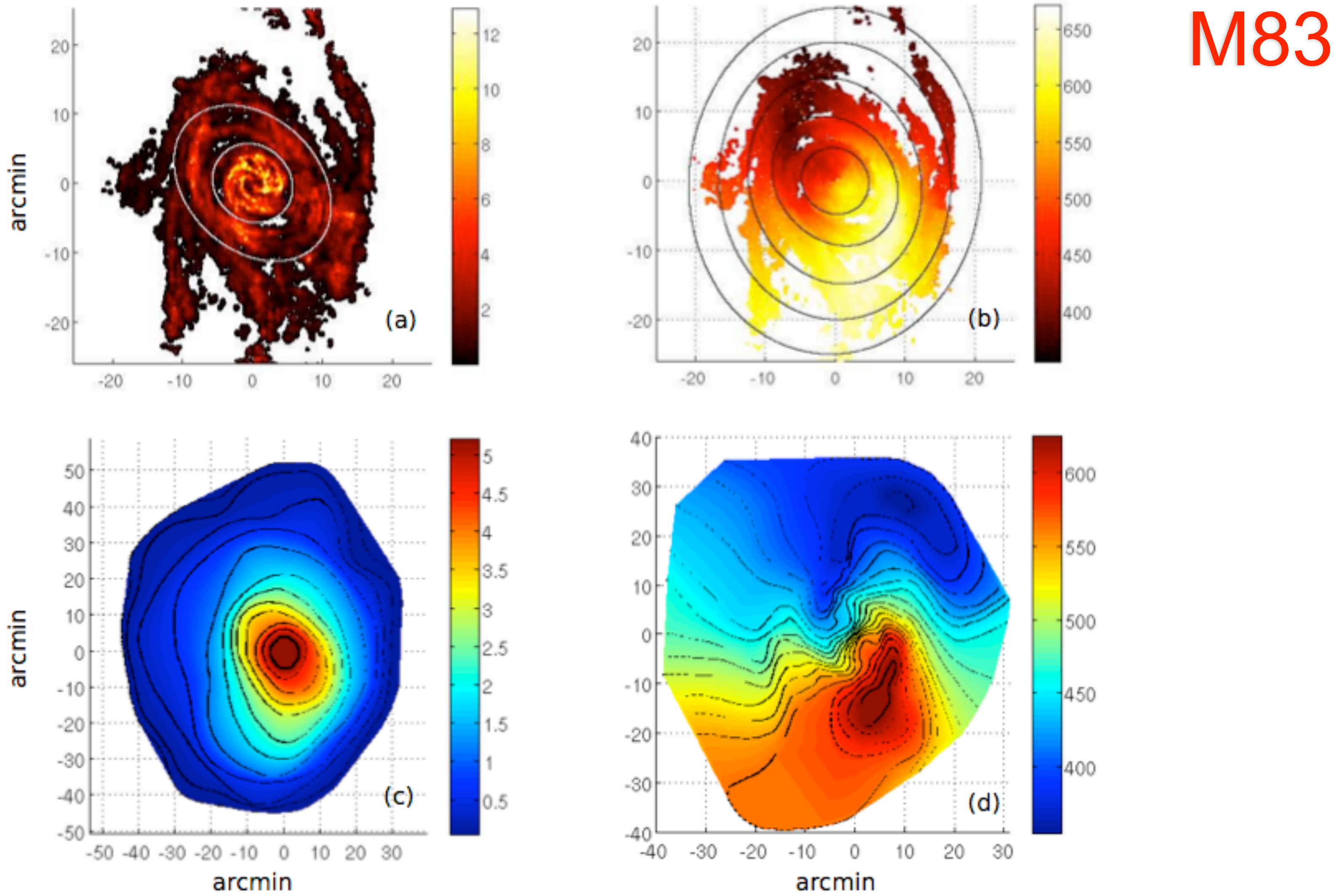

Figure 1. (a) The zeroth moment in units of $M_\odot$ pc^{-2} of the THINGS map. The white ellipses correpond to the black vertical lines ($R = 6', 12.75'$) shown in Fig. 3b, which define the region of the bright HI ring. (b) The first moment in units of km s^{-1} of the THINGS map. Each black ellipse is a result of a tilted circular ring at radii 5′, 10′, 15′, 20′, 25′, with a PA and an inclination extracted from the tilted-ring analysis. To associate structures with the corresponding radii, these ellipses serve as a coordinate system for the fiducial model with $V_{\max} = 180$ km s^{-1}. (c) Reconstructed HI intentisty map in units of column density $M_\odot$ pc^{-2} of the Effelsberg map. (d) Reconstructed line-of-sight velocity, $V_{\rm los}$ [km s^{-1}], of the Effelsberg map. The contours shown in (c) and (d) are extracted from HB81 and are used to reconstruct the Effelsberg map.

M83

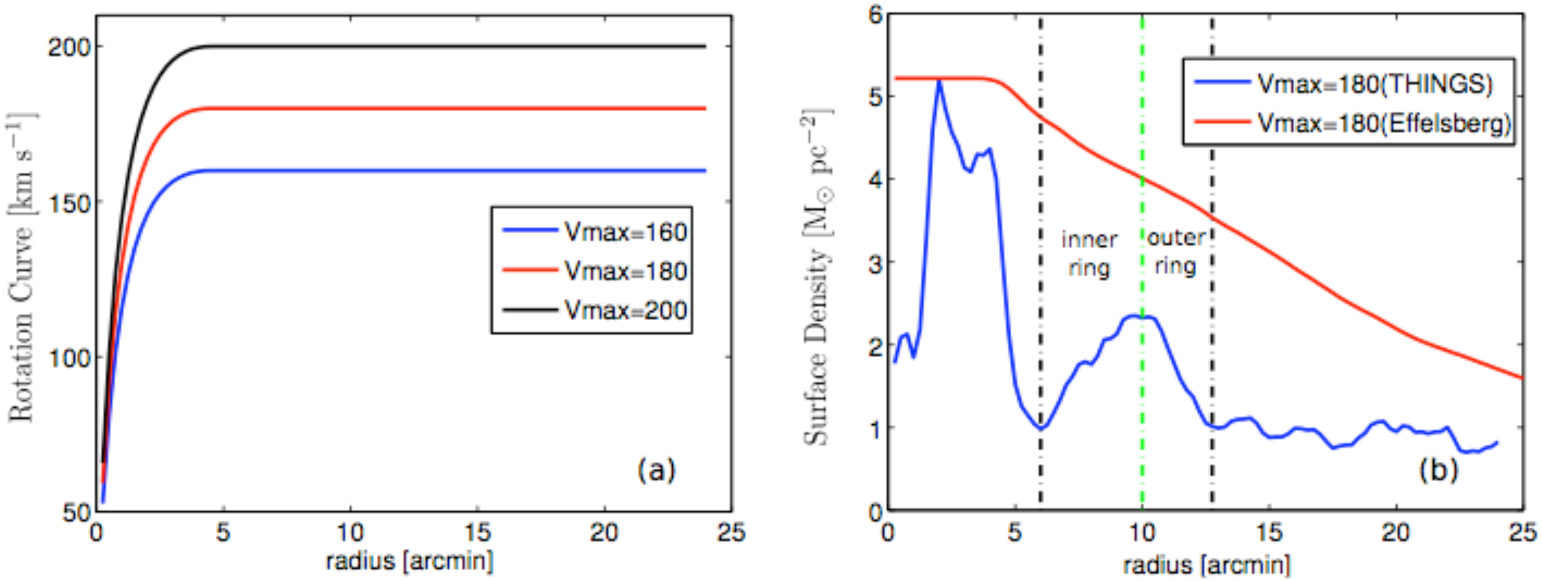

Figure 3. (a) The Brandt-type flat rotation curves as described in Eq. (13). Due to the low inclination of M83, we bracket the real situation with a range of different rotation curves and corresponding fit parameters from the tilted ring model. We assume $n = 0.8$, $R_{\rm max} = 4.5'$, $V_{\rm max} = 160, 180, 200$ km s^{-1}. As suggested in HB81, we take the model with $V_{\rm max} = 180$ as our fiducial case, which will then be justified in § 5. (b) The averaged surface density of the THINGS map (blue curve) and of the Effelsberg map (red curve). They are extracted from the fiducial model. The black vertical lines situated at $6'$ and $12.75'$ define the region of ring structure, which is also shown as the area enclosed by the white ellipses in Fig. 1a and the black ellipses in Fig. 7. The green vertical line marks the location of the density peak and further divides the ring into an inner ring and an outer ring.

M83

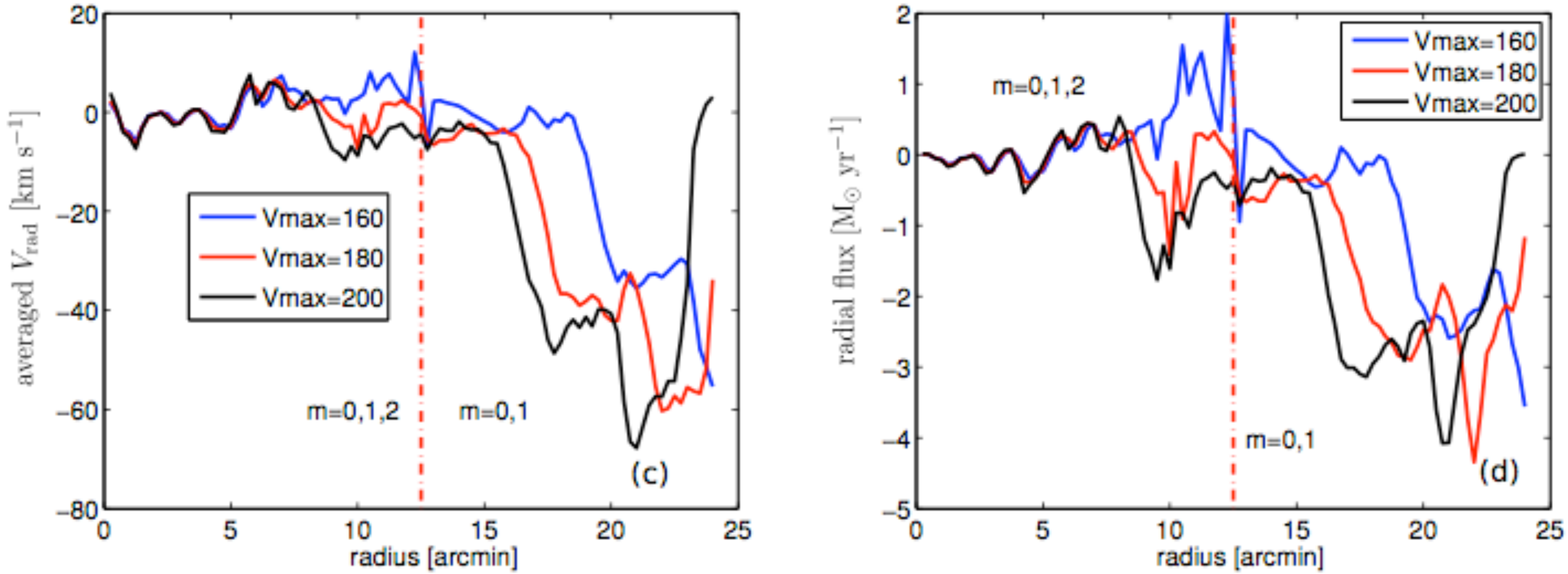

Figure 5. (a) PA and (b) inclination models used to infer radial motion of the gas in the THINGS map. (c) The inferred radial velocity. (d) The inferred radial mass flow. PA and inclination inside the vertical line ($R = 12.5'$) are extracted from the THINGS map, while in the other part we extrapolate these quantities from the Effelsberg map. The Fourier coefficients are fitted for the harmonics $m = 0, 1, 2$ for the radial regime to the left of the vertical line, while only $m = 0, 1$ for the outer parts of the map. In the outer disk, the radial shift is due the different inclinations corresponding to the different models. In all models, the common features are the prominent radial inflow in the outer disk, epicyclic motion in the transition zone (where the HI is organized into a ring like structure, see also Fig. 7 and an indication of moderate radial inflow in the inner disk.

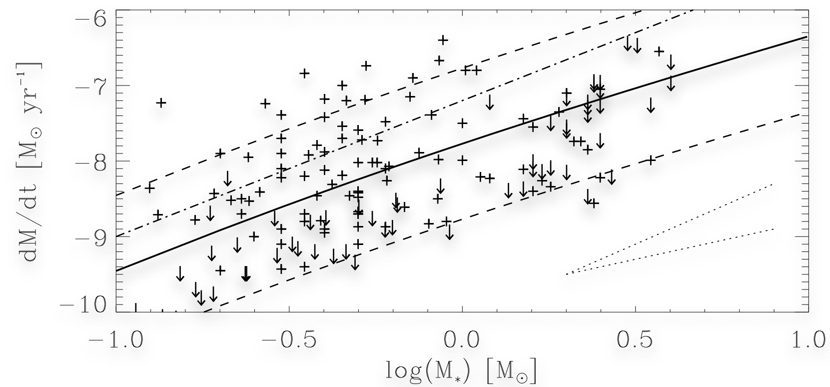

Fig. 7. Prediction of the accretion rate onto the disk as a function of the mass of the star. The solid line corresponds to a mean density of $\bar{n} = 100\,\mathrm{cm}^{-3}$ while the two dashed lines are for $\bar{n} = 1000\ \mathrm{cm}^{-3}$ (upper curve) and $\bar{n} = 10\ \mathrm{cm}^{-3}$ (lower curve). To guide your eye the dotted lines indicate the slope of the relations $\dot{M} \propto M_*^2$ and $\dot{M} \propto M_*$. We compare with data from Calvet et al. (2004), Mohanty et al. (2005), Muzerolle et al. (2005), and Natta et al. (2006) as displayed in Figure 3 of Garcia Lopez et al. (2006), where crosses indicate detections and arrows upper limits. The dot-dashed line is the fit proposed by Natta et al. (2006).

Lecture 1+2: ISM dynamics

- phases of the ISM
- how to observe the ISM
- formation of molecular clouds in convergent flows
  - chemistry
  - dynamics
- origin of ISM turbulence